# Optimal Traffic Control : Cooperative Eco-driving Strategies at Signalized Intersection

Ziqing Wang

**THÈSE DE DOCTORAT DE L'ÉTABLISSEMENT UNIVERSITÉ BOURGOGNE FRANCHE-COMTÉ**

**PRÉPARÉE À L'UNIVERSITÉ DE TECHNOLOGIE DE BELFORT-MONTBÉLIARD**

École doctorale n°37

Sciences Pour l'Ingénieur et Microtechniques

Doctorat d'Automatique

par

ZIQING WANG

# Optimal Traffic Control: Cooperative Eco-driving Strategies at Signalized Intersection

Thèse présentée et soutenue à Belfort, le 29 June 2023

Composition du Jury :

| | | |
|---|---|---|
| AHMED NAIT SIDI MOH | Professeur à l'Université Jean Monnet | Rapporteur |
| SAID HAYAT | Directeur du GIS-GRAISyHM chez IFSTTAR | Rapporteur |
| PIERRE BORNE | Professeur à École Centrale de Lille | Président |
| MOHAMED BENREJEB | Professeur à ENIT Tunisie | Examinateur |
| NICOLAS GAUD | Maître de conférence (HDR) à l'Université Bourgone Franche-Comté, UTBM | Examinateur |
| MAHJOUB DRIDI | Maître de conférence (HDR) à l'Université Bourgone Franche-Comté, UTBM | Codirecteur de thèse |
| ABDELLAH EL MOUDNI | Professeur à l'Université Bourgone Franche-Comté, UTBM | Directeur de thèse |

N° | X | X | X |

école doctorale **sciences pour l'ingénieur et microtechniques**

**Title:** Optimal Traffic Control: Cooperative Eco-driving Strategies at Signalized Intersection

**Keywords:** Eco-driving strategy, signalized intersection, stochastic optimazation, intelligent transportation, energy consumption

**Abstract:**

The cooperative automation of connected and autonomous vehicles (CAVs) has great potential to address a number of safety, mobility, and sustainability issues of our current transportation systems. One key aspect of this innovation lies in cooperative longitudinal motion control, which has been a focal point of extensive research. This dissertation studies how to reduce the energy consumption of vehicles by making high-level driving decisions of different type vehicles. The first part of this dissertation considers the problem of eco-driving for Plug-in Hybrid Electric Buses (PHEBs), a spatial PHEB velocity optimization formulation with communication to traffic information is proposed to minimize the energy consumption or travel time, the simulation results validate the energy savings or time savings of the proposed velocity planning strategy. The second part addresses the problem of traffic environment randomness at signalized intersections. A Stochastic Eco-Driving System (S-EDS) is proposed for Hybrid electric Vehicle (HEV) to minimize the energy cost of individual HEV. The performance of the proposed system is evaluated through many cases that were built with an applied S-EDS in traffic simulation environment SUMO (Simulation of Urban MObility). The final statistical results of simulation groups proved the effectiveness of the stochastic eco-driving system in fuel economy. The third part presents a data-driven trajectory planning strategy for Connected and Automated Vehicles (CAVs), which can ensure probabilistic collision avoidance and improve the fuel economy along signalized corridors, the results from the numerical simulation using the NGSIM (Next Generation SIMulation) data set show the proposed method's efficacy in improving the fuel economy.

**Titre :** Optimal Traffic Control: Cooperative Eco-driving Strategies at Signalized Intersection

**Mots-clés :** Stratégie d'éco-conduite, carrefour à feux, gestion de l'énergie, transport intelligent, consommation d'énergie

**Résumé :**

L'automatisation coopérative des véhicules connectés et autonomes (VCA) présente un potentiel considérable pour résoudre divers problèmes liés à la sécurité, la mobilité et la durabilité de nos systèmes de transport actuels. Un aspect essentiel de cette innovation concerne le contrôle coopératif du mouvement longitudinal, qui a été l'objet d'une recherche approfondie. Cette thèse étude comment réduire la consommation d'énergie des véhicules en prenant des décisions de conduite de haut niveau pour différents types de véhicules. La première partie de cette thèse considère le problème de l'éco-conduite pour les bus électriques hybrides rechargeables (PHEB), une formulation d'optimisation de la vitesse spatiale modèle avec communication aux informations de trafic est proposée pour minimiser la consommation d'énergie ou le temps de déplacement. Les résultats de simulation valident les économies d'énergie ou de temps de la stratégie de planification de la vitesse proposée. La deuxième partie aborde le problème en considérant le caractère aléatoire de l'environnement de circulation aux intersections signalisées, Un système d'éco-conduite stochastique (S-EDS) est proposé pour les véhicules électriques hybrides (HEV) afin de minimiser le coût énergétique. La performance du système proposé est évaluée à travers de nombreux cas construits dans un environnement de simulation de trafic SUMO (Simulation of Urban MObility) avec S-EDS appliqué. Les résultats statistiques finaux des groupes de simulation prouvent l'efficacité du système d'éco-conduite stochastique en termes d'économie de carburant. La troisième partie présente une stratégie de planification de trajectoire basée sur les données pour les véhicules connectés et automatisés (CAV), qui peut assurer l'évitement probabiliste des collisions et améliorer l'économie de carburant le long des couloirs signalisés, les résultats de la simulation numérique utilisant l'ensemble de données NGSIM (Next Generation SIMulation) montrent l'efficacité de la méthode proposée pour améliorer l'économie de carburant.

UBFC UNIVERSITÉ BOURGOGNE FRANCHE-COMTÉ

Université Bourgogne Franche-Comté
32, avenue de l'Observatoire
25000 Besançon, France

# ACKNOWLEDGEMENTS

Undeniably, pursuing a doctoral degree is a challenging journey, made even more difficult by the unprecedented circumstances of the past three years during the COVID-19 pandemic. This period has left an indelible mark on all of us, making it seem as if time had come to a standstill.

In such trying times, I would like to express my heartfelt gratitude to my supervisors, Prof. Abdellah EL MOUDNI and Mahjoub DRIDI, for their unwavering support and guidance throughout my Ph.D. studies and research at the NIT-O2S Lab. Their patience, encouragement, and open-mindedness have been invaluable, especially during my lowest moments. I am deeply grateful for the opportunity to study and grow abroad, made possible by their faith in me. I would also like to extend my sincere appreciation to the China Scholarship Council (CSC) program for their financial support, and to UTBM for providing a comfortable and inspiring environment for my thesis work. Despite my limited French language proficiency, the warm and patient demeanor of everyone I encountered made me feel truly welcome.

Lastly, I would like to thank my dear friends Liu Wenheng, Luo Hongyuan, Wang Gaoshuai, Hao Xinyang, Ao Yunjin, Li Wenbo, ..., for their kind help, and Feng Linfei, Zhang Teng, and Mira BOUSALEH, for their unwavering support and companionship. Without their encouragement, completing this dissertation might have been impossible.

Finally, I owe a special debt of gratitude to my parents and my boyfriend, Li Jiaming, whose love and support have been the foundation for me to passionately pursue my academic research.

Life is a continuous process of creating certainty amidst uncertainties, and each of us has the power to shape our own unique and infinite game of life.

# PUBLICATIONS

**Conference:**

[1] Wang Z, Dridi M, El Moudni A. Ecological Velocity Planning of Plug-in Hybrid Electric Bus Through Signalized Intersections[C]//2021 International Conference on Computational Intelligence and Knowledge Economy (ICCIKE). IEEE, 2021: 355-359.

[2] Wang Z, Dridi M, El Moudni A. Data-driven Trajectory Planning Strategy for Connected Vehicles at Signalized Intersection[C]//2022 17th International Conference on Control, Automation, Robotics and Vision (ICARCV). IEEE, 2022: 111-118

**Journal :**

[1] Wang Z, Dridi M, El Moudni A. Stochastic Eco-driving System for Hybrid Electric Vehicles at Signalized Intersection. IET Intelligent Transport System (Under Review)

[2] Wang Z, Dridi M, El Moudni A. Co-optimization of Eco-driving and Energy Management for Connected HEV/PHEVs near Signalized Intersections: A review Applied Sciences (Accept)

# CONTENTS

# ABBREVIATIONS

| | |
|---|---|
| **PHEV** | Plug-in Hybrid Electric Vehicle |
| **HEV** | Hybrid Electric Vehicle |
| **PEV** | Pure Electric Vehicle |
| **PHEB** | Plug-in Hybrid Electric Bus |
| **EMS** | Energy Management Strategy |
| **ITS** | Intelligent Transportation System |
| **V2V** | Vehicle to Vehicle Communication |
| **V2I** | Vehicle to Infrasructure Communication |
| **SPaT** | Signal Phrase and Timing |
| **CAV** | Connected and Automated Vehicle |
| **CAHEV** | Connected and Automated Hybrid Electric Vehicle |
| **HDV** | Human-Driven Vehicle |
| **Eco-driving** | Ecological Driving |
| **Co-optimization** | Cooperative Optimization |
| **ITS** | Intelligent Transportation System |
| **ICE** | Internal Combustion Engine |
| **ECM** | Equivalent Consumption Minimization |
| **PMP** | Pontryagin's Maximum Principle |
| **DP** | Dynamic Programming |
| **DDP** | Deterministic Dynamic Programming |
| **SDP** | Stochastic Dynamic Programming |
| **ACC** | Adaptive Cruise Control |
| **PCC** | Predictive Cruise Control |
| **MPC** | Model Predictive Control |

# General Introduction

Urban cities have been focusing on energy shortages and environmental issues in recent years. The transportation sector, which accounts for nearly three-quarters of the total petroleum consumption, is the most energy-consuming system. According to reports [118], energy consumption in the U.S. transportation sector accounted for approximately 28% of total U.S. energy use in 2021. Moreover, the International Energy Agency (IEA) states that the transportation sector, which has the highest reliance on fossil fuels, contributed to 37% of CO2 emissions from end-use sectors during the same year, causing the share of transportation in global energy-related carbon dioxide emissions to increase by two percentage points, reaching 26% [57]. It is evident that the majority of our daily energy consumption is attributed to our movements. In response to reducing energy consumption and emissions related to transportation, scholars and researchers have proposed many approaches which can be summarized based on two technical aspects.

The first aspect is to use alternative energy sources as much as possible to replace traditional fossil fuels, such as the promotion of new energy taxis, buses, subways, passenger cars, and trains; the so-called new energy sources are obtained from renewable resources like hydrogen, solar, and wind. With these new energy sources, new powertrain types have been created for the purpose of using electricity that comes from these renewable energy sources. For instance, Hybrid Electric Vehicles (HEVs) and Pure Electric Vehicles (PEVs) have been developed, which offer better fuel efficiency compared to traditional Internal Combustion Engine (ICE) vehicles. However, even though we surmise the widespread adoption of PEVs and HEVs could alleviate energy shortages, charging infrastructure limitations and range anxiety are major obstacles to their large-scale rollout. While, unlike PEVs, HEVs are formed by adding additional energy sources and storage systems, which offer a temporary solution to the above two issues under existing conditions. Therefore, they are a suitable choice during the transition period before moving to large-scale PEVs. Such a trend is also reflected in the market share performance as Fig.1 shows. The market share of HEVs has increased significantly, capturing 3.2% of the light vehicle market in 2013 and 5.5% in 2021. PHEVs sales began in 2011, and their market share has grown every year. As of 2021, PEVs accounted for 3.2% of the light vehicle market. Consequently, the Energy Management System (EMS) of these vehicles has become an increasingly important issue.

In order to better understand the following reviewed EMS solutions, Fig.2 illustrates the structural differences between the three types of three Electrical Vehicles (EVs). In the case of a Hybrid Electrical Vehicle (HEV), both an engine (ICE) and an electric drive

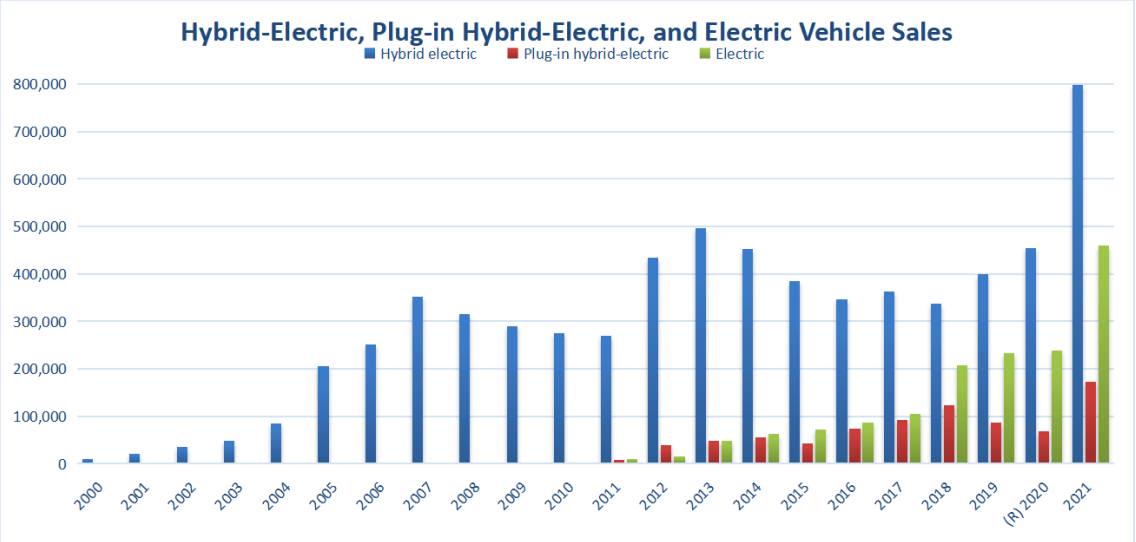


Figure 1: Sales illustration of HEV/PHEV on the US market [118]

power the drivetrain. The electric motor's battery is charged by regenerative braking and a generator connected to the ICE, allowing for the use of smaller engines and improving fuel efficiency. And for a Plug-in HEV (PHEV), the battery is charged not only by regenerative braking and the generator but also by an external electric power source. Finally, a Pure EV (PEV) is solely powered by its battery, which is charged using an outside electric power source.

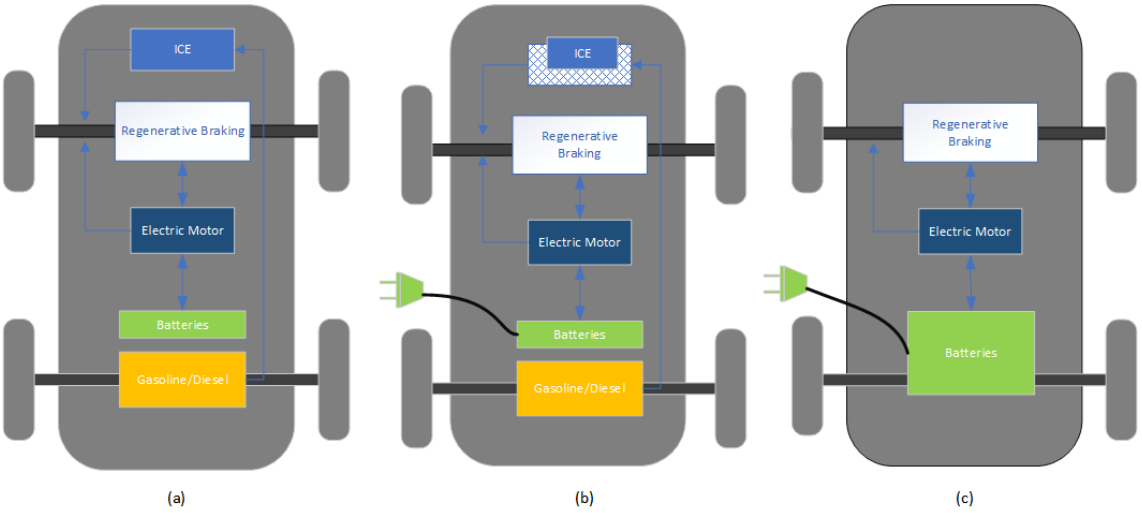


Figure 2: Basic structure of different EV types. (a) HEV (b) PHEV(c) PEV

Meanwhile, the second aspect focuses on novel driving techniques that prioritize environmental sustainability in transportation systems, such as Ecological Driving (Eco-Driving) strategies. The concept of Eco-driving involves optimizing and regulating the speed of vehicles based on various factors such as the route information and surrounding environment, such as speed limits, locations of stop signs, and Signal Phase and Timing

(SPaT) information provided by the Intelligent Transportation System (ITS) technology. More details, such as the use of Connected Vehicles (CVs) can lead to enhanced road safety, smoother traffic flow, and energy conservation through Vehicle-to-Vehicle (V2V) and Vehicle-to-Infrastructure (V2I) communication. V2V enables vehicles equipped with communication technology to exchange information, thereby preventing collisions and enabling coordinated movement. On the other hand, V2I enables vehicles to communicate with roadside units and infrastructure, such as traffic signals, which allows for better coordination between them. The transportation system has evolved with the integration of smart and connected technologies, as shown in Fig.3, not only for vehicles but also for the road network, which has become smarter with the deployment of intelligent traffic infrastructures and sensors.

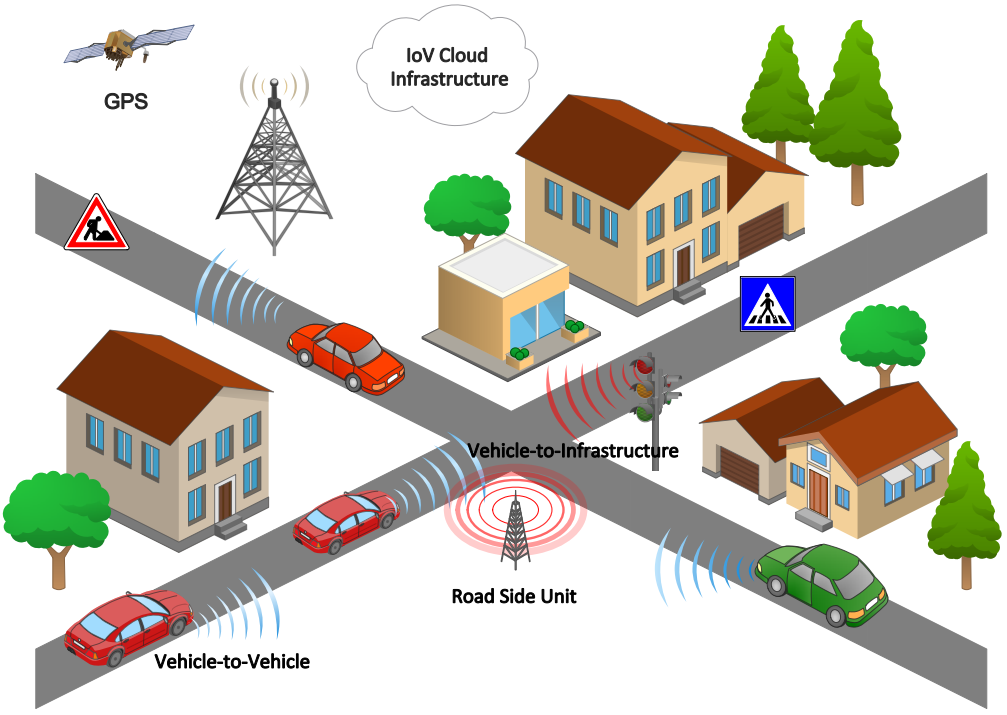


Figure 3: Schematic of ITS technology

Therefore, with the rapid development of intelligent transportation systems (ITS) and the increasing emphasis on sustainable mobility, connected hybrid electric vehicles (HEVs) and plug-in hybrid electric vehicles (PHEVs) have emerged as crucial components in the global effort to reduce emissions, improve energy efficiency, and achieve sustainable transportation. The integration of advanced energy management systems (EMS) and eco-driving strategies in connected HEV/PHEVs has the potential to address these challenges by optimizing single-vehicle and transportation system performance. The choice of this topic is motivated by the growing demand for effective solutions that can harness the benefits of connected vehicle technologies and cooperative systems to enhance the performance of HEV/PHEVs in diverse traffic conditions. The importance of this topic

lies in its potential to provide valuable insights for researchers, policymakers, and practitioners, guiding the development of innovative EMS and eco-driving strategies that can maximize fuel economy, reduce emissions, and improve traffic flow.

## PLAN OF THE THESIS

In this thesis, there are total five chapters as follows.

Chapter 1 introduces definition and main difference between HEV, PHEV, and PEV in terms of their operation, as well as state-of-the-art about existing EMS for HEV/PHEV, eco-driving strategies for CAV, and cooperative optimization of EMS and eco-driving strategies for CAHEV. Then conclude the review part and point out our contribution in this study.

Chapter 2 presented a velocity planning strategy for PHEBs focused on energy and time savings. Firstly mathematical model is established for the PHEB, its components, and traffic signals, then the velocity planning problem is formulated using a DP framework. To simplify the computation, we proposed a 2D-DP method that uses optimal SOC from empirical data. Our simulation utilized the optimal SOC curve from the energy management system without velocity optimization as a substitute for empirical data. We solved sub-problems as time-discrete nonlinear optimization problems using DP and treated the velocity planning problem as a deterministic spatial-discrete nonlinear optimization problem. The simulation results showed a 3.98% energy reduction and a 4.84% time saving. Despite its limitations, such as assuming deterministic intersection and bus-stop information and potential inaccuracies in energy distribution ratios, the strategy can serve as a precursor for online EMS to reduce energy consumption.

Chapter 3 proposed a stochastic eco-driving system for power-split HEVs, featuring co-optimization of vehicle dynamics and hybrid powertrain operations. The system consists of a stochastic eco-driving decision subsystem and a hybrid powertrain control decision subsystem. The upper-level decision subsystem utilizes a dual-driven approach to suggest optimal set speeds or predict trajectories, while the hybrid powertrain control subsystem employs a rule-based strategy to optimize energy consumption at intersections. Simulations in SUMO traffic environment demonstrate energy reductions of 6.49% and 4.17% compared to groups without the system. The system's independence from full traffic infrastructure connectivity is a major advantage, as universal connectivity is costly and unlikely in the near future. Data- and model-driven optimization shows promise for future traffic data and intelligent transportation systems. Although real traffic data was not used, our method can be easily extended to various traffic environments and multiple intersections.

Chapter 4 developed a data-driven trajectory planning strategy for connected vehicles, addressing uncertainty in shared information. We first reviewed the Gaussian sampling-

based method for handling chance constraints in trajectory planning. Inspired by this, we developed a strategy that solves the optimal control problem by transforming the chance constraint into a deterministic equivalent interval for each time step, using a Gaussian Process Regression prediction model. We evaluated our approach using the Next Generation SIMulation (NGSIM) dataset, simulating various scenarios and examining vehicle trajectory and fuel consumption performance under different probability values. The results demonstrated improvements in fuel economy, validating the effectiveness of our strategy. Future research could involve extending this approach to longer routes with more signalized intersections, further refining the method and potentially achieving even greater efficiency improvements in complex traffic situations.

Chapter 5 concludes the whole thesis and discussed potential research directions and opportunities in this field.

# 1

# Introduction of EMS, Eco-driving and co-optimization

## 1.1/ Architecture of HEVs/PHEVs

To fully understand the potential of HEV/PHEVs as an approach for sustainable transportation, it is important to examine the architecture of HEV/PHEVs and EMS that govern their performance. EMS is the core determinant of HEV/PHEV performance and is closely linked to the vehicles' architecture. Thus we will provide a comprehensive overview highlighting the key components that make up these vehicles and their respective roles in the energy management process.

Generally, the structure of HEVs/PHEVs offers additional flexibility to optimize their engine operation regions compared with ICE vehicles, as the latter can only adjust their engine speed to regulate their torque in response to a driver's power demand. Then the key characteristics of HEV/PHEVs which are different from the ICE vehicles, are listed as follows [102],

- Recover the regenerative braking energy as much as possible
- Reduce the idling energy cost by turning off the engine
- Achieve an optimal distribution of power among various power sources
- Reduce the size of the ICE while ensuring that the vehicle's maximum requirements are still met
- Tend to be more complex and costly as they necessitate additional controllers
- Have a weight that is 10-30% greater than that of ICE vehicles

Anyway, as depicted in Fig.2, a motor assists the engine to operate in a higher efficiency area in an HEV/PHEV, which is able to achieve better fuel efficiency. To accomplish this, HEVs/PHEVs need to determine how to distribute power among various power sources

(e.g., the engine and battery) in response to varying driving conditions. Typically, there are three types of HEV powertrains, which are also utilized in PHEVs except that PHEVs have a charging port that allows the battery to be charged directly from the grid. The three types are series hybrid, parallel hybrid, and combined(series-parallel) hybrid respectively [4]. In a series hybrid powertrain system, a motor/generator set is powered by the engine to drive the vehicle; In a parallel hybrid system, either use the battery with a motor/generator set or the engine to drive the vehicle according to the torque demand; In a combined hybrid system, vehicles has the ability to operate as a series or parallel hybridization.

### SERIES HYBRID

Specifically, the IC engine acts as an Auxiliary Power Unit (APU) and thus extends the range of a purely electric vehicle in a series hybrid drive system, as shown in Fig.1.1. One of the advantages of this configuration is that the IC Engine can be employed at a point where efficiency and emissions are at their highest levels because it is not dependent on the mechanical requirements of the vehicle in this form. Furthermore, the loss brought on by the gears or clutch is reduced by the lack of a mechanical connection between the vehicle and the IC Engine, and using the Electric Motor enables the continued use of regenerative braking. Nevertheless, this configuration requires IC Engine, Electric Generator, and Electric Motor and the added weight could offset the benefits described earlier. Based on these characteristics, series HEV/PHEVs are more suitable for low-speed operating conditions in urban areas and not for highway driving conditions.

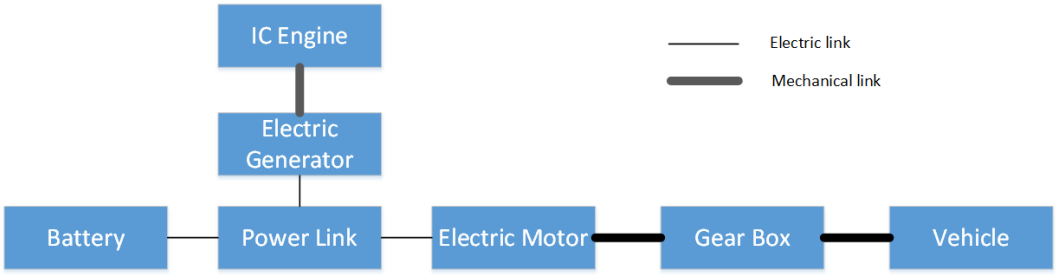


Figure 1.1: Series Hybrid Configuration

### PARALLEL HYBRID

In a parallel hybrid drive system, both the IC Engine and Electric Motor operate simultaneously. As illustrated in Fig.1.2, compared to the series hybrid system, the parallel configuration requires only the IC Engine and Electric Motor, eliminating the Electric Generator and reducing the total weight and complexity. Furthermore, the auxiliary power effect of the electric motor enables a reduction in the power of the IC Engine and battery capacity. Additionally, because the IC Engine remains mechanically connected to the drive system,

the energy utilization of the engine in the parallel hybrid system is relatively high, resulting in higher fuel efficiency than in the series hybrid drive system. However, the IC Engine's operating conditions are influenced by the driving conditions, and frequent changes in driving conditions can cause the engine to operate inefficiently, resulting in increased emissions compared with the series type. Therefore, the parallel hybrid system is better to match the operating conditions where the car is driven steadily at medium and high speeds and is most suitable for driving on intercity roads and highways.

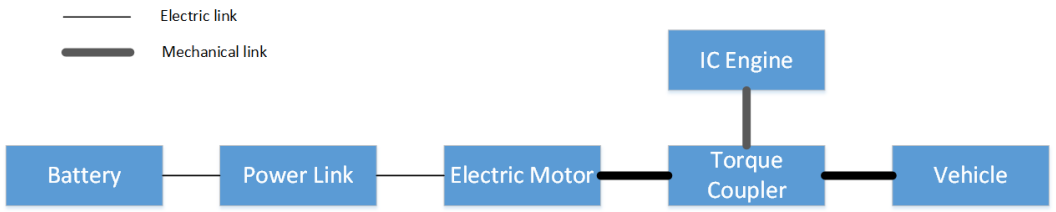


Figure 1.2: Parallel Hybrid Configuration

### COMBINED HYBRID

The combined hybrid system (Fig.1.3) combines the characteristics of the series and parallel hybrid systems, compared to the series hybrid system, it incorporates additional transmission routes for mechanical power, while compared to the parallel hybrid system, it introduces more transmission routes for electric power. The combined hybrid system gains flexibility by dividing the power between the motor and the generator and this complex configuration generally makes it more costly and difficult to control. But the advantages of this combined hybrid system are also obvious, on the one hand, it can be applied to a variety of vehicle operating conditions, and the vehicle's economy and emissions can be guaranteed whether on the inter-city arterial road or on the highway, on the other hand, this system is suitable for all size of vehicles.

In the subsequent study, different types of hybrid type were selected for different scenarios according to their characteristics. After having examined the architecture of HEV/PHEVs, we can now turn our attention to the Energy Management Strategies (EMSs) that are commonly used in HEV/PHEVs, as well as the key factors that influence their design and optimization. By examining the EMS in detail, we can gain a deeper understanding of how these strategies are developed and optimized to ensure maximum efficiency and performance in various driving conditions.

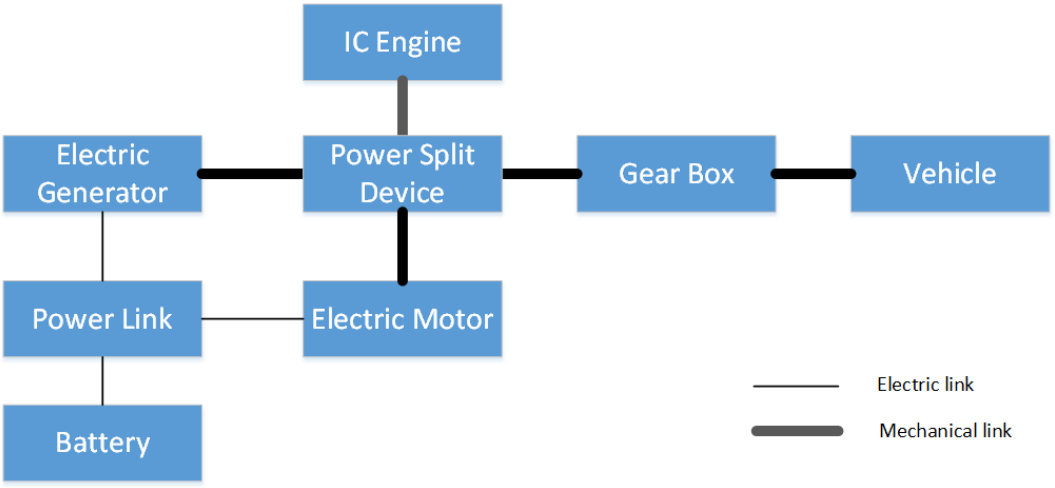


Figure 1.3: Combined Hybrid Configuration

## 1.2/ LITERTURE REVIEWS

### 1.2.1/ ENERGY MANAGEMENT STRATEGY FOR HEV/PHEVS

EMS is critical as it determines the allocation and flow of energy between the powertrain components and energy storage system. By optimizing the EMS, HEV/PHEVs can achieve higher efficiency and better performance in a wide range of driving conditions. In this section, we will examine the different types of EMS that are commonly used for HEV/PHEVs. Through a detailed analysis of EMS, we aim to provide a comprehensive understanding of the key principles and strategies that underlie the design and optimization of HEV/PHEVs.

The presence of two power sources in HEVs/PHEVs allows for the regulation of energy allocation to achieve greater environmental friendliness. Normally, the energy management problem of hybrid power is formulated as the following [119],

$$\begin{aligned} &\min_{x,u} J(x,u) \\ &\text{s.t. } G(x) \leq 0 \end{aligned} \tag{1.1}$$

where $x \in X$ denotes the state variables of the hybrid system, such as vehicle distance, speed, State of Charge (SOC), fuel consumption, etc. The control variable $u \in U$ is usually defined as the ratio of power or torque demand. The constraint conditions $G(x)$ represent limitations on power or velocity, torque, and the final value of SOC. The objective function $J$ can be defined to minimize fuel consumption, and exhaust emissions, delay battery aging, or maintain vehicle mobility or combinations of these objectives.

Based on the above formulation, numerous efforts have been made to develop more efficient powertrain systems and Energy Management Strategies (EMSs) for HEV/PHEVs.

Fig.1.4 illustrates the related classification of strategies based on the approach adopted.

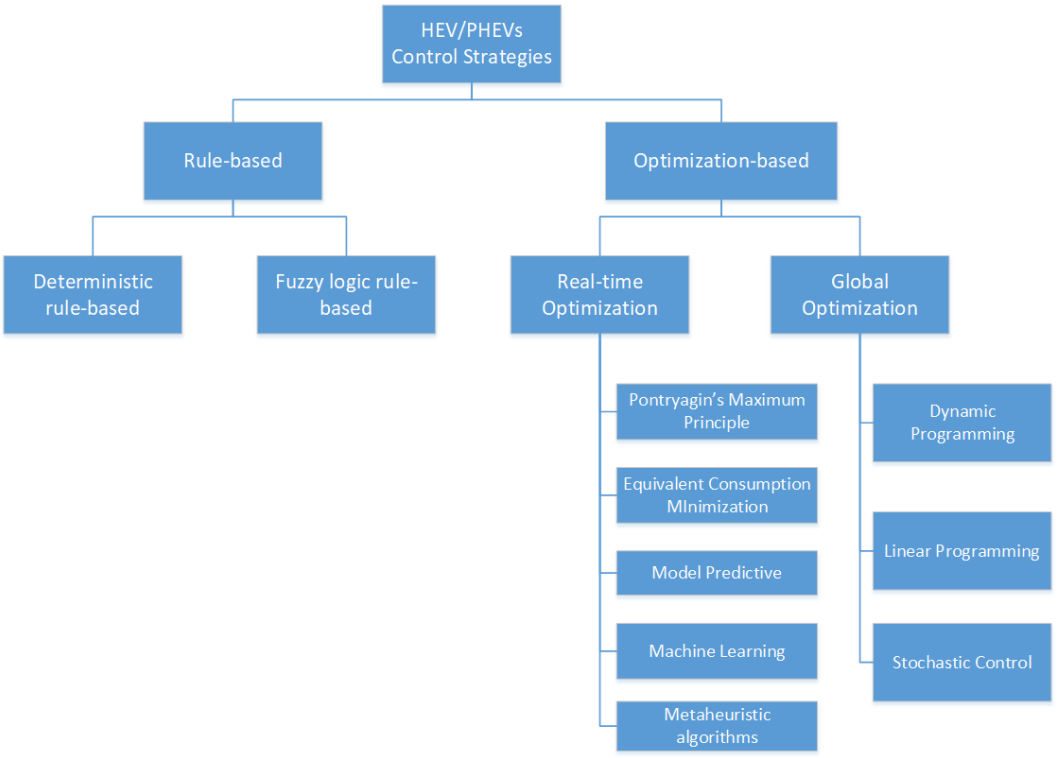


Figure 1.4: Classification of HEV/PHEVs Control Strategies, source:[47]

#### 1.2.1.1/ RULE-BASED EMS

Rule-based control strategies are usually extracted from the existing control experience to meet the characteristics of each component, belonging to the class of real-time strategy. The main research directions can be divided into two categories, the first category is based on a deterministic logic threshold, the earliest as in literature [16], the researchers divided the operation of PHEV into Charging Depleting (CD) and Charging Sustaining (CS) mode by setting SOC threshold value, the other is using fuzzy logic, like [2, 37]. Rule-based EMSs have shown promising results since the early 2000s, but they are not guaranteed to be optimal since they are based only on instantaneous outputs. In fact, these rules are determined by the car manufacturer using standard speed profiles that do not always accurately represent real-world conditions.

#### 1.2.1.2/ OPTIMIZATION-BASED EMS

The optimization-based strategies are derived from optimization theory, specifically optimal control theory. And the solution to this Optimal Control Problem (OCP) can be divided into two main classes: those that attempt to compute a local solution in real-time, usually online, and those that compute a global solution, typically offline [63, 61].

### REAL-TIME OPTIMIZATION

The real-time strategies aim to determine the allocation of power sources at each time step while simultaneously minimizing the cost function (e.g., fuel economy, power, emissions). This class of strategy has been widely developed in recent years due to its relative ease of implementation. It can be subdivided as follows:

- Pontryagin's Maximum Principle (PMP), which is the main method in optimal control theory, obtains the optimal control variable by solving the extreme values of the Hamilton function at each moment. It is easy to be implemented in order to find the optimal control, see in [22, 93].

- Equivalent Consumption Minimization (ECM) is developed by calculating the total fuel consumption as the sum of the fuel used by the ICE and equivalent fuel consumption for the electric motor. This unifies the electric power and combustion power [5]. It is also a form of PMP that is proven to yield the maximum fuel economy under certain conditions [18]. An adaptive method [74] has been developed based on ECM, which refreshes the equivalent factor while taking into account driving conditions. The equivalent consumption is calculated in real-time as a function of the current system output. This method enables the system to work without any information about future driving conditions [48].

- Model Predictive Control (MPC) is an advanced method of process control that is used to control a process while satisfying a set of constraints. In the context of EMS for HEV/PHEV, it is a strategy that combines online system parameter updates with optimal control to predict future velocities and optimize fuel consumption based on them. A typical example can be found in [25], where the authors formulated the energy management problem of combined HEV as a nonlinear optimal control problem with constraints. Two different cost functions were defined and the MPC strategy was used to determine the power split between the IC Engine and electrical machines at each sample time. Results showed significant improvement in fuel economy with compared to those of an available controller in the commercial Powertrain System Analysis Toolkit (PSAT) software. For more reviews of MPC-based EMS, please refer to [66].

- Machine learning in recent years is a popular and useful technique for addressing various problems in many research fields, including as an EMS method for HEV/PHEVs. It has great potential to improve the computation process and adaptability. The applications of machine learning to energy management can be generally classified into two categories [100]. The first involves using a single algorithm, such as reinforcement learning algorithms [52, 95], to derive the energy management policy. The second category involves combining other information or algo-

rithms with machine learning methods, such as predictive algorithms, trip information, and MPC [21, 32, 33, 38].

- Metaheuristic algorithms are a type of computational intelligence paradigms that are especially useful for solving complex optimization problems with large search space of likely solutions [81]. They use general methods that can be applied to different types of optimization problems, without relying on specific knowledge, and aim to find near-optimal solutions within a reasonable amount of computation time. They are often used in engineering, science, and business to solve a wide range of optimization problems, including those encountered in HEV/PHEV EMSs. The most commonly used metaheuristic algorithms in HEV/PHEVs EMSs are Simulated Annealing(SA), Genetic Algorithm(GA), and Particle Swarm Optimization (PSO) [13, 9, 15], these algorithms do not require derivative calculations but harness alternative methods to populate candidates for the optimal solution. This solution search depends on certain parameters that facilitate getting rid of local minima, although convergence to global optima cannot be generally ensured [61].

#### GLOBAL OPTIMIZATION

The concept of Dynamic Programming (DP) is essential in developing strategies to find an optimal global solution. DP applies Bellman's optimality principle and solves complex problems by breaking them into simpler subproblems. Normally, Deterministic Dynamic Programming (DDP) has been used to obtain a theoretical lower bound for consumption on specific speed profiles [10]. but it has a curse of dimensionality where the computational cost increases exponentially with the number of state and control variables, making it limited to small systems and difficult to use in real-time. Some works have proposed dimension reduction techniques for the state or control space to overcome this limitation [12, 11]. Additionally, future trips information can be considered in the EMS formulation in order to minimize the total trip fuel consumption, which can be described as a mixed-integer linear programming problem[49], or using a stochastic control (Stochastic Dynamic Programming) framework [6, 14].

In conclusion, EMS is a crucial aspect for HEV/PHEV, playing a vital role in achieving their energy efficiency and reducing their environmental impact. The various optimization techniques offer a range of options for designing EMS that meet the specific requirements of different HEV/PHEV applications. Furthermore, the integration of eco-driving strategies with EMS can result in improvement in more aspects, such as significant fuel savings, increased safety, and driving comfort. In order to fully understand the complex integration technique, we will explore the various eco-driving strategies that are not limited by HEV/PHEV first in the next section.

### 1.2.2/ Eco-driving Strategy for Connected Vehicles

As mentioned before, Eco-driving is a relatively low-cost and immediate approach to reduce fuel consumption and emissions significantly [86], as the driver plays a major role in determining vehicle performance. Meanwhile, eco-driving has various definitions and scopes in the literature, for example, the authors in [35] defined it as vehicle purchase and post-purchase decisions, and in [75], the authors pointed out that eco-driving behavior including driving, cabin comfort, trip planning, load management, fuelling, and maintenance six classes, the driving behavior is further divided into acceleration/deceleration, cruise, idling and driving mode selection and parking. However, In the following context, eco-driving is narrowed to the driving behaviors or the control a driver has over the vehicle during a journey that can influence fuel consumption and emissions. The typical research methods used to study eco-driving technology include laboratory testing, on-road experiments, and numerical modeling.

#### Laboratory testing

There are various methods to measure different driving styles, including the use of a chassis dynamometer, engine dynamometer, or driving simulator. Engine dynamometer testing requires following specific procedures set out in regulations for the testing of the engine and exhaust after-treatment system [127]. Similarly, the chassis dynamometer requires standard operation by the operator. These kinds of dynamometers are located in the laboratory and designed to meet regulatory standards. The testing results from the laboratory dynamometer are highly precise and reliable, and influencing factors such as test cycles, road resistance, and climate conditions can be fully controlled. In addition, a driving simulator is also commonly used to study driving behaviors, comprising a fixed-base car mock-up equipped with a steering wheel, acceleration, and brake pedals and indicators, with road scenarios displayed on a screen. The driver will operate the driving simulator according to the virtual traffic environment. The primary advantage of driving simulators offers a safe and effective way to examine various factors that impact driver performance [56].

#### On-road experiments

On-road experiments provide valuable data for evaluating the actual driver performance with the eco-driving strategy, they are generally less accurate and repeatable than laboratory testing. Due to the absence of standard testing cycles, on-road experiments are highly affected by uncertainties in traffic conditions, driver behaviors, and transient operation[39]. And the commonly used on-road research methods for eco-driving include Portable Emissions Measurement Systems (PEMS), data loggers, odometer reading and fuel use, and surveys [86].

### NUMERICAL MODELLING

Numerical modeling is a commonly used tool to evaluate the performance of new eco-driving and eco-routing algorithms, the reason why it becomes popular is that allows researchers to study the effectiveness of new eco-driving strategies or algorithms without conducting field experiments, saving greatly in both research time and cost. Meanwhile, the limitation is that results are generally less accurate and reliable than those of laboratory testing and on-road experiments.

Anyway, if novel eco-driving strategies are proposed, two significant scenarios are typically considered: freeways [41, 60], and signalized intersection on urban roads [24, 84, 94, 98]. Since the first scenario is beyond the scope of this thesis, we will focus on investigating the literature on the second scenario. There are a variety of existing dynamic eco-driving models that differ in their conceptual design, problem solution formulation (including mathematical formulation, interacting modules, input space, and more), and the energy and traffic models used to translate the eco-driving service to energy and vehicle dynamics [104]. In the early models of dynamic eco-driving, the fuel-optimal speed trajectory is estimated and advised using the equipped vehicle's dynamic status, location information, and SPaT data. For instance, Mandava et.al [17] proposed arterial velocity planning, which aimed to maximize the probability of encountering a green light when approaching a signalized intersection. Building on this concept, Barth. et. al [24] developed the model further to estimate energy-efficient (de)acceleration profiles based on remaining green/red time and distance between the vehicle and intersection. However, despite the aforementioned models considering similar inputs for fuel-optimal speed profile estimation, they used different methodologies to process inputs, and all their assumptions were based on the absence of other surrounding traffic interference.

Next, to account for the impact of other surrounding traffic factors, the concept design of the eco-driving strategy was adjusted to consider queue discharge information and the status of the preceding vehicle. So in order to implement the advice speed in actual complex traffic conditions, the authors [20] proposed the Predictive Cruise Control (PCC) model, which minimized travel time under both free-flow and stop-and-go traffic conditions while providing energy-efficient (de)acceleration strategies. In addition to traffic signal and preceding vehicle factors, Queue Length Estimation (QLE) techniques, which are based on commonly installed induction loop sensor systems, help the predictive speed assistance system to show fuel savings of 8–11% [28]. Similar research can be found in [34, 44, 54].

Although V2I technology has made it easier to obtain real-time SPaT information on signalized intersections with pre-timed signal control, the use of accurate future SPaT information is challenging in practice due to time drift in pre-timed traffic signals and fluctuations in the traffic environment. To address this challenge, probabilistic signal timing information has been designed based on real-time SPaT data and historically averaged

timing data per signal status [31]. For instance, Green Light Optimized Speed Advisory (GLOSA) has been enabled for fully and semi-adaptive traffic lights using empirical signal and detector data as a solution developed from a traffic signal control perspective [43]. And from another perspective of the transportation system, vehicle control, the eco-driving problem for CAVs has been formulated as a data-driven chance-constrained robust optimization problem, and DP has been employed to solve the optimization problem in order to improve the controller's robustness in the face of uncertain signal timing with/without the distribution of the random variable [92, 106]. Despite these developments, obtaining precise and accurate future SPaT information remains challenging due to technological barriers and the dynamic operation of actuated coordinated, and adaptive traffic signals. However, as CAV driving technology continues to develop, new possibilities may open up to address this challenge.

Last but not least, the dynamic eco-driving control for platoons of vehicles at signalized intersections, the concept has attracted the interest of some researchers. One of the main methods to solve the effects of platooning is by accurately identifying the leading vehicles of each phase and giving slightly different advice to each vehicle in the platoon. For example, in [51], the algorithm is designed to account for real-time signal information and traffic conditions, and group vehicles into platoons based on their permutations, and the simulation results significantly reduce fuel consumption and emissions, while also minimizing travel time and improving traffic flow. Similarly, [76] develops algorithms by characterizing the optimal speed profiles for platoon-based optimization and highlights the importance of accurately estimating the vehicle's position and speed again, especially for platooning scenarios. In addition to the homogeneous CAV fleet, the heterogeneous traffic flow, including both CAVs and human-driven vehicles (HDVs), is also a hot issue that needs to be addressed urgently, in [117], where a suggestion-based control framework based on MPC is proposed to optimize fuel efficiency in heterogeneous urban traffic, the authors considered the recommended velocity from CAVs are non-binding with HDVs, which means the driver of HDV can choose to follow or not to follow the suggested velocity. In the simulation, this assumption is expressed as a certain probability $\beta$. At last, the simulation results show the proposed control strategy's efficacy. Even though research on dynamic eco-driving for platoons has received limited attention so far, it provides a basis for significantly improving the energy-saving and emission-reduction potential of existing models.

Here conclude the main elements for developing eco-driving models near the signalized intersections:

- Optimization problem formulation and methods

  Most proposed eco-driving systems employ mathematical programming to estimate optimal speed profiles for energy and/or traffic efficiency objectives. These objectives include improving energy efficiency (minimizing vehicle tractive force/fuel

consumption [34, 54, 68]), traffic efficiency (minimize idling time [24, 20, 53]), or a combination of safety, energy consumption, emissions, and traffic flow efficient objectives [98, 106, 117]. Generally speaking, for models that incorporate a fuel consumption model, energy efficiency calculations are integrated with optimal problem solutions. While for others, speed trajectories are derived from simulation tools and input into fuel consumption and emissions models. At the same time, various optimization frameworks have been proposed for different objectives, such as MPC approaches based on trip time and kinetic energy loss [20], fuel-optimal speed profiles estimation based on a linear combination of traffic efficiency and emissions [44], and optimal controllers based on the formation of tight and fast-moving platoons for fuel efficiency optimization [68].

- Analysis boundary

  The analysis boundary for a dynamic eco-driving system typically includes the area of the road network where the system can affect CAVs. This area comprises both the upstream road section leading to the signalized intersection and the downstream section where benefits of eco-driving strategies [104].

- Vehicle dynamic model and energy model

  In many research works, constant acceleration [17, 44, 34] and non-linear acceleration models [7, 98] were considered and adopted to estimate optimal speed profiles for eco-driving strategy. Besides these traditional vehicle dynamics models, trigonometric functions were developed to replicate the increase/decrease of an equipped vehicle speed profile while considering the comfortable objective in [24]. These vehicle models are employed to depict the progression of a vehicle's speed from the current speed to the target speed, and eventually to the desired speed. Regarding the energy models, they can be classified based on their transparency into white-box, grey-box, and black-box models, according to [64]. White-box models are constructed based on the physical or chemical processes of the engine, black-box models treat the entire vehicle or the engine alone as a black box, and grey-box models are the most suitable energy models for evaluating eco-routing and eco-driving systems because its balance between accuracy and simplicity.

Furthermore, the efficiency of CAV operation depends heavily on the drivers'compliance, if drivers do not follow the recommended speed advice by CAV technology, the benefits of the system will reduce a lot, but the human-related factor is so unpredictable in reality, as the human can be influenced on so many factors, like personal traits, cognitive and psychomotor functions, situational factors, acceptance and trust [91], which now is gradually become an important topic and will get more attention. In the following section, we will analyze deeper into the integration of eco-driving strategies with energy management systems for hybrid and plug-in hybrid vehicles. By doing so, we aim to explore the poten-

tial synergies and opportunities for improvement in both environmental sustainability and energy efficiency.

### 1.2.3/ CO-OPTIMIZATION OF ECO-DRIVING STRATEGY AND EMS FOR HEV/PHEVS

As mentioned earlier, the integration of eco-driving and EMSs of HEV/PHEVsis essential for enhancing the energy-saving and environmental-friendly potential of vehicular traffic. The effectiveness of EMSs depends on predicting future states of vehicular traffic, like velocity and surrounding traffic information, these data can be partially obtained through ITS technology. As a result, co-optimization of eco-driving strategy and EMS for HEV/PHEVs further developed. Current literature can be classified into two categories based on different scenarios, namely single-vehicle, double/multi-vehicle scenarios.

#### 1.2.3.1/ SINGLE-VEHICLE SCENARIO

In the past decade, most research literature in the cooperative optimization of eco-driving and energy management systems (EMS) for HEV/PHEVs focuses on the single-vehicle scenario, where the most valued target is to optimize the power split considering traffic or road information and progressively taking the safety constraints into account, but rarely considering other vehicle's interactions, like overtaking and lane-changing.

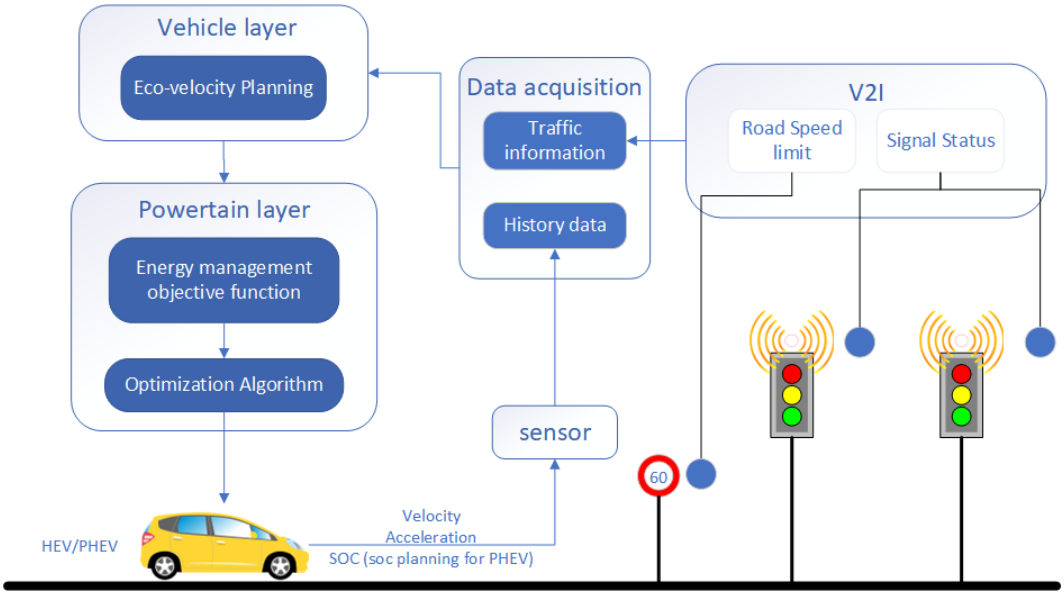


Figure 1.5: The Scenario of Single-Vehicle, cooperative optimization logic based on V2I information

- Cooperative Optimization for HEV

In most cases, the cooperative optimization framework for HEV is normally designed to minimize energy consumption by optimizing velocity trajectories first, then the power split is optimized by tracking the optimal velocity provided recommended by the eco-velocity planning system, as the Fig.**??** shows, the main idea is based on a two-level framework, consisting of the vehicle level and the powertrain level. However, the complex nature of driving in real-world scenarios makes it impractical to optimize the entire velocity trajectory. Therefore, the analysis boundary is typically restricted near to the intersection, allowing better integration of EMS with the traffic and road conditions such as SPAT information and speed limits. Numerous methods have been proposed to tackle the two-layer problem. For instance, if only considering one signalized intersection, [58] decomposes the hybrid optimal problem into two subproblems. First, the optimal velocity trajectory is computed by solving a nonlinear time-varying optimal problem using the Krylov subspace method to improve computational efficiency. Second, the optimal torque split ratio and gear shift schedule are determined by combining Pontryagin's minimum principle (PMP) and numerical methods in the bi-level MPC framework. While considering continuous intersections, [69] introduces a novel cooperative optimization framework for HEVs, similarly, which is designed to minimize energy consumption by optimizing velocity trajectories first, then optimizing the power split based on a genetic algorithm to solve the complex fuel consumption model of HEVs. Simulation results of the proposed optimal speed algorithm are compared to the results of a real driving test and a single-intersection optimization algorithm. These comparisons show that the proposed strategy is more effective in reducing fuel consumption and intersection passing time. Finally, an example of considering as many real traffic scenarios as possible, [108] developed an MPC-based strategy that fully considered the three main objectives: safe driving, energy management, and exhaust emission reduction. To address these objectives, the study designed a driving scenario classifier to determine the corresponding vehicle mode. And the simulation was conducted in a realistic urban traffic environment by using Simulation of Urban MObility (SUMO), and the results demonstrated that the proposed strategy guaranteed safe driving throughout the entire trip, reduced fuel consumption and exhaust emissions, and kept the battery in a healthy SOC range. The study showed the effectiveness and robustness of the proposed strategy for potential online applications.

The studies mentioned above focus on the intersection as a specific scenario and determine the constraints based on the real-time state of the signalized intersection. However, there is another way of considering the signalized intersection scenario that includes their possible encounters in the uncertainty of future traffic information. One such approach is proposed by [115], which uses a novel statistical traffic model to generate stochastic driving behavior and formulates the EMS of HEV as a bi-level hierarchical optimization problem. This formulation leads to an effective upper-level problem that can be solved online as a global optimization using a low-

dimension deterministic DP and can be optimized offline using Stochastic Dynamic Programming (SDP), which is embedded with stochastic traffic behavior in the lower level. Simulation results show reasonable over-consumption compared to deterministic optimization and manageable computational times for both offline and online parts. Another recent work by [124] proposes an adaptive co-optimization method of speed planning and EMS with dynamic probabilistic constraints. The proposed composite sequence generation model enables dynamic probabilistic constraints by predicting the future speed distribution of the preceding vehicle based on the probability relationship among future speed sequence, historical speed sequence, and macroscopic traffic state of downstream road segments. This effectively models the macro and micro disturbance from a random traffic environment and improves the prediction accuracy by about 10% compared to pure sequence generation models, with over a 57% decrease in distribution divergence. Simulation results indicate a 14.81% increase in driving safety and relatively high energy efficiency compared to existing co-optimization methods under the same car-following tasks.

- Cooperative Optimization for PHEV

  Compared with HEV's cooperative optimization, PHEVs differ only by an additional degree of freedom, which corresponds to the ability to deplete the battery for electric traction and recharge the battery pack, whereas the PHEV's EMS will be more complicated because the SOC planning for PHEV is hoped for battery depletion during a journey [8]. To tackle this challenge, typical work such as [72] has integrated an eco-driving assistance system with the co-optimization of vehicle dynamics and powertrain operations. In this approach, the vehicle dynamic optimization is approximated using the trigonometric speed profile, and the powertrain operation optimization is formulated as a nonlinear constrained optimization problem, which is solved using Mixed Integer Nonlinear Programming (MINP). The performance of the proposed system is evaluated at different vehicle automation levels and achieves an average 24% fuel savings for typical urban driving conditions. [96, 97] present the design of an ecological adaptive cruise controller (ECO-ACC) for PHEV considering a deterministic traffic signal phase and timing (SPaT) over the entire route, the hardware-in-the-loop (HIL) simulation results validate the energy savings of the receding-horizon control framework in various traffic scenarios. As the machine learning methods introduced, [110] propose an innovative deep learning-based queue-aware eco-approach and departure (DLQ-EAD) system for a Plug-in Hybrid Electric Bus (PHEB), which is able to provide an online optimal trajectory for the vehicle considering both the downstream traffic condition (i.e. traffic lights, queues) and the vehicle powertrain efficiency. The simulation shows that the proposed DLQ-EAD can achieve 18.7%-24.0% energy efficiency improvements for a single PHEB on various traffic congestion levels. In addition, back to the traditional optimization methods, like mentioned in the previous HEV part, many studies

[36, 30, 77, 82] did not deal with the signalized intersection as a special scenario, proposed the eco-driving base EMS for PHEV based on a velocity optimization algorithm by utilizing the velocity bounds via V2V and V2I communication, and the power split of connected PHEVs and fuel economy can be optimized over a given prediction horizon. Generally, the first step is to plan a global optimal SOC trajectory with the available traffic information. Then fuel economy is further improved by optimizing the velocity and power split at different levels. However, the driver's behavior in this type of method is often ignored in the simulation results, the performance is dependent on the driver's behavior in real conditions.

The analysis of single-vehicle scenarios in HEV and PHEV has demonstrated that cooperative optimization strategies can play a crucial role in shaping future green transportation. As we continue to advance our understanding of double/multi-vehicle scenarios, the lessons we will learn from these optimization strategies will pave the way for a more sustainable, efficient, and environmentally friendly transportation ecosystem.

#### 1.2.3.2/ DOUBLE/MULTI-VEHICLE SCENARIO

The previous subsections concluded the integration of ITS information and EMS of single-vehicle scenarios, these ideas can also be applied to double/multi HEV/PHEVs to further enhance overall performance or for a fleet with regards to fuel economy and traffic efficiency.

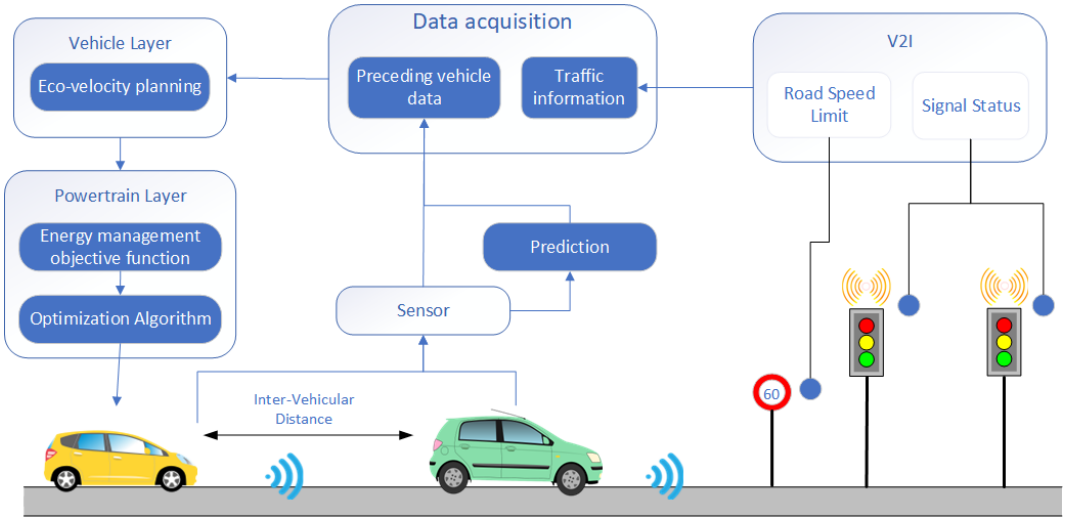


Figure 1.6: The Scenario of Double-Vehicle considering the safety constraints with preceding vehicle

- Double-Vehicle Scenario

  The advent of ITS technology has made it more convenient to acquire V2I/V2V information about the surrounding traffic. In the double-vehicle scenario, cooperative

optimization is typically carried out using a car-following model that takes into account the interaction between the two vehicles in order to balance fuel economy and safety. According to [102], two categories of strategies can be distinguished for double-vehicle scenario optimization. The first category is mainly based on Adaptive Cruise Control (ACC) systems, which aim to increase driving comfort, reduce traffic accidents, and improve traffic flow throughput[3]. Instead of the safety and traffic efficiency objectives, the integration of ACC and EMS means the optimization of them simultaneously, adding the target to improve fuel economy. In the car-following scenarios, the velocity of the preceding vehicle has a great impact on the following vehicle as an input for devising the following vehicle's EMS. A typical example is [55], the authors developed an ACC system based on a nonlinear MPC for intelligent HEVs that simultaneously considers traffic safety, fuel economy, and ride comfort to enhance energy efficiency and control system integration. However, this combination of ACC and EMS is usually carried out by predefining the preceding vehicle's velocity, which can be done by following certain rules. A similar work is [90], an adaptive tube-based nonlinear model predictive control (AT-NMPC) approach is introduced for designing autonomous cruise control systems, which guarantees robust satisfaction of the specified constraints, even in the presence of uncertainties and enhances the system's performance by adapting to changes in the vehicle control-oriented model. Using a different approach in [87], an ecological ACC based on motion-dependent heuristic dynamic programming is developed to achieve multi-objective optimization. As Fig.1.6 illustrated, the aforementioned point about the pre-defining velocity of the preceding vehicle based on traffic light time when a signalized intersection is taken into account, and the second category is based on Predictive Cruise Control (PCC). EMSs utilizing PCC are designed to make the most of future information by predicting the velocity of the preceding vehicle and using a predictive control algorithm to determine the optimal velocity and power split for the subject vehicle considering the traffic disturbances [19]. Specifically, the PCC-based EMSs are designed with the goal of maximizing the use of future information, achieved through the prediction of the preceding vehicle's velocity. An example is [46], which suggests an estimation method based on actual and past inter-vehicle distance data and information on traffic and upcoming traffic lights, employing a set of nonlinear, autoregressive (NARX) models to predict traffic behavior, using cooperative adaptive cruise controller (CACC) to achieve better fuel economy because of the advantages of information prediction. Moreover, some machine learning methods are introduced to the part of the preceding vehicle's prediction due to the complexity and stochastic of dynamic traffic, such as the Bayes network model used in [79], which shows a better prediction performance than the "constant acceleration" and "constant velocity" methods. Gaussian Process model is used in [88], which predicts leading vehicle velocity based on time series data and mean traffic flow speed drawn from cloud data. By the way, these machine-learning

methods can also be leveraged to optimize complex systems with inconsistent objectives and stringent constraints. For example, [121] integrated completely ACC and EMS, proposed Deep Deterministic Policy Gradient-based ECOlogical driving strategy (DDPG-ECO) based on deep reinforcement learning, the weights of multiple objectives are analyzed to optimize the training results, simulation results showed that the DDPG-ECO approach achieved over 90% of the performance of DP-based methods, while also ensuring good car-following performance. In conclusion, the integration of ACC and EMS aims to reduce fuel consumption by using specific driving cycles to approximate the velocity of the preceding vehicle, without taking into account dynamic driving conditions. On the other hand, the integration of PCC and EMS more focus on predicting preceding vehicles' state through dynamic traffic information, further improving fuel economy. Both approaches prioritize safety and fuel economy in optimizing controls.

- Multi-Vehicle Scenario

  In the multi-vehicle scenario, which has the potential to reduce air resistance for each vehicle and in turn, can increase road capacity, reduce fuel consumption, and improve road safety [103]. Therefore, there has been increased attention on the cooperative optimization of EMSs and eco-driving for HEV/PHEVs platoon and making great efforts towards proposing holistic approaches in this area. The most classic framework as shown in Fig.1.7, which is presented in [59, 73], is a hierarchical energy management control strategy for a group of connected HEVs. At the higher level, MPC is used to incorporate SPAT information to predict the optimal velocity profile over a finite time horizon. At the lower level, the adaptive ECMS and DP are used separately controllers to achieve power distribution by tracking the optimal speed of each HEV's higher-level controller. The effectiveness of the proposed control strategy is validated through simulation results. However, it should be noted that the propulsion and recuperation efficiencies of HEVs are considered to be constant in this work. To reflect operating characteristics precisely, [101] considers the efficiency feedback of the two characters based on the above hierarchical energy management control strategy. The fuel economy of the system can be improved, and additional benefits can be achieved by synergizing the reduction of red light stopping, collision avoidance, and cooperative platoon information. Around the same time, [109] proposed a real-time MPC scheme for connected HEVs that relies on look-ahead traffic information, a chain GP-based predictor is utilized to obtain the preceding vehicle's speed, assuming that the vehicle aims to maintain an average speed that is reflected through the traffic density. The simulation results show that the proposed method can avoid violations of the spacing corridor to ensure traffic safety, and reduce energy consumption without requiring significant emergency acceleration or braking behavior. Moreover, several related works such as [70, 85, 112] have confirmed the fuel-saving potential in platoons of HEV/PHEVs.

However, optimizing the control strategy for a platoon and EMS of each HEV simultaneously can be challenging due to the highly coupled nature of the nonlinear augmented system. Most current literature assumes a perfectly homogeneous traffic flow, overlooking human-related factors. As heterogeneous traffic flow becomes more prevalent in multi-vehicle scenarios in the near future, it will further increase the complexity of traffic conditions, posing a more significant challenge to improving both the mobility of the traffic system and fuel economy.

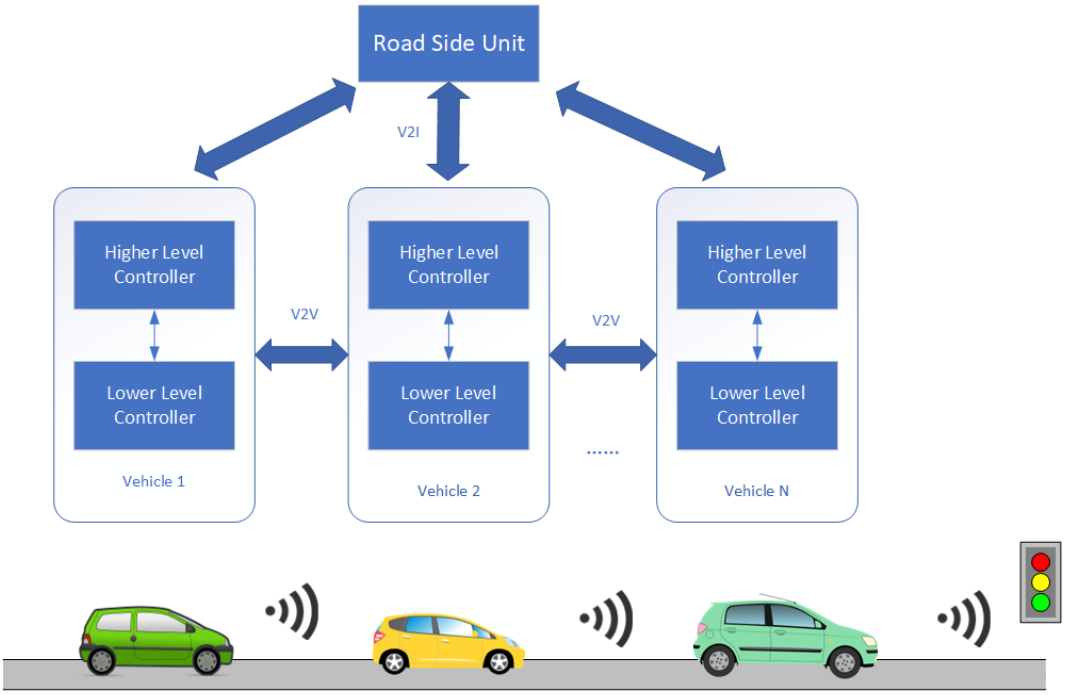


Figure 1.7: The Hierarchical Control Framework of Multi-Vehicle Scenario

## 1.3/ CONCLUSION AND OBJECTIVE OF THE THESIS

As seen from the review of existing EMS, eco-driving strategies, and cooperative optimization of EMS and eco-driving strategies, EMS approaches typically require driving conditions when applied to real vehicles. This is because real-time power demand directly impacts the power distribution and energy consumption calculations of the energy management system, which in turn affect other performance aspects such as vehicle comfort and emissions. Given the mutual coupling characteristics of humans, vehicles, and the environment, driving conditions are primarily influenced by drivers and surrounding traffic.

Generally, there are two ways to obtain driving information: one is through applying various prediction algorithms to forecast future working conditions based on historical data analysis, and the other is by integrating ITS, which includes road load sensing units and moving edge computing units. The ITS background provides an effective application

framework for energy management strategies that integrate traffic information into vehicle control systems. This involves obtaining traffic data outside the driver's visual range through sensors or ITS, increasing the vehicle's perception range, and combining historical driving condition information recorded by on-board VCUs. During this process, eco-driving strategies optimize traffic perspectives, and these two techniques will be seamlessly integrated within the future ITS context.

However, there are still challenges to be addressed in the transition period, for example, a typical problem that need to face is the heterogeneous traffic environment. The automobiles could be categorized Human-Driven Vehicles (HDVs), connected PEV/HEV/PHEVs in the near future, the mixed traffic streams will face heterogeneous dynamics and stability. The control problem for this must respond effectively to re al-world traffic conditions while maintaining string stability to ensure safe transitional platoon maneuvers. In addition to meeting queue control requirements, another issue that deserves consideration is the interaction with HDV. In realistic traffic conditions, lane-changing and merging maneuvers posed by human occur frequently. How do we deal with the traffic risks associated with the uncertainty of human behavior is also a question worthy of in-depth study.

Therefore, to lay the foundation for solving these complex problems, three main tasks have been undertaken as follows.

- A deterministic data-based eco-driving strategy for a PHEB is proposed that aims to reduce energy consumption and save time. By simplifying the 3D-DP problem to a 2D-DP method and utilizing a DP framework, our approach led to a 3.98% energy reduction and 4.84% time saving in simulations.
- A stochastic data-based eco-driving system is developed for power-split HEVs, focusing on co-optimizing vehicle dynamics and hybrid powertrain operations. Our dual-driven approach in the eco-driving decision subsystem and rule-based strategy in the hybrid powertrain control subsystem led to energy reductions of 6.49% and 4.17% in SUMO traffic simulations. The system's independence from full traffic infrastructure connectivity and adaptability to various traffic environments make it could be a promising solution for future intelligent transportation systems.
- A data-driven trajectory planning strategy for connected vehicles is introduced for addressing uncertainty in shared traffic information. The proposed approach effectively improved fuel economy, as demonstrated using the real-world Next Generation SIMulation (NGSIM) dataset.

# 2

# A DETERMINISTIC DATA-BASED ECO-DRIVING STRATEGY

## 2.1/ INTRODUCTION

In general, the intersection is an area of concern for researchers, according to [23], fuel reduction of approximately 22% could be obtained by receiving phase-shifting information of the traffic lights and computing the optimal velocity in advance. In addition, bus-stops are the similar area with intersections, we can think of it as a signalized intersection that is always in a red-light period when buses arrive.

The rapid development of ITS provides huge opportunities to improve the overall performance of Energy Management Strategies (EMS) for Connected and Automated Hybrid Electrical Vehicles (CAHEVs). In this context, Plug-in Hybrid Electrical Bus (PHEB) as a suitable public transportation attracts researcher's attention. Normally, the researchers achieve the purpose of reducing fuel consumption and being environment friendly by planning the trajectory of the subject vehicle, which is defined as a vehicle trajectory optimization problem. But we need to consider more information for PHEB ,the powertrain operation is considered as the first dimension–EMS, which is complicated as there are two energy sources flow and we want to use electric as much as possible in order to ensure the low cost of energy consumption. And the other dimension-vehicle (longitudinal) dynamic optimization, which is gradually become possible by connected traffic information. Therefore, based on the above background, as we try to simplify the first eco-driving strategy problem for CAHEV as much as possible, a specific example of velocity planning problem for a series PHEB on a fixed route with signalized intersections is modeled and simulated in this chapter. The objective is to minimize energy consumption or travel time under the premise of safety and we treat this problem as a spatial optimization formulation and via Dynamic Programming (DP) to solve.

This chapter is organized as follows. Section 2.2 represents the PHEB vehicle modeling and its components modeling. The fixed traffic signal is presented using mathematical model in Section 2.3. Section 2.4 introduce the dynamic programming and the calculation

steps. Then based on the DP framework, the velocity planning problem considering the fixed traffic signals constraints is formulated in the section 2.5. The section 2.6 illustrate the method that constructed 3 Dimensional (3D)-DP, and simplified 3D-DP to 2D-DP by adopting empirically optimal SOC. Finally, section 2.7 presents the simulation results that consists of SOC optimization under a standard driving cycle and velocity optimization under an actual bus route condition and section 2.8 conclude this chapter.

## 2.2/ PHEB VEHICLE MODELING

In the contemporary automotive industry and transportation research, numerical simulation of vehicles using mathematical models has become a standard method for evaluating energy consumption. Generally, the numerical method is widely applicable, and there are two common approaches to the describe vehicle simulation process, namely ”backward” simulation and ”forward” simulation [40], which can greatly affect the behavior of the model. In the backward scheme, a target speed is provided by a driving cycle and the necessary propulsion force is calculated from Newton’s second law. The vehicle speed and the calculated propulsion force are then propagated from the vehicle model, through the transmission model, and to the prime mover where the required input power for the engine model is determined. This approach is referred to as backward because the data flows backwards through the powertrain, as depicted in Fig.2.1b. While in the forward scheme, a target speed is similarly provided by a driving cycle, but it passes through a driver model, the driver controls the longitudinal vehicle interfaces such as the accelerator and brake pedals based on the difference between the target and the actual vehicle speed. The engine torque is propagated forward through the transmission model to the vehicle model; where the traction sustains the propulsion force. Again, Newton’s second law provides the vehicle acceleration which is integrated for speed and position. The position is fed back to the driving cycle to find a target speed, which closes the computation loop. The effort flows in the opposite direction in the powertrain compared to the backward method and the approach is therefore called forward. Both schemes are commonly used in science and engineering. The backward method is often used when treating control problems, for example optimal control of battery management or finding the best configuration. And forward simulation is more common when predicting the influence from the environment, when the driver impact is of concern, or when investigating specific components [105]. Therefore, the backward simulation is chosen for the following study in this chapter.

### 2.2.1/ VEHICLE MODEL

In this chapter, a series PHEB is chosen as the research subject, as indicated by Fig. 2.2, the PHEB powertrain has four main parts, including the battery part that can be external

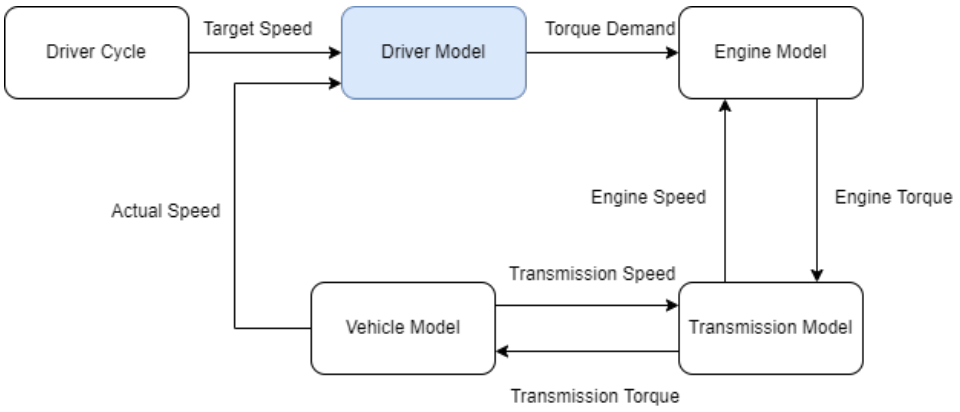


(a) Forward (dynamic) vehicle simulation

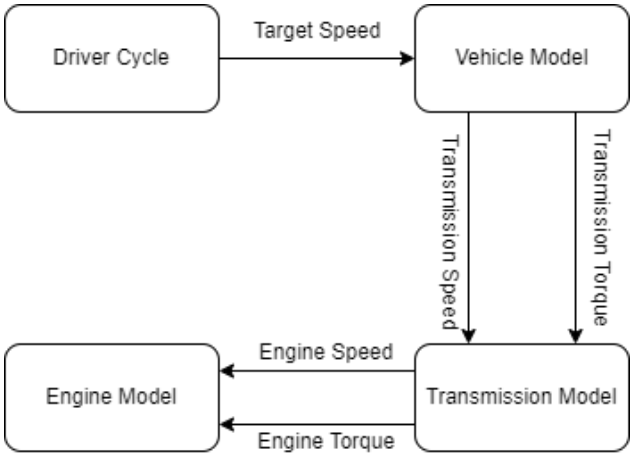


(b) Backward (quasi-static) vehicle simulation

Figure 2.1: Vehicle simulation process classification, source:[40]

recharge, the Auxiliary Power Unit (APU) consists of an Internal Combustion Engine (ICE) and an Integrated Starter Generator (ISG), the final drive by dual motor connected to the rear wheel, the high voltage control unit consists of generator controller and a drive motor controller. As the series structure indicated in the chapter 1, the mechanical energy is convert to electrical energy through the ISG and the wheel motor is driven to meet the vehicle running demand to keep the vehicle running normally. Some vehicle characteristics of PHEB are shown in TABLE 2.1.

Since our main goal is to improve fuel economy, the lateral dynamic is ignored and the longitudinal dynamic equation [67] models vehicle model that calculated by

$$P_{req} = \frac{v}{3600\eta_T}\left(Gf\cos\alpha + G\sin\alpha + \frac{C_D A V^2}{21.15} + \delta m\frac{dv}{dt}\right) \tag{2.1}$$

where $P_{req}$ is the total power required by vehicle, $G$ is gravity, $\alpha$ is route slope, $v$ and $V$ vehicle speed $(m/s)$ and $(km/h)$, $f$ is rolling friction coefficient.

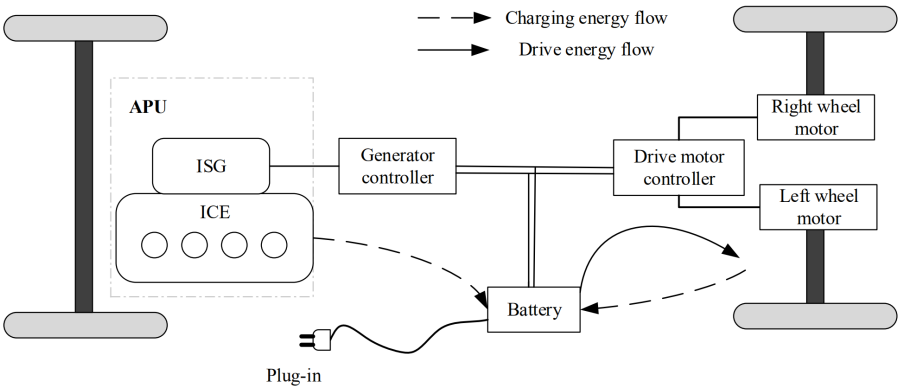


Figure 2.2: PHEB powertrain architecture

Table 2.1: Vehicle Parameters

| | Parameter | Mark | Value |
|---|---|---|---|
| Vehicle | Vehicle mass | $m(kg)$ | 14500 |
| | Air drag coefficient | $C_D$ | 0.65 |
| | Front area | $A(m^2)$ | 8 |
| | Transmission efficiency | $\eta_T$ | 0.97 |
| | Rotational mass coefficient | $\delta$ | 1.07 |
| Battery | Open circuit voltage | $V_{oc}(V)$ | 340 |
| | Capacity | $Q_b(Ah)$ | 180 |

## 2.2.2/ POWERTRAIN MODEL

### 2.2.2.1/ APU MODEL

As mentioned before, APU consists of an IC Engine and an IS Generator (ISG), therefore, to model the APU part, we first model the engine and generator separately, and according to the different principles, this modeling process can be divided into two categories: theoretical and experimental modeling. Theoretical modeling is based on a detailed analysis of the internal characteristics and operating processes, which can accurately describe the operating states, but there are disadvantages such as complicated model construction, some parameters are hard to get and low time efficiency for simulation. As a result, the experimental modeling is generally used for simulation, which is based on experimental data and often ignored the internal working process, established the mapping relationship between the performance parameters, and then extends the non-test points by using data interpolation. Then a table look-up is applied in the simulation process, it does not reflect the transient operating characteristics but is simple to implement and time efficient for simulation studies. The Fig.2.3 shows the ICE and ISG 3D maps based on the experimental modeling respectively. The fuel consumption efficiency of ICE at different speeds and torque is shown in Eq.2.2, similarly, Eq.2.3 represents the ISG experimental model-

ing.

$$m_f = f(n_e, T_e) \tag{2.2}$$

where $n_e$ is the ICE speed (RPM), $T_e$ is the output torque of the ICE (Nm), $m_f$ is the fuel consumption rate (g/kWh), $f$ is the mapping between engine speed, torque and fuel consumption rate.

$$\eta = f(n_m, T_m) \tag{2.3}$$

where $n_m$ is the ISG speed, $T_m$ is the motor torque, whose positive and negative values represent the two operating states of motor and generator respectively. $\eta$ is the ISG efficiency, $f$ is the function which described the relationship between speed, torque and efficiency.

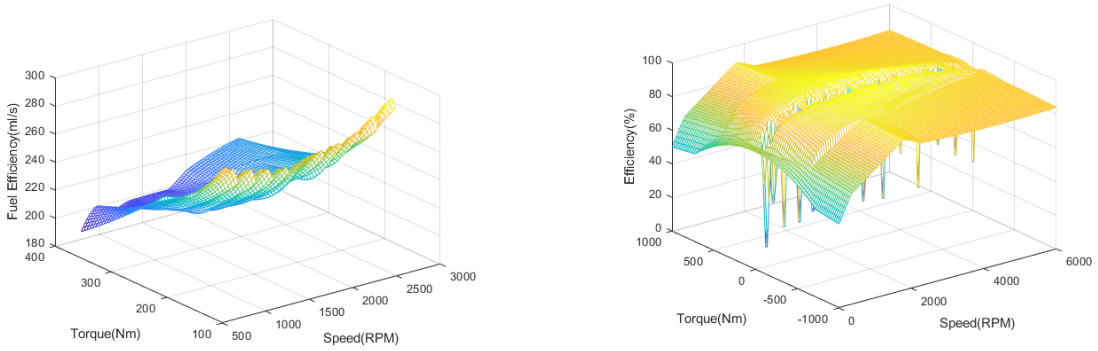


(a) ICE 3D map

(b) ISG 3D map

Figure 2.3: 3Dmap

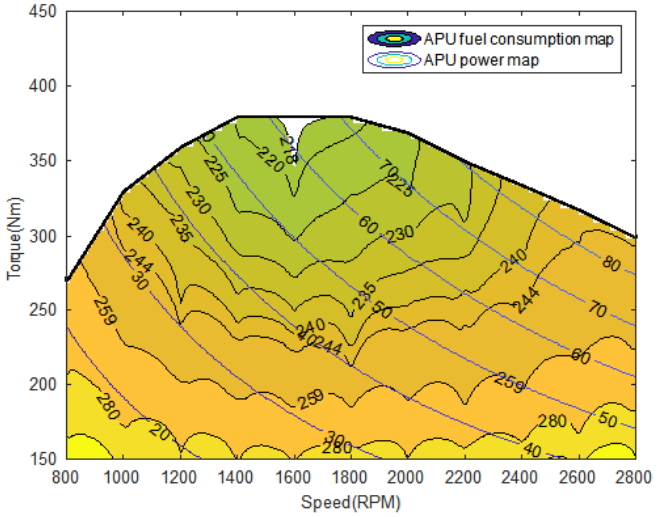


Figure 2.4: APU map

From the Fig.2.2, the direct connection of ICE and ISG is considered as APU module and

the fuel consumption rate of APU can be calculated by the ratio of fuel efficiency of the ICE to the efficiency of the ISG for a combination of speed and torque by discrete the engine speed and torque and the generator speed and torque into several values within a certain range. As a result, fig. 2.4 shows the power map and fuel consumption map of APU.

Next, as we all know, if the engine is defined to operate at its optimal operating point during the control process, excess energy loss can be effectively avoided. Similar to the above method, the output power of the APU can be found for a combination of speed-torque by discretizing the engine speed-torque and generator speed-torque and combining them with the motor efficiency. In this case, if the output power is known, interpolate the torque for each APU speed to get the corresponding fuel consumption rate, and then find the operating point with the lowest fuel consumption, which is the optimal operating point of the APU for that output power. The red line in fig.2.5a represents the optimal operating point of the APU.

By replacing the vertical coordinate in fig.2.5a with the fuel consumption rate, the minimum fuel consumption rate is obtained for different discrete values of the APU's output power, and the curve in fig.2.5b is called the minimum fuel consumption curve for the APU's equal power. In the subsequent calculation, the default APU operating point is always located on the minimum fuel consumption curve.

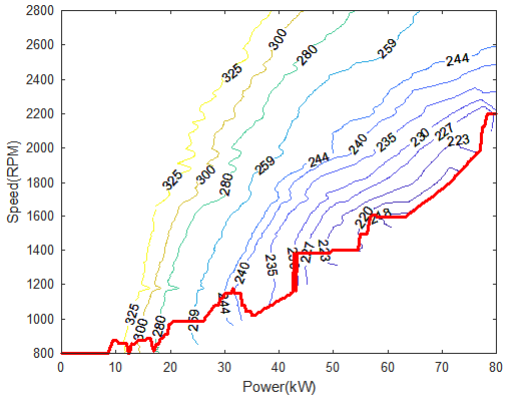


(a) APU optimal operating points

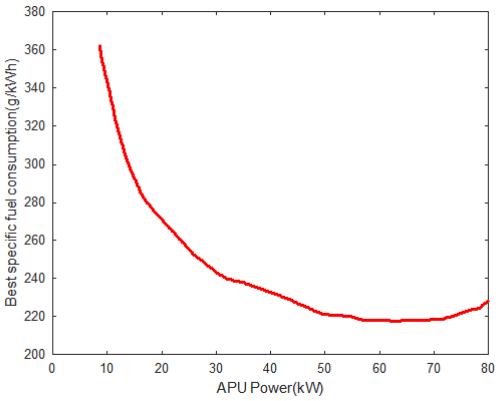


(b) APU minimum fuel consumption curve

### 2.2.2.2/ WHEEL-SIDE DRIVE MOTOR MODEL

Similar to the ISG model, the wheel-side drive motor still uses experimental model. However, the wheel-side drive motor is direct source power transmission, its operation mode is divided into two types: on charge mode and discharge mode. In the series PHEB architecture, it can provide driving torque on discharge mode and it can also act as a generator on charge mode during regenerative braking state, converting mechanical en-

ergy into electrical energy and storing it in the battery to increase the distance range. And to taking into account of battery life, we set the maximum reused electrical energy as 30kW. So the output power of wheel-side drive motor $P_m$ can be written as

$$P_m = \begin{cases} P_{req}/eff_m & P_{req} \geq 0 \\ \max\left(P_{req} \cdot eff_m, -30\right) & P_{req} < 0 \end{cases} \tag{2.4}$$

where$P_{req}$ is the vehicle required power that calculated by Eq.2.1, $eff_m$ is the efficiency of the wheel-side drive motor, it can be calculated through Fig. 2.6.

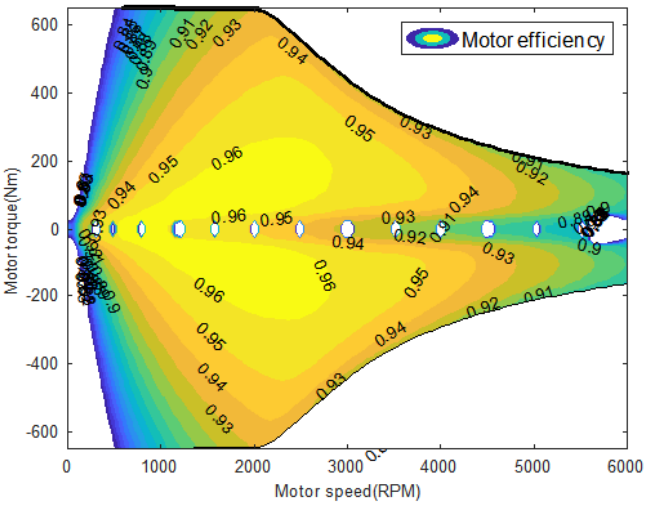


Figure 2.6: Motor efficiency map

### 2.2.2.3/ BATTERY MODEL

Another important component of the PHEB is the power battery, the structure of its composition is in the form of Cell-Battery-Pack. The voltage of the power cell is 3.2$V$ and the nominal capacity is 2.3 $Ah$. Then 78 cells are connected in parallel to form a power battery with total capacity of 180 $Ah$. Finally, 100 power battery are connected in series to form a power pack with a total output voltage of 340V and a total capacity of 180Ah. In the simulation, the inconsistency of battery is ignored and the internal resistance and open circuit voltage of battery are assumed to be the same, so the charging/discharging characteristic curves with SOC can be obtained as shown in Fig.2.7. As the core energy storage element, the internal chemical reaction is complicated during the charging/discharging process. To describe the battery model as simple and accurate as possible, the widely used equivalent electrical circuit is established for simulate, as Fig.2.8 indicated. And

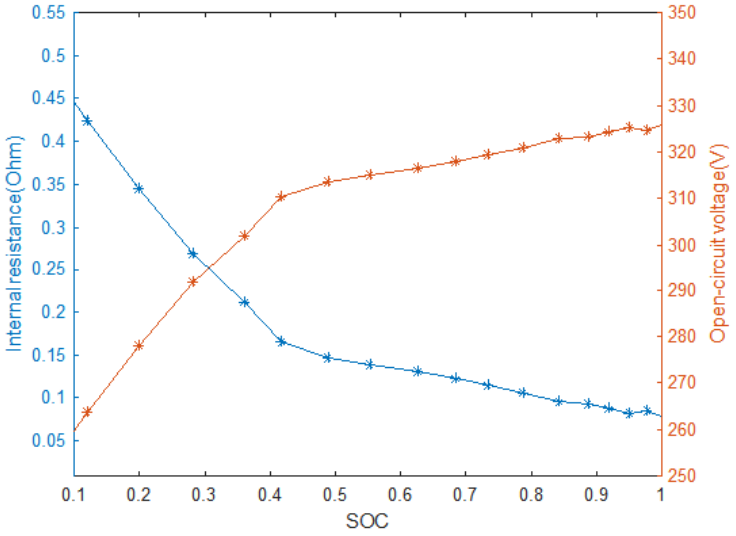


Figure 2.7: Open-circuit voltage and internal resistance

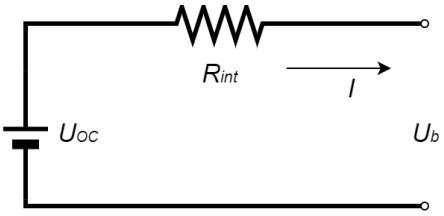


Figure 2.8: Equivalent electrical circuit

based on the $R_{int}$ internal resistance equivalent circuit, there is,

$$\begin{cases} V_{oc} = n \cdot U_{oc} \\ R_b = n \cdot R_{\text{int}} \\ U_b = V_{oc} - I \cdot R_b \\ 1000 \cdot P_b = I \cdot U_b \end{cases} \tag{2.5}$$

Therefore, $I$ can be calculated,

$$I = \frac{V_{oc} - \sqrt{V_{oc}^2 - 4000 R_b \cdot P_b}}{2R_b} \tag{2.6}$$

where $U_{oc}$ is the open circuit voltage of battery, $V_{oc}$ is the pack voltage, $n = 100$ is the number of battery, $U_b$ is the terminal voltage of battery, $R_{int}$ is the equivalent internal resistance of battery, $R_t$ is the equivalent internal resistance of pack, $I$ is the charging/discharging current, specifying that the current here is positive when discharging and negative when charging. $P_b$ is the output power of pack.

Then according to Coulomb Counting method, the State-Of-Charge of power battery dy-

namics can be expressed as

$$S\dot{O}C = -\frac{I}{Q_b} = -\frac{V_{oc} - \sqrt{{V_{oc}}^2 - 4000 R_b P_b}}{2 Q_b R_b} \tag{2.7}$$

where $Q_b$ is the total power pack capacity.

## 2.3/ Fixed Traffic Signal Modeling

Fixed traffic signs are space indexed and time varying during vehicle driving [92]. We suppose the length of the target driving route is $s_f$ , the position of the i th traffic signal is denoted by $s^i$, therefore

$$s^i \epsilon \left[0, s_f\right] \quad i = \{1, 2, 3, \ldots I\} \tag{2.8}$$

where *I* is total number of traffic signals along the route. It's worth noting that these traffic signs include not only *M* traffic signals but also *N* stops signs, naturally $M + N = I$. In addition, each traffic light has an independent periodic clock. For every intersection, we denote the clock period at intersection *i* as $c_f^i \in R^+$, while the red-light duration is indicated by $c_r^i$,

$$c_r^i \in \left[0, c_f^i\right] \quad i = \{1, 2, 3, \ldots..M\} \tag{2.9}$$

Denote by $c_0^i$ the clock time when the vehicle departs from its origin, and $t_p^i$ is the time at which the subject vehicle passes through the *i*th the intersection in the travelling time domain, the corresponding time in the periodic traffic signal clock timing can be calculated as,

$$c_p^i = \left(c_0^i + t_p^i\right) \bmod c_f^i \quad t \in R^+ \tag{2.10}$$

$c_p^i$ is the vehicle passing time in the signal-cycling clock. According to the basic safety rule, $c_p^i$ has a bound

$$c_p^i > c_f^i \tag{2.11}$$

## 2.4/ Dynamic Programming

Dynamic Programming is a mathematical optimization method that was developed by Richard Bellman in the 1950s and has been applied in numerous fields. Especially for discrete problems, where the dynamic programming method becomes a very useful tool in the absence of analytical mathematics [29]. Its main idea is to simplify a decision by breaking it down into a sequence of decision steps over time, which means sub-problems can be nested recursively inside larger problems, so that can be solved easily. The following part will state the DP algorithm for a basic optimal control problem as an example [106].

Denoting the cost at the $k$th step by $g_k(x_k, u_k)$, the cost function can be summed step by step,

$$J = \sum_{k=0}^{N-1} g_k(x_k, u_k) + g_N(x_N) \tag{2.12}$$

According to Bellman's principle of optimality equation, the objective is to minimize the following cost-to-go function at each stage $k$:

$$\begin{aligned} V_k(x_k) &= \min\{g_k(x_k, u_k) + V_{k+1}(x_{k+1})\} \\ &= \min\{g_k(x_k, u_k) + V_{k+1}(f(x_k, u_k))\} \end{aligned} \tag{2.13}$$

where $V_k(x_k)$ is value function ("cost-to-go" function). It represents the minimum cost from stage $k$ to stage $N$, given that the state is initialized to $x_k$ at stage $k$. And the terminal cost at $k = N$ is given by the boundary,

$$V_N(x_N) = g_N(x_N) \tag{2.14}$$

Assume the optimal control and state variable trajectories for the basic optimal problem are $U^*$ and $X^*$, respectively, then

$$\begin{aligned} U^* &= \left[u_0^*, u_1^*, u_2^*, \ldots, u_{N-1}^*\right]^T \\ X^* &= \left[x_0^*, x_1^*, x_2^*, \ldots, x_N^*\right]^T. \end{aligned} \tag{2.15}$$

Based on the terminal condition, the optimal control policy can be computed by the following backward recursive algorithm starting from step $N-1$ to 0:

$$\begin{aligned} u_k^* = \underset{u_k \in \mathcal{U}_D}{\operatorname{argmin}} &\{g_k(x_k, u_k) + V_{k+1}(f(x_k, u_k))\} \\ &\forall x_k \in \mathcal{X}_D \end{aligned} \tag{2.16}$$

where $\mathcal{U}_D$ and $\mathcal{X}_D$ are the feasible control and state variable constraint sets, $f(x_k, u_k)$ described this basic control system dynamics.

## 2.5/ Problem Formulation

The main objective of the vehicle trajectory optimization is to minimize travel time or energy consumption. For the PHEB, the energy consumption can be computed by fuel consumption and battery consumption respectively (Eq.2.17), while it depends on power splitting between APU model and battery model, the cost function $J$ can be expressed as

$$P_{req} = P_{bat} + P_{apu} \tag{2.17}$$

$$J = \lambda \cdot \sum_{1}^{s_f} \left| m_{fuel}\left(v, P_{apu}, P_{bat}\right) \right| \Delta t + (1-\lambda) \cdot \left| t\left(s_f\right) \right| \tag{2.18}$$

where $\lambda$ is a tuning weight, $s_f$ is the trip distance, $m_{fuel}$ is energy consumption , $v$ is velocity, $P_{apu}$ is APU output power, $P_{bat}$ is power provided by the battery. $\left| t\left(s_f\right) \right|$ is normalized cumulative travel time at destination for making the unit consistent.

First, the velocity, travel time, and state of charge are state variables, the velocity at bus stops is calculated by considering $v(s)$ as a small positive constant.

$$x = [v(s), t(s), SOC] \tag{2.19}$$

$$\frac{dv}{ds}(s) = \frac{a(s)}{v(s)}, \quad \frac{dt}{ds}(s) = \frac{1}{v(s)}, v(s) > 0 \tag{2.20}$$

Next, the APU output power and vehicle acceleration are control variables $u = \left[P_{apu}, a\right]$. Besides, during the calculation, the following vehicle physical constraints should be considered,

$$\begin{gathered} v^{\min} \leq v \leq v^{\max} \\ v(0) = v\left(s^i\right) = v^{\min}(s) \cdots i \in \{1, 2, 3, 4 \ldots N\} \\ a^{\min}(s) \leq a(s) \leq a^{\max}(s) \end{gathered} \tag{2.21}$$

Eq. 2.11 forces buses to pass through signalized intersections only at green-light duration.

Finally, as we treat this problem as a spatial trajectory formulation, a maximum arrival time $t_f$ needs to be imposed at the final stage to balance energy consumption and traveling time.

$$t\left(s_f\right) \leq t_f \tag{2.22}$$

## 2.6/ METHODOLOGY

### 2.6.1/ CONSTRUCTION OF DYNAMIC PROGRAMMING

Global optimization solution is necessary to analyze planning strategy performance. According to the problem formulation, if we gave the current state and traffic signals information can be fully known in advance through V2I technology, which means the red-light duration $c_r^i$ is known and deterministic mathematically. In this case, DP is chosen to solve this deterministic global optimal planning problem. To guarantee the location of bus stop and traffic light, a distance sampling is utilized. Trading off computation complexity and result precision the mesh step is determined to be 1 meter, Fig. 2.9a shows three dimensions(3D)-DP structure diagrams, the process of solving the optimization problem starts from the final stage, and then from the stage that the last stage minus 1 meter, until the entire problem is solved. At each stage, the power distribution between the APU model and the battery model will have a significant impact on the calculation of transfer

function between stages. Therefore, it's essential to optimize the energy management in the transfer function at each step, but this will lead to a computation "dimensional disaster". In order to solve this problem and considering there are generally fixed commuting routes for PHEBs, in other word, drivers are like to face similar traffic situations every day so we can get some empirical EMS results that simplify the 3D-DP to 2D-DP, the Fig. 2.9b described 2D-DP structure.

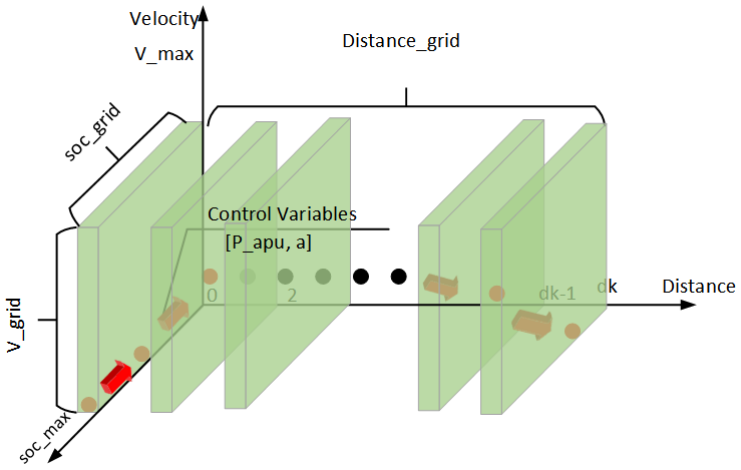


(a) 3D-DP structure diagram

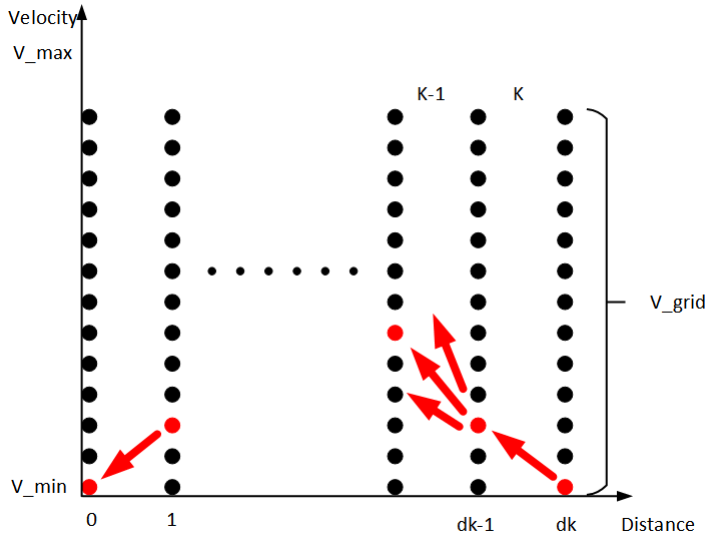


(b) 2D-DP structure diagram

Figure 2.9: Dynamic Programming Construction

### 2.6.2/ SOC BOUNDARIES WITHOUT OPTIMAL VELOCITY PLANNING

Therefore, here we will use the optimal energy contribution results without velocity optimization to substitute these empirical data mentioned in the previous section. The sub-

problem regarding EMS allocation can be described as,

$$J_s = \sum_{k=1}^{N-1} L(x(k), u(k), k)\Delta t = \sum_{k=1}^{N} \left(c_{fuel} P_{apu}(k) + c_{grid} P_{bat}(k)\right) \Delta t \tag{2.23}$$

where $c_{fuel}$ is the current fuel energy price, $c_{bat}$ is the current electricity energy price, and the state variable $x(k)$ in this context represents SOC value and the control variable is $P_{bat}$,

$$V_k(SOC(k)) = \min\left\{(g_k(SOC(k), P_{bat}(k)) + V_{k+1}\left(SOC(k), P_{bat}(k)\right)\right\} \tag{2.24}$$

And the following constraints have to be satisfied,

$$\begin{aligned} P_{apu}^{\min} \leq P_{apu} \leq P_{apu}^{\max} \\ P_{bat}^{\min} \leq P_{bat} \leq P_{bat}^{\max} \\ SOC^{\min} \leq SOC \leq SOC^{\max} \end{aligned} \tag{2.25}$$

$P_{apu}^{\min}$, $P_{apu}^{\max}$, $P_{bat}^{\min}$ and $P_{bat}^{\max}$ are the minimum and maximum output power of APU and battery, respectively. In the calculation process, similar to the above 3D-DP structure, it start from the last stage to find the optimal $J_s$ for each state of each stage recursively, and store them in a data table, then from a given initial state to find the optimal sequence.

## 2.7/ SIMULATION

### 2.7.1/ DP-BASED EMS OPTIMIZATION RESULTS

Before we use the actual road condition to simulate, the PHEB vehicle and powertrain model need to be validate first. Thus, we will use a standard driving cycle to validate the vehicle model for controlling and the sub-optimization model. The Urban Dynamometer Driving Schedule (UDDS) cycle, is also called the US FTP-72 driving cycle, represents a pure city route consisting of frequent stops. Fig.2.10 illustrated the speed profile, the total distance is 12.07 $km$, and the whole time is 1372 $s$.

Considering the large battery capacity of PHEB, we repeated the UDDS driving cycle 7 times as input to validate the vehicle model and test the SOC planning model without velocity optimization that will be applied in the subsequent simulation process. Fig.2.11 shows the performance of PHEB with SOC initial value equal to 0.4, the output power of APU and battery add up to meet the entire required power, and the APU always runs in its minimum fuel consumption zone when it's on. For comparison further, we compare the SOC curve with different initial values of SOC (Fig.2.12), when $SOC_0 = 0.6$, batteries can freely utilize their stored energy without exceeding the maximum allowable battery power, so the final SOC has not yet reached 0.3. While for the rest cases where the SOC initial value is less than 0.6, the output power of the APU and battery is evenly distributed

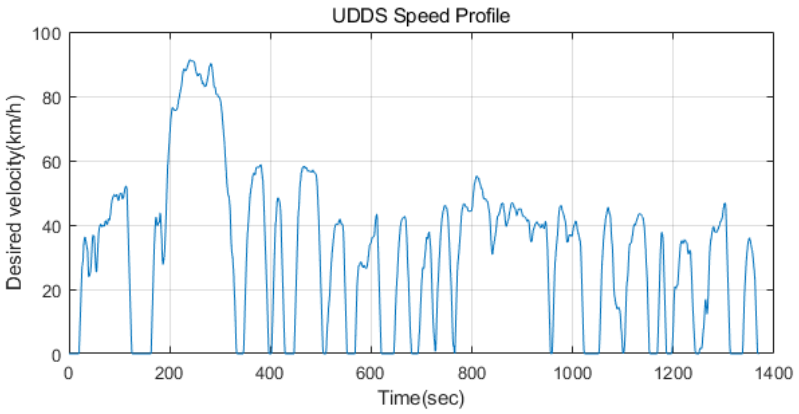


Figure 2.10: UDDS speed profile

during the operation of PHEB to achieve the minimum energy consumption. The final cost of different initial SOC is recorded in TABLE 2.2, as the initial SOC decrease, total cost consumption increases, because there is less energy stored in the battery at first so the vehicle have to rely more on the engine to meet the required power.

Table 2.2: Total cost of different initial SOC

| | initial SOC | | | |
|---|---|---|---|---|
| | 0.6 | 0.5 | 0.4 | 0.3 |
| Cost($) | 13.68 | 18.08 | 24.23 | 32.94 |

### 2.7.2/ Driving Condition in Real World

After validating the vehicle model and the SOC optimization model, a small fragment of city bus route data including 4 intersections and 9 bus stations is obtained from a lot of actual road condition data. This short but typical route segment is chosen for developing and verifying, which is shown in Fig. 2.13. The operation time of this route segment is 930 seconds, the distance is 3.72km and the velocity range is from 0km/h to 60 km/h. The position and timing information for this route segment are shown in TABLE 2.3.

### 2.7.3/ Velocity Optimization Results

A new optimized velocity profile is obtained by the proposed velocity optimization strategy according to the previous subsection, the results are shown in the Fig. 2.14.

First, it can be indicated clearly that PHEB will cost shorter time by the optimized velocity than the original route data, because of the participation of $\Delta t$ in objective function, the subject bus takes about 930.0 seconds to complete this journey with the original speed plan, but with the optimized velocity planning, it only takes 921.4s or 885.1s respectively

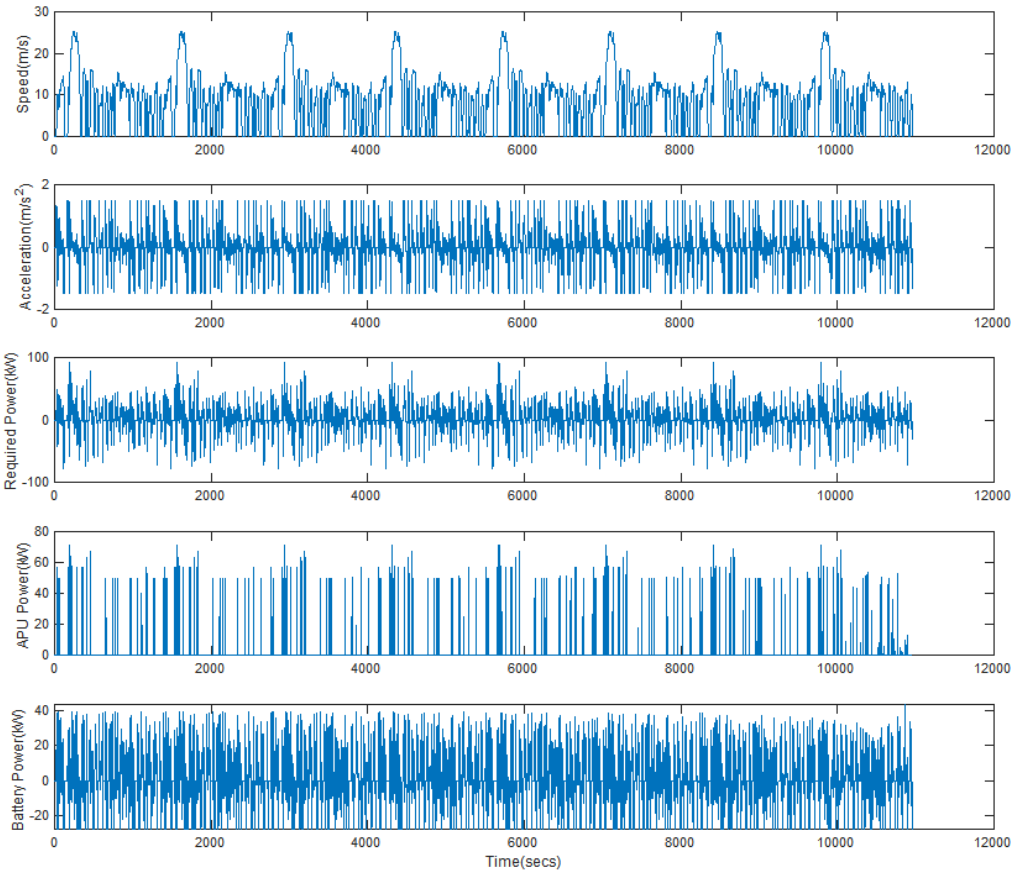


Figure 2.11: PHEB performance using DP optimal strategy with $SOC_0 = 0.4$

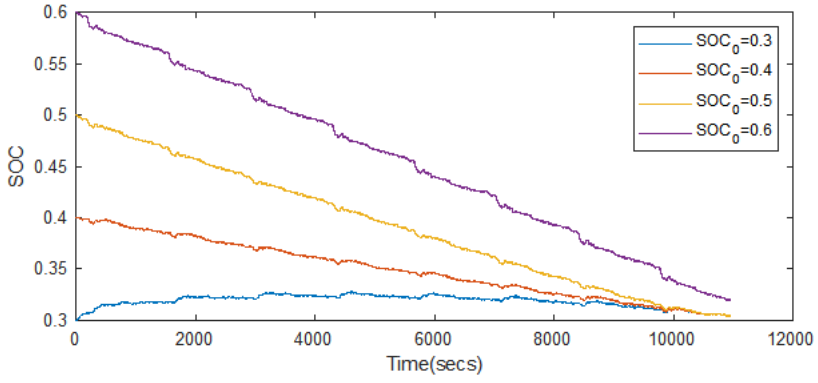


Figure 2.12: $SOC$ as a function of $SOC_0$

by the choice of target is minimum energy consumption or minimum travel time as described in TABLE 2.4. Also, for the facility of calculation, we convert the energy consumption to price cost with the different unit prices of fuel and electricity. As the balance of time

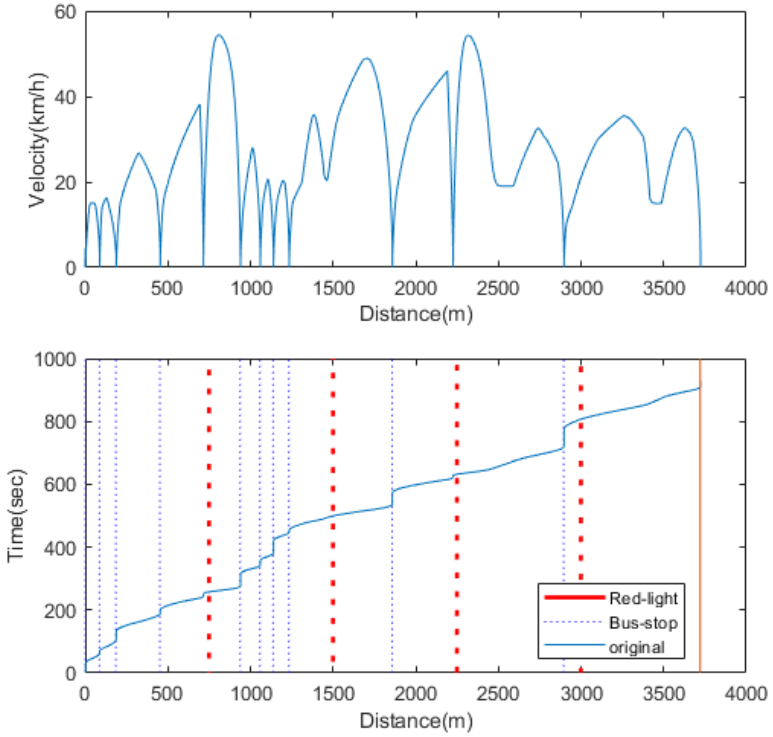


Figure 2.13: Actual road

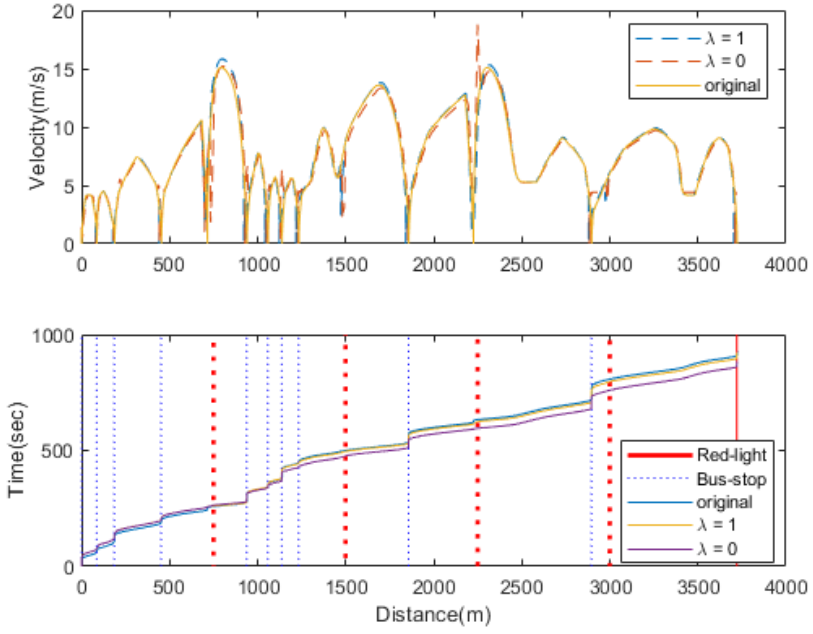


Figure 2.14: The result of optimized velocity profile

reduction, we have to sacrifice the fuel economy during the journey, thus the price cost by the original velocity file is cheaper, it cost 3.27 dollars. However, as for the situation of $\lambda = 0$, which means the fastest velocity planning, it cost 3.44 dollars for entire trip.

Table 2.3: Traffic information of real route

| **No.** | | $s_M^i$ | $c_0^i$ | $c_f^i$ | $c_r^i$ | | $s_N^i$ | Stop time(s) |
|---|---|---|---|---|---|---|---|---|
| 1 | light | 750 | 15 | 60 | 20 | stop | 86 | 6 |
| 2 | light | 1500 | 25 | 60 | 20 | stop | 186 | 21 |
| 3 | light | 2250 | 0 | 60 | 20 | stop | 452 | 11 |
| 4 | light | 3000 | 5 | 60 | 20 | stop | 938 | 38 |
| 5 | | | | | | stop | 1058 | 14 |
| 6 | | | | | | stop | 1137 | 39 |
| 7 | | | | | | stop | 1233 | 5 |
| 8 | | | | | | stop | 1857 | 37 |
| 9 | | | | | | stop | 2895 | 57 |

At the same time, the situation of $\lambda = 1$ only cost 3.14 dollars, which is beyond our expectation in the performance of fuel consumption.

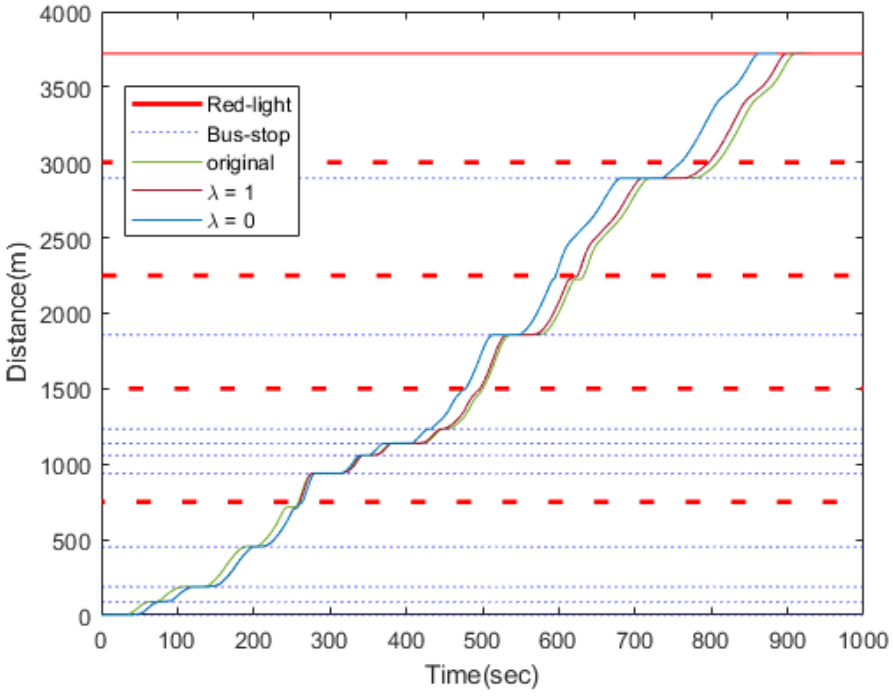


Figure 2.15: The result of optimized velocity for comparison

Besides, we can see clearly from Fig 2.15 that the main velocity adjustment occurs when the PHEB encounters traffic signals and bus stations, the faster acceleration and deceleration in these places greatly reduce the travel time of the entire trip, but equally, these behaviors are not friendly to the vehicle fuel economy. It is also worth noting that the optimized velocity sequence accomplish the purpose of time-saving from global perspective, for example, when the PHEB passed through the first intersection, the original data indicated that the bus waiting for a few seconds, but the optimized velocity reduce stop as much as possible, the optimized decision is to choose go-slow in advance. Another

Table 2.4: Comparison of arrival time and energy consumption results

| | Arrival time(s) | Energy consumption($) |
|---|---|---|
| $\lambda = 0$ | 885.1 | 3.44 |
| $\lambda = 1$ | 921.4 | 3.14 |
| Actual road without optimization | 930 | 3.27 |

example is when at the bus station before the third intersection, the strategy of $\lambda = 0$ chooses to accelerate fast for catching the last green-time duration, while the strategy of $\lambda = 1$ chooses to wait few seconds at the third intersection by the bound of stop time at the bus stop, which makes the travel time longer than the former situation but shorter than the original velocity planning, in this case, the fuel-saving potential of the intersection is still worth exploring. From the perspective of time, the saving of time has positive meaning for alleviating traffic congestion in some certain situation especially like morning and evening peak periods in the city.

## 2.8/ CONCLUSION

In this chapter, we proposed a velocity planning strategy focusing on energy consumption saving and time-saving for PHEB. At first, the mathematical model of PHEB vehicle, its components and traffic signals are built respectively, then the velocity planning problem considering traffic signals for PHEB is proposed and formulated based on DP framework. In order to solve the problem and to avoid the heavy computational duty, we proposed the method which simplified 3D-DP to 2D-DP by adopting an optimal SOC that obtained the empirical data. And in our simulation, the optimal SOC curve is obtained from the energy management system without velocity optimization for replacing the empirical data. During this process, we formulated this sub-problem as a time-discrete nonlinear optimization problem and also solved by DP. Then considering the location constraints of traffic signs, the velocity planning problem is treated as a deterministic spatial-discrete nonlinear optimization problem. Finally, the simulation results indicated that the proposed strategy can reduce energy consumption by 3.98%, and time-saving by 4.84%. Consequently, the velocity optimization strategy can be used as an antecedent for on-line EMS to reduce the energy consumption. However, there exist some limitations to the proposed strategy and implementation. First, we assumed all the intersection and bus-stop information is deterministic and known in advance, which is an extremely ideal situation. Second, the energy consumption will be greatly impacted by the ratio of APU power and battery power, so if we calculate the energy consumption on the premise of determined energy distribution ratio, the result may differ greatly from the application in the real world. Thus, on one hand, the diversity of traffic scenarios should be considered, the SPaT and bus station information will be set to uncertain, on the other hand, the accuracy of planning system and the reliability of control system should also be improved further.

# 3

# A STOCHASTIC DATA-BASED ECO-DRIVING STRATEGY

## 3.1/ INTRODUCTION

In Chapter 2, we focused on deterministic traffic information, assuming that we could obtain precise and accurate data in advance. This allowed us to develop a velocity planning and energy management strategy based on empirical State of Charge (SOC). In this chapter, we will shift our focus to the more realistic scenario in which traffic information, particularly in intersection areas near traffic lights, is stochastic in nature. By acknowledging the inherent uncertainties in traffic data, we will now explore the development of an optimal velocity profile for power-split hybrid electric vehicles that accounts for these stochastic elements. Specifically, in this study, we propose and assess a stochastic eco-driving system for hybrid electric vehicles (HEVs) that co-optimizes vehicle dynamics and hybrid powertrain operations. This system comprises two interconnected subsystems: a stochastic eco-driving decision subsystem and a hybrid powertrain control decision subsystem. The upper-level stochastic eco-driving decision subsystem takes into account the randomness of the traffic environment, employing a dual-driven (data and model) approach to recommend optimal desired set speeds or predict trajectories through stochastic optimization. Meanwhile, the hybrid powertrain control decision subsystem employs a rule-based control strategy tailored to the specific characteristics of intersections, optimizing the host HEV's energy costs. We evaluate the performance of our proposed stochastic eco-driving system using simulation cases created in the SUMO traffic simulation environment. The results demonstrate a significant decrease in the groups that applied the proposed stochastic eco-driving system in energy consumption compared to groups without the stochastic eco-driving system.

The remaining of this chapter is structured as follows: Section 3.2 introduces the primary research problem of this chapter. Section 3.3 outlines the essential traffic flow model, Eco-Approach and Departure (EAD) model, Gaussian Process Regression (GPR) model. The HEV model is detailed in Section 3.4. In Section 3.5, the co-optimization problem for

HEVs at a signalized intersection is formulated mathematically, and a stochastic eco-driving system is established using a bi-level approximation for co-optimization, which is solved by dividing it into two optimization objectives. Section 3.6 documents the process of collecting traffic data necessary for constructing the GPR model. Finally, simulation results and analysis are presented in Section 3.7, while the conclusion and discussion can be found 3.8.

## 3.2/ PROBLEM STATEMENT

An accurate road section (intercepted from a residential area in Belfort, France), as shown in Fig.3.1, it is a typical road section found in many places, such as residential communities, industrial parks, etc. Such road sections are generally characterized by non-congested traffic flow, and the duration of the green (and yellow) and red signals is coordinated according to the actual traffic situation so that vehicles can pass through the intersection from a certain distance within a signal cycle. However, there are some accidental interference situations. For instance, cars on the main road (Rue de Luxembourg) are susceptible to the sudden impact of the merged turning of the vehicles on both sides of the road (Rue de Jérusalem and Rue d'Amsterdam) and the opposite direction, or even if a pedestrian presses the pass button. This kind of interference often prolongs the passing time of the vehicles at signalized intersections. As mentioned in

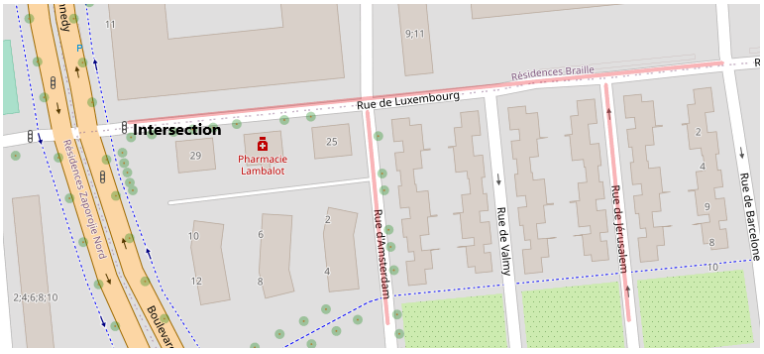


Figure 3.1: A typical real road section with the conventional environment from a residential area in Belfort, France

Chapter 1, HEVs will gradually become the market's mainstream as a substitute for the development of large-scale Connected and Automated Electric Vehicles (CAEVs). And it is not realistic to upgrade all the V2I infrastructure very soon for the typical road sections like Fig.3.1. Therefore, this study focuses on the bi-level optimization of vehicle dynamic and powertrain operation at a signalized intersection, especially given the uncertainty environment. As shown in Fig.3.2, we consider a signalized intersection with a single lane, the vehicles in this lane of the signalized intersection entrance can turn left, go straight and turn right. And for simplicity, we ignore human factors such as lane changing, overtaking, and pedestrian behavior first, and consider the disturbance caused

by other vehicles from/to the connecting road. These random occurrences occasionally force vehicles to slow down, making the arrival time at intersection uncertain. However, thanks to the past driving experience of this route, we can build a model to describe the relationship between the crossing time of this intersection and the driving-affected factors through Gaussian Process Regression, by predicting the crossing time with the possibility to co-optimize the vehicle velocity and hybrid powertrain system.

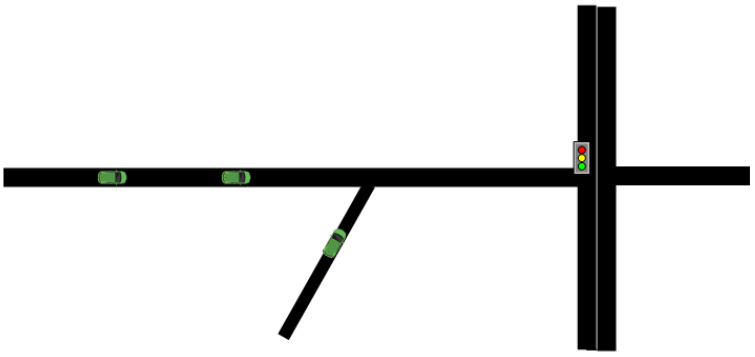

Figure 3.2: Random interventions scenario

## 3.3/ Eco-driving at Signalized Intersection

### 3.3.1/ Eco-Approach and Departure (EAD) at signalized intersection

Normally, when a vehicle approaches a signalized intersection, four possible passing scenarios [72] could happen as shown in Fig. 3.3,

1) Scenario 1: The host vehicle might speed up slightly to rush through the intersection before the red light, but still under the maximum speed limit of the intersection. The maximum speed limit is the smaller value between the speed of preceding vehicle and the maximum speed specified at the intersection.

2) Scenario 2: The most ideal situation, the host vehicle pass the intersection smoothly at cruising speed with the sufficient green light signal regardless of whether there is a preceding vehicle.

3) Scenario 3: The host vehicle has to slow down because the preceding vehicle's speed limit, but there's still enough green light signal left time to pass.

4) Scenario 4: The host vehicle have to stop since some uncertainty such as the vehicle or passenger coming out of the side road, which made the preceding vehicle could not pass within the green-yellow signal, and it's the worst situation compared to the previous 3 cases because the fuel consumption and travel time of host vehicle may increase greatly due to passing-with-stop.

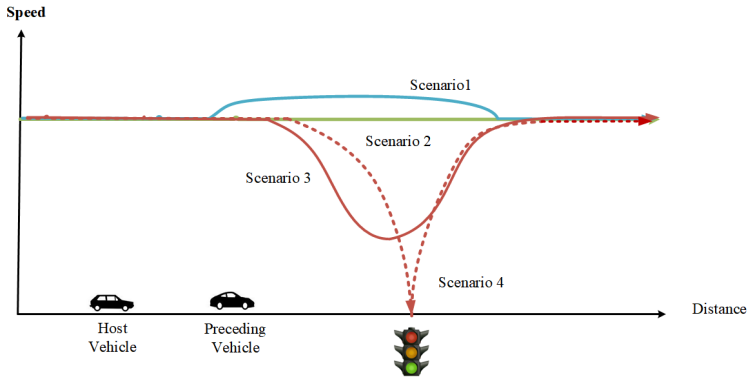


Figure 3.3: Illustration of 4 passing scenarios through an intersection

Moreover, for the above four scenarios, if the real-time information of signal timing are given in advance, the eco-driving trajectory for host vehicle is easy to be planned based on the distance to intersection $d$, the current speed $v_c$, the desired time to arrival at the intersection $T_d$ and uniform speed $v_u = d/T_d$, then the speed $v(t)$ at every time step $t$ for scenario 1 and 3 can be determined based on the trigonometric speed profiles. And the trigonometric model was proposed in [24], its objective is to minimize vehicle tractive power without compromising the driving comfort which constrained by the maximum jerk $du_M$. After testing in authors'follow-up works[42, 65, 89],the fuel saving of trigonometric model-based speed profile achieved 10%-15%. Therefore, according to the Eq.3.3, shown at the top of next page, the speed profiles for scenario 1 and 3 can be determined, where $m$ and $n$ determine the shape of the speed profile and satisfy,

$$\begin{cases} |n \cdot (v_u - v_c)| \leq a_{\max} \\ |n \cdot (v_u - v_c)| \leq d_{\max} \\ \left|n^2 \cdot (v_u - v_c)\right| \leq du_M \\ n \geq \frac{\frac{\pi}{2}-1}{T_d} \end{cases} \tag{3.1}$$

$$m = \frac{-\frac{\pi}{2}n - \sqrt{\left(\frac{\pi}{2}n\right)^2 - 4n^2 \cdot \left[\left(\frac{\pi}{2}-1\right) - T_d \cdot n\right]}}{2\left[\left(\frac{\pi}{2}-1\right) - T_d \cdot n\right]} \tag{3.2}$$

where $a_{max}$, $d_{max}$ denote the max acceleration and deceleration and $du_M$ is the maximum jerk. $m$ and $n$ also are the dominant variables to control the fuel efficiency in the acceleration and deceleration process. Given a value of $n$, the choice of $m$ is affected by the specific time that the vehicle reach to the intersection.

Similarly, for scenario 4, the host vehicle's trajectory could also be planned by Eq.3.4,

where $g_s^2$ denotes the start time of the second green time and $m$, $n$ satisfied,

$$\begin{aligned} n &= m \\ m &= \frac{\pi \cdot v_u}{d} \end{aligned} \tag{3.5}$$

$$v(t) = \begin{cases} v_u - (v_u - v_c)\cos(mt) & t \in \left[0, \frac{\pi}{2m}\right) \\ v_u - (v_u - v_c)\frac{m}{n}\cos\left[n \cdot \left(t - \frac{\pi}{2m} + \frac{\pi}{2n}\right)\right] & t \in \left[\frac{\pi}{2m}, \frac{\pi}{2m} + \frac{\pi}{2n}\right) \\ v_u + (v_u - v_c)\frac{m}{n} & t \in \left[\frac{\pi}{2m} + \frac{\pi}{2n}, \frac{d}{v_u}\right) \\ v_u - (v_u - v_c)\frac{m}{n}\cos\left[n \cdot \left(t - \frac{d}{v_u} + \frac{\pi}{n}\right)\right] & t \in \left[\frac{d}{v_u}, \frac{d}{v_u} + \frac{\pi}{2n}\right) \\ v_u - (v_u - v_c)\cos\left[m \cdot \left(t - \frac{d}{v_u} - \frac{\pi}{2m} - \frac{\pi}{2n}\right)\right] & t \in \left[\frac{d}{v_u} + \frac{\pi}{2n}, \frac{d}{v_u} + \frac{\pi}{2m} + \frac{\pi}{2n}\right) \\ v_c & t \in \left[\frac{d}{v_u} + \frac{\pi}{2m} + \frac{\pi}{2n}, +\infty\right) \end{cases} \tag{3.3}$$

$$v(t) = \begin{cases} v_u - (v_u - v_c)\cos(mt) & t \in \left[0, \frac{\pi}{2m}\right) \\ v_u - (v_u - v_c)\frac{m}{n}\cos\left[n \cdot \left(t - \frac{\pi}{2m} + \frac{\pi}{2n}\right)\right] & t \in \left[\frac{\pi}{2m}, \frac{\pi}{2m} + \frac{\pi}{2n}\right) \\ v_u + (v_u - v_c)\frac{m}{n} & t \in \left[\frac{\pi}{2m} + \frac{\pi}{2n}, g_s^2\right) \\ v_u - (v_u - v_c)\frac{m}{n}\cos\left[n \cdot \left(t - g_s^2 + \frac{\pi}{n}\right)\right] & t \in \left[g_s^2, g_s^2 + \frac{\pi}{2n}\right) \\ v_u - (v_u - v_c)\cos\left[m \cdot \left(t - g_s^2 - \frac{\pi}{2m} - \frac{\pi}{2n}\right)\right] & t \in \left[g_s^2 + \frac{\pi}{2n}, g_s^2 + \frac{\pi}{2m} + \frac{\pi}{2n}\right) \\ v_c & t \in \left[g_s^2 + \frac{\pi}{2m} + \frac{\pi}{2n}, +\infty\right) \end{cases} \tag{3.4}$$

### 3.3.2/ TRAFFIC FLOW MODEL

The mathematical concept of traffic flow modeling for conventional cars is presented in this subsection. Generally, microscopic traffic models express the acceleration and deceleration of each vehicle as a function of the velocity of the preceding vehicle, speed difference, and safe headway between vehicles [98]. Our traffic simulation is based on a discrete-time framework and we only consider the longitudinal motion dynamics of vehicles, thus the car-following models are used to infer driving behavior at a signalized intersection and the vehicle dynamic motion could be expressed at every timestep $t$ as

$$\begin{aligned} y_h(t+1) &= y_h(t) + v_h(t)\Delta t + 0.5u_h(t)\Delta t^2 \\ v_h(t+1) &= v_h(t) + u_h(t)\Delta t \end{aligned} \tag{3.6}$$

where $y_h$, $v_h$, and $u_h$ are the position, velocity, and acceleration of host vehicle, and $\Delta t$ is the step size. The vehicle velocity depends on input acceleration $u_i$ in Eq. 3.6, which is calculated according to a microscopic car-following model called the Intelligent Driver Model (IDM), the instantaneous acceleration $u_h(t)$ with its preceding vehicle is calculated by

$$\begin{aligned} u_h(t) &= a\left[1 - \left(\frac{v_h(t)}{v^{des}}\right)^4 - \left(\frac{s^*\left(v_h(t), \Delta v_h(t)\right)}{\Delta y_h(t)}\right)^2\right] \\ s^*\left(v_h(t), \Delta v_h(t)\right) &= s_0 + v_h t_{hw} + \frac{v_h \Delta v_h}{2\sqrt{ab}} \end{aligned} \tag{3.7}$$

where $v^{des}$ is the desired velocity of the host vehicle, $s_0$, $t_{hw}$ is the minimal distance, the

desired time headway to the preceding vehicle respectively, *a*, *b* is the maximum acceleration and comfortable deceleration (positive number), and $\Delta v_h = v_h - v_p$, $\Delta y_h = y_h - y_p$ are the distance gap and velocity difference of host vehicle and the preceding vehicle.

## 3.4/ HEV Powertrain Model

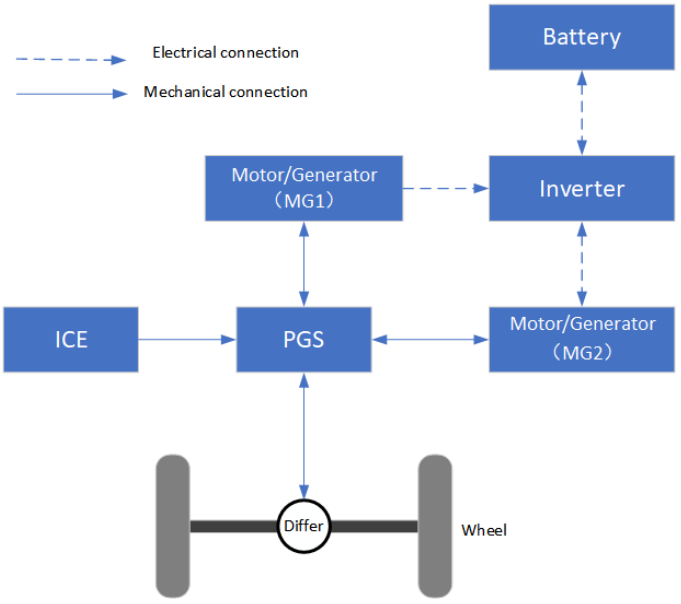


Figure 3.4: Power-split HEV architecture

Generally speaking, there are three typical types of HEV powertrains: series, parallel, and series-parallel as mentioned in Chapter1. This work focused on a power-split (also known as a series-parallel hybrid) HEV, as Fig.3.4 shows, consists of PGS (Planetary Gear Set), an ICE (Internal Combustion Engine), two EMs (Generator and Motor), energy storage system (battery). The PGS bonded ICE and EMs together, the sun gear, carrier gear, and ring gear are connected to motor/generator (MG1), ICE and motor/generator (MG2). Meanwhile, the TABLE 3.1 records the basic characteristics of this HEV.

The PGS, as a result of mechanical connection through gear teeth, satisfy the following relationship, where *c*, *r*, *s* indicate the carrier gear, the ring gear, and the sun gear.

$$(N_R + N_S)\,\omega_c = \omega_s N_S + \omega_r N_R \tag{3.8}$$

Moreover, at each time step, the energy flow of power-split HEV can be described as Eq. 3.9, where $P_{req}$ is the tractive power demand, $T_i$, $\omega_i$ denote the torque and speed, $i \in \{\text{engine}, MG1, MG2\}$.

$$P_{req} = T_{\text{eng}}\,\omega_{\text{eng}} + T_{MG1}\omega_{MG1} + T_{MG2}\omega_{MG2} \tag{3.9}$$

Table 3.1: Vehicle parameters

| | Parameter[Symbol] | Value |
|---|---|---|
| Vehicle | Vehicle mass[$m$] | 1750kg |
| | Front area[$A$] | $3.8m^2$ |
| | Air drag coefficient[$C_D$] | 0.33 |
| | Air density[$\rho$] | $1.293kg/m^2$ |
| | Tire radius[$R_{tire}$] | 0.298 |
| | Rolling resistance coefficient[$\delta$] | 0.015 |
| Powertrain | Transmission efficiency[$\eta_T$] | 0.97 |
| | Final differential gear ratio[$g_f$] | 4.113 |
| | Sun gear teeth number[$N_S$] | 30 |
| | Ring gear teeth number[$N_R$] | 78 |
| IC Engine | Max Power | 57kW |
| Motor/Generator(1) | Max Power | 50kW |
| | Rated Power | 25kW |
| Motor/Generator(2) | Max Power | 30kW |
| | Rated Power | 15kW |
| Battery | Capacity[$Q_b$] | 6.5Ah |
| | number of cells | 240 |

Suppose that the connection between the components are rigid and the energy losses can be ignored, and consider the force analysis, the dynamic equations that govern the mechanical path are

$$\begin{aligned} \omega_c = \omega_{ICE}, \omega_r = \omega_{MG2}, \omega_s = \omega_{MG1} = \frac{g_f}{R_{\text{tire}}} v \\ J_{MG1}\frac{d\omega_{MG}}{dt} = T_{MG1} + F \times N_S \\ J_{eng}\frac{d\omega_{eng}}{dt} = T_{eng} - F \times (N_S + N_R) \\ J_{MG2}\frac{d\omega_{MG2}}{dt} = T_{MG2} - \frac{T_{out}}{g_f} + F \times N_R \end{aligned} \tag{3.10}$$

where $v$ is the speed of HEV, $g$ is the gravity acceleration, $\alpha$ is the road angle, $J_i$ is the lumped inertia, $F$ is the interaction force between the differential gears, $T_{\text{out}}$ is the sum of the powertrain output torque. To reduce the number of dynamic states, the inertial losses $J_i\,(d\omega_i/dt)$are ignored and set to zero in the control-oriented model[25].

The fuel consumption is selected as the target of the fuel economy, a empirical break-specific fuel map (Fig.3.5) of engine is used to relate the fuel flow rate, $\dot{m}_f$ described as,

$$\dot{m}_f = BSFC\left(T_{eng}, \omega_{eng}\right)\frac{P_{eng}}{3600} \tag{3.11}$$

Another important evaluated indicator when consider the energy consumption for an HEV is the electricity consumption, the dynamic equation of the state of charge (SOC) can be

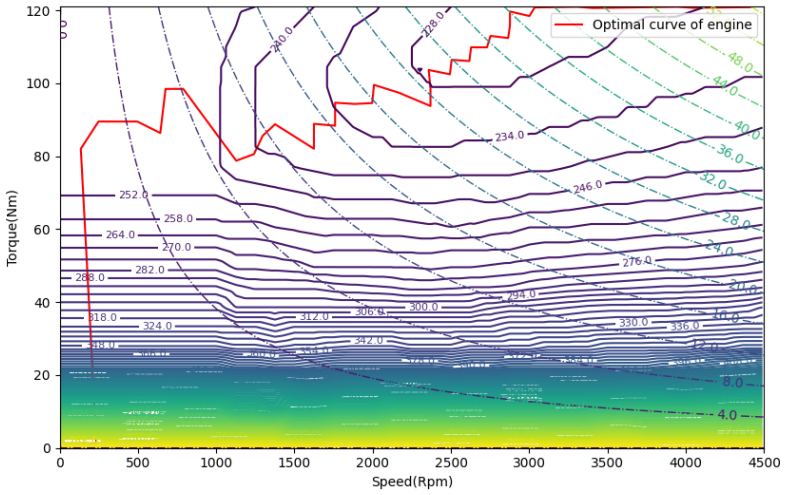


Figure 3.5: BSFC map of ICE

represented by

$$S\dot{O}C = -\frac{V_{oc} - \sqrt{V_{oc}^2 - 4P_{bat}R_{bat}}}{2Q_bR_b} \tag{3.12}$$
$$P_{bat} = \eta_{MG1}^{k_1} T_{MG1}\omega_{MG1} + \eta_{MG2}^{k_2} T_{MG2}\omega_{MG2}$$

where $R_{bat}$, $P_{bat}$ and $V_{oc}$ are internal resistance, power of battery and the open-circuit voltage respectively. As for $\eta_{MG1}^{k_1}$,$\eta_{MG2}^{k_2}$ denotes the efficiency of MG1, MG2 (Fig. 3.7), when $T_i\omega_i > 0$, $k_1 = 1$ denotes the discharging state, and $T_i\omega_i < 0$ , $k_1 = -1$ denotes the charging state. Furthermore, $V_{oc}$ and $R_{bat}$ are generally dependent on both the SOC and the temperature, since we only consider the situation at normal operating temperature of $25°\mathrm{C}$, the map of $V_{oc}$ and $R_{bat}$ are shown in Fig 3.6.

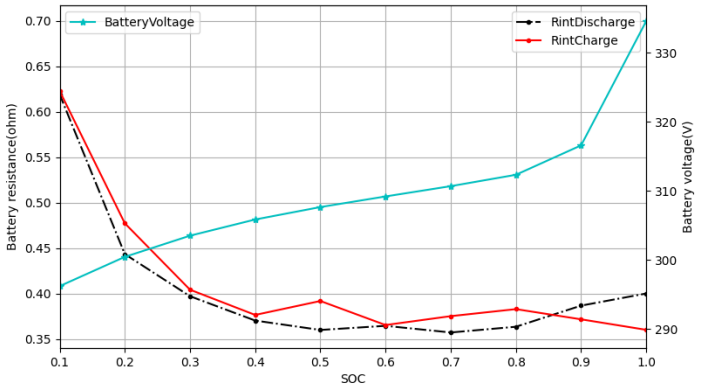


Figure 3.6: Maps of the open circuit voltage and the internal resistance

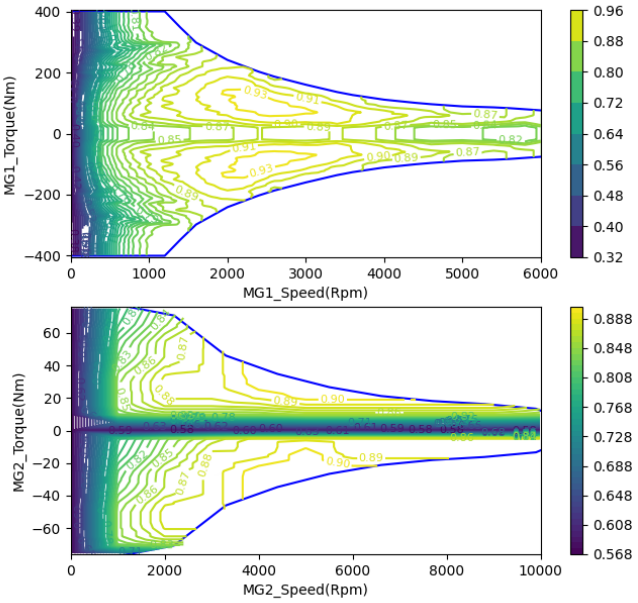


Figure 3.7: MG1 and MG2 efficiency map and torque boundary

## 3.5/ METHODOLOGY

### 3.5.1/ CO-OPTIMIZATION FORMULATION AT AN INTERSECTION

The co-optimization of this power-split HEV at an intersection is formulated as a nonlinear constrained optimization problem. We only consider longitudinal velocity and assume no road grade, the total energy consumption cost of crossing an intersection for an HEV is optimized to minimize, which can be written as,

$$\min \sum_{t=t_{en}}^{T} \left( c_{fuel} m_f(t) + c_{ele} m_e(t) \right) \tag{3.13}$$

subject to

$$\int_{t=t_{en}}^{T} v(t) = L \tag{3.14}$$

$$v^{\min} \leq v(t) \leq v^{\max} \tag{3.15}$$

where $c_{fuel}$, $c_{ele}$ is the fuel and electricity price separately, $m_e(t)$ is the instantaneous electricity consumption, it can be calculated by $P_{bat}(t)/3600$, $T$ is the time to cross the intersection, $t_{en}$ is the moment at occurrence of traffic light change, $L$ is the given road section distance, $v^{\min}$ and $v^{\max}$ are boundaries of $v(t)$. In addition to the distance limit of the

velocity optimization, the constraints to optimize the powertrain of HEV are,

$$P_{\text{req}}(t) = \frac{v(t)}{3600\eta_T}\left(mg(f\cos\alpha + \sin\alpha) + \frac{C_D A v(t)}{21.15} + \delta m u(t)\right) \tag{3.16}$$

$$P_{eng}\left(\omega_{eng}(t), T_{eng}(t)\right) = P_{req}(t) - P_{bat}(t; SOC_0)\ \forall t \tag{3.17}$$

where $SOC_0$ is the given initial SOC, $P_{req}(t)$ is the required traction power at every time step. Besides, the boundaries of related variables are,

$$\begin{cases} \omega_i^{\min} \le \omega_i(t) \le \omega_i^{\max} \\ T_i^{\min} \le T_i(t) \le T_i^{\max} \\ P_{eng}^{\min} \le P_{eng}(t) \le P_{eng}^{\max} \\ P_{bat}^{\min} \le P_{bat}(t) \le P_{bat}^{\max} \\ SOC^{\min} \le SOC(t) \le SOC^{\max} \end{cases} \tag{3.18}$$

### 3.5.2/ Gaussian Process Regression Model

Based on the previously analysis, we consider that the crossing time $T$ to pass through an intersection for such a vehicle is uncertain because the exact information of the traffic signal is unknown. However, it's possible to use past driving data to estimate the crossing time $T = t_{cross}$, thus the following variables related to the important factors which can influence the traffic flow are defined,

1) Crossing time $\tau_n$, and $\tau_n = t_c - t_{en}$, $t_{en}$ is the moment at occurrence of traffic light change, $t_c$ is the moment that vehicle cross through the intersection

2) States of traffic signal $\delta_n(t_{\text{en}})$ , where $\delta_n(t_{\text{en}}) = 0$ denotes signal switching from green to yellow and to red and $\delta_n(t_{\text{en}}) = 1$ denotes a signal switching from red to green

3) Velocity $v_n(t_{\text{en}}) \in \mathbb{R}^+$

4) Distance to the intersection $d_n(t_{en}) \in \mathbb{R}^+$

Firstly, the crossing time $\tau_n$ as the most important indicator should be recorded, here it's worth noting that the crossing time calculated from the moment $t_{en}$ at the occurrence of traffic light change to ensure the validity of the collected data and the accuracy of estimation possibilities. Next, the state of traffic signal $\delta_n(t_{\text{en}})$ since the crossing time start at the occurrence of traffic light change, when $\delta_n(t_{\text{en}}) = 0$, a vehicle with fast velocity and nearing the intersection seems to have the higher possibility to cross without stop, and when $\delta_n(t_{\text{en}}) = 1$, a vehicle may or may not cross depending on the velocity $v_n(t_{\text{en}})$ and distance to the intersection $d_n(t_{\text{en}})$, but still, there's a possibility that vehicles fail to cross if there are some unexpected situations, such as the preceding vehicle has to slow down due to the appearance of passenger or other cars from both sides of the road, which

also are hazardous behaviors, then the vehicle fails to cross and brakes aggressively to stop. It's clear that the crossing time of each vehicle $\tau_n$ has stochastic nature, and is impacted by predictor variables $\delta_n(t_{\text{en}})$, $v_n(t_{\text{en}})$, $d_n(t_{\text{en}})$. Therefore, a kernel-based probabilistic model called Gaussian Process Regression (GPR) model is defined for predicting the crossing time $t_{cross}$ is presented below. GPR is a nonparametric, bayesian approach to regression that has been widely used for regression and classification tasks in the area of machine learning [107], its benefits are working well on small datasets, having the ability to provide uncertainty measurements on the predictions, and making the prediction more versatile by providing the opportunity of specifying custom kernels [27]. In order to learn the probabilistic relation between a set of the above-mentioned variables and their conditional dependencies, the training dataset is collected from a series of intersection scenario simulations, and after having $D = \{(f_n, \tau_n) \mid n = 1, 2, \ldots, N\}$, where $f_n = \{d_n, v_n, \delta_n\}$ is input vector, $\tau_n$ is response vector, the GPR model $f_{\text{GPR}}$ is defined to fit the training dataset . The output of $f_{\text{GPR}}$ is a multivariate Gaussian with mean $\mu_n$ and covariance matrix $\Sigma_n$, and the elements of covariance matrix is determined using squared-exponential kernel function. Next, if the new input vector $(d_{\text{new}}, v_{\text{new}}, \delta_{\text{new}})$ is received, the crossing time distribution $t_{cross}$ is predicted from the model $f_{\text{GPR}}(d_{\text{new}}, v_{\text{new}}, \delta_{\text{new}})$, we can obtain the mean $\mu_{cross}$ and covariance matrix $\Sigma_{cross}$ $(t_{\text{cross}} \sim N(\mu_{\text{cross}}, \Sigma_{\text{cross}}))$(Fig.3.8).

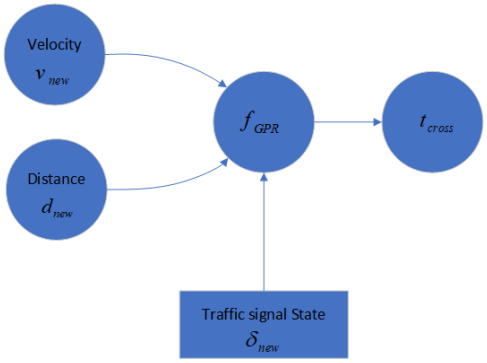


Figure 3.8: Gaussian Process Regression Model Structure

The standard deviation $\sigma_{\text{cross}}$ is obtained from the covariance matrix, and the probability $P_{cross}$ of a vehicle crossing the intersection for any arbitrary time is calculated using the Gaussian cumulative distribution function[98],

$$P(t_{\text{cross}} \mid \tau_n, f_n, z_{\text{new}}) = \frac{P(t_{\text{cross}}, \tau_n \mid f_n, z_{\text{new}})}{P(\tau_n \mid f_n, z_{\text{new}})} \tag{3.19}$$

$$P_{\text{cross}} = P(t_{\text{cross}} \leq t_{\text{r}}) = P\left(Z_{\text{r}} \leq \frac{t_{\text{r}} - \mu_{\text{cross}}}{\sigma_{\text{cross}}}\right) \tag{3.20}$$

where $t_r$ is the red signal timing, $Z_r$ follows the standard normal distribution. The failure probability of crossing $P_{\text{fail}}$ is the complement of $P_{\text{cross}}$.

### 3.5.3/ BI-LEVEL APPROXIMATION OF CO-OPTIMIZATION

As shown in Fig 3.9, a system driven by model and data is designed to obtain the optimal or near-optimal solution for the above-formulated co-optimization problem. First, a stochastic eco-driving decision system composed of learning-based on the past traffic data model (GPR model) and EAD model is built to evaluate the probability of crossing $P_{cross}$ the intersection and to obtain the desired set speed $v_s^*$ for the host HEV, the optimal trajectory problem is considered as a stochastic optimization problem and according to this subsystem, vehicle adjust the velocity from where the it can observe a change of traffic signal, and the minimum limit of SOC ($SOC_{MIN}$) is compared with the initial value of SOC detected $SOC_0$ at the same time, once $SOC_0 > SOC_{MIN}$, the optimal speed of host HEV is planned by real-time calculation based on IDM model and desired set speed and the pure electric mode will be locked in consideration of the above co-optimized objective function, but if $SOC_0$ is not satisfied $SOC_0 > SOC_{MIN}$, the optimal energy management for HEV can be formulated as a nonlinear constrained optimization problem based on the predicted speed planning with the probability of crossing, and is implemented to powertrain in real-time.

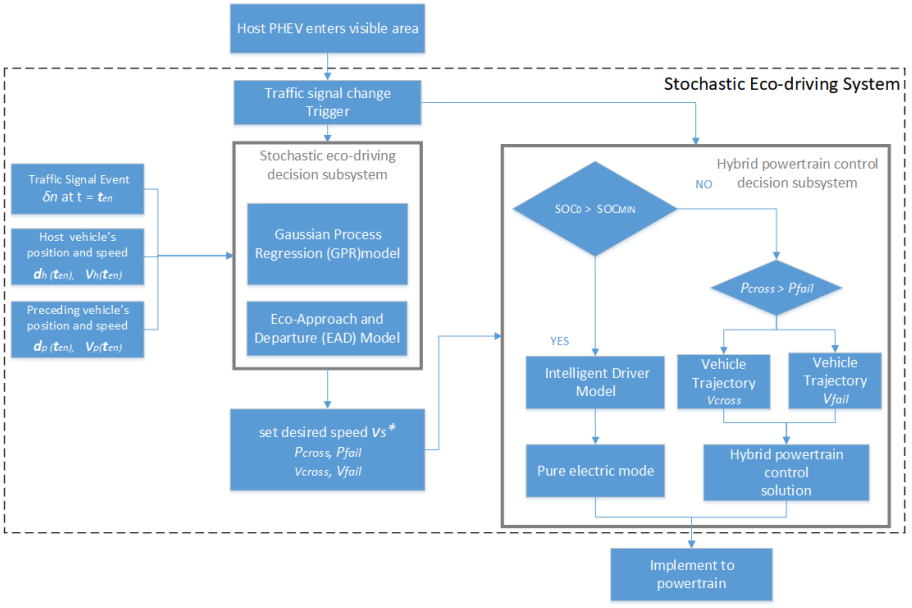


Figure 3.9: Flowchart of the proposed system with co-optimization of velocity and powertrain

#### 3.5.3.1/ STOCHASTIC ECO-DRIVING PROBLEM FORMULATION

Before we begin to describe the stochastic eco-driving system, recall that the car-following model described in Eq. 3.7, where the parameter $v_{des}$ denote the desired speed of the host vehicle and can be handled as a simple optimization problem with only one control

variable as the Eq. 3.21 shows, $P_{req}$ is a function of $v_h$ and $u_h$ Eq. 3.16. According to optimized $v_{des}$ and suggested EAD trajectory [89]of the preceding vehicle, the optimal speed planning of host HEV is able to be implemented easily no matter in which event ($\delta_n = 0$ or $\delta_n = 1$). Moreover, in case of preventing the sharp change of deceleration caused by the sudden drop of $v_{des}$, the desired speed can be implemented by tuning the set speed $v^s$, as the equation (3.22) shows, where $\varphi$ is the adjustment factor and $\varphi < 1$.

$$\min \sum_{t=t_{en}}^{T} P_{req}\left(v_h, u_h\left(v^{des}\right)\right) \tag{3.21}$$

$$v^{\text{des}}\ (t, v^s) = \begin{cases} v^s & \text{if } v^s \geq v^{\text{des}}\ (t-1) \\ \varphi v^{\text{des}}\ (t-1) + (1-\varphi) v^s & \text{otherwise} \end{cases} \tag{3.22}$$

In order to solve this formulated optimization problem, $v^s$ is is discretized by speed step into a set of possible solutions, which is also constrained by $v^s_{min} \leq v^s \leq v^s_{max}$, so the optimal (desired) set speed $v^{s*} \in \left\{v^s_{\min} + k\Delta v\right\}$, where $k = 0, 1, 2, \ldots, K$, speed step $\Delta v = 0.1$ m/s and $K = \left(v^s_{\max} - v^s_{\min}\right)/\Delta v$, for each $v^s$, the trajectory is able to be calculated by Eq. 3.6 and Eq. 3.7 assuming a preceding vehicle, if there's any, driving in the EAD way, such as Eq. 3.3, after the corresponding $v_h$ and $u_h$ of each time step are calculated in the entire horizon, the objective $P_{req}$ is determined accordingly. Therefore, K+1 target values are obtained from the given set of possible solutions, and the desired set speed $v^{s*}$ is selected corresponding to the minimum target value.

Then recall the GPR model that driven by a small amount of experienced traffic data and presented in previous subsection 3.5.2, based on estimated probability $P_{\text{cross}}$ of host vehicle crossing the intersection, the aforementioned simple deterministic optimization problem can be changed in a stochastic manner as,

$$\sum_{t=t_{en}}^{T_c} P_{\text{cross}} P^{\text{cross}}_{req}\left(v_h, u_h\left(v^s, t\right)\right) + \sum_{t=t_{en}}^{T_f} P_{\text{fail}} P^{\text{fail}}_{req}\left(v_h, u_h\left(v^s, t\right)\right) \tag{3.23}$$

It is worth noting that the crossing time of the preceding vehicle remains an important factor if there's a preceding vehicle and the safety distance between the preceding vehicle and the host vehicle is close enough. Still, in this case, the possibility of the host vehicle crossing the intersection is considered equal to the chance of the preceding, which could be determined by the GPR model as well. Thus let's assume that there is always a preceding car. When there is no data of the preceding vehicle in reality, the speed of the preceding can be considered to be the same as the host HEV, and the position of the preceding car is calculated by $d_p = d_h + S_s$, $S_s$ is the safe following distance, the value equals to 30-60m according to the speed of host vehicle. In this way, we solve the optimization problem by proposing a stochastic eco-driving decision subsystem; the overall procedure is summarized in Algorithm 1, will advise either to slow down early to avoid the high fuel consumption of emergency deceleration or increase acceleration appropriately to have a

higher probability of crossing the intersection without stopping when there's a preceding vehicle, and if not, predict the trajectory of crossing the intersection with the consideration of the possibility.

**Algorithm 1** Stochastic Eco-driving Decision Subsystem

**Input:** $d_h(t_{en})$, $v_h(t_{en})$, $d_p(t_{en})$, $v_p(t_{en})$

**Output:** $v^{s_*}$, $P_{\text{cross}}$, $P_{\text{fail}}$, $v_h^{\text{cross}}$, $v_h^{\text{fail}}$

Initialize $\delta_n$ at $t_{en} = t$, visible distance of signal $x_J$, distance after the intersection $x_d$, empirical fixed traffic signal time $t_g$, $t_r$
Estimate $P_{\text{cross}}$ and $P_{\text{fail}}$ from $f_{GPR}\left(d_p(t_{en}), v_p(t_{en}), \delta_n\right)$
**if** ($\delta_n == 1$ and $t_r < \frac{x_J - d_p}{v_p} \leq t_r + t_g$ )or($\delta_n == 0$ and $\frac{x_J - d_p}{v_p} < t_g$ ) **then**
    Set the preceding vehicle pass through the intersection with steady cruise speed $v_p$
**else**
    **if** $\delta_n == 1$ **then**
        $T_d = t_r + 3$ and $v_u = d_p / T_d$ ▷ 3s is the buffer time
    **else**
        $T_d = t_g - 3$ and $v_u = d_p / T_d$
    **end if**
    Compute the trajectory of preceding car by the EAD model Eq(3.3)
**end if**
Compute the fail trajectory of preceding vehicle by Eq(3.4)
Discrete $v^{s_*} \in V^{s_*} = \left\{v^s_{\min} + k\Delta v\right\}$ and $K = \left(v^s_{\max} - v^s_{\min}\right)/\Delta v$
**for** each $v^s \in V^{s_*}$ **do**
    $P_{req}^{\text{cross}} := 0$, $P_{req}^{\text{fail}} := 0$, $t := 0$
    **while** $d_h <= x_J + x_d$ **do**
        Calculate $u_h(t)$ by IDM Eq(3.7)
        Update $d_h^{\text{cross}}$, $v_h^{\text{cross}}$ using traffic model Eq(3.6)
        Compute $P_{req}^{\text{cross}} = P_{req}^{\text{cross}} + P_{req}^{\text{cross}}(v_h, u_h(v^s))$
    **end while**
    $t := 0$
    **while** $d_h <= x_J + x_d$ **do**
        Calculate $u_h(t)$ by IDM Eq(3.7)
        Update $d_h^{\text{fail}}$, $v_h^{\text{fail}}$ using traffic model Eq(3.6)
        Compute $P_{req}^{\text{fail}} = P_{req}^{\text{fail}} + P_{req}^{\text{fail}}(v_h, u_h(v^s))$
    **end while**
    Calculate $J(k) = P_{\text{cross}} P_{\text{req}}^{\text{cross}}(v_h, u_h(v^s)) + P_{\text{fail}} P_{\text{req}}^{\text{fail}}(v_h, u_h(v^s))$
**end for**
Find optimal $v^{s_*}$ corresponding to the minimum $J$
Record $v_h^{\text{cross}}$ and $v_h^{\text{fail}}$ corresponding to the optimal $v^{s_*}$

#### 3.5.3.2/ POWERTRAIN OPTIMIZATION PROBLEM FORMULATION

Except for the vehicle dynamic optimization, the operation of HEV is still a valuable part of improving fuel economy. Typically, the optimal energy management for HEV is formulated as a nonlinear constrained optimization problem and the objective is to minimize the total fuel consumption along the given required tractive power as the same expression as Eq. 3.13, and the constraints conclude Eq. 3.8-Eq. 3.12 and Eq. 3.16-Eq. 3.18, such formulation is suitable for traditional mathematical optimization methods with high complexity, which are difficult to be implemented in real-time[72]. So in order to facilitate on-line optimization based on the predicted optimal trajectory from stochastic eco-driving system, the energy management optimization problem can be reformulated as,

$$\min \sum_{t=t_{en}}^{T} \sum_{l=1}^{N} x_t^l \frac{P_{\text{eng}}(t,l)}{\eta_{\text{eng}}(t,l)} \tag{3.24}$$

subject to:

$$\sum_{t=1}^{j} \gamma \left( P_{\text{req}}(t) - \sum_{l=1}^{N} x_t^l P_{\text{eng}}(l) \right) \leq C \quad \forall j = 1, \ldots, T \tag{3.25}$$

$$\sum_{n=1}^{N} x_t^l = 1 \tag{3.26}$$

$$x_t^l = \{0, 1\} \tag{3.27}$$

where $N$ is the number of discretized power levels for the engine, $l$ is the engine power level index, $P_{\text{eng}}(l)$ is the $l$-th discretized level of the engine power; $x(t,l)$ is a binary variable, either 1 or 0, the objective means to choose the optimal ICE power level for each time step in order to achieve the highest fuel efficiency. Besides, $\gamma()$ models the SOC change as a function of required demand power $P_{\text{req}}$, $C$ is the gap of the battery pack's SOC between the initial and the minimum. For the constraint Eq. 3.25, if $\Delta SOC$ is precalculated for each associated engine power level based on the given power demand at each time step from predicted velocity, it can be replaced by,

$$\begin{aligned} SOC_0 - SOC_{\max} &\leq \sum_{t=t_{en}}^{j} \text{selec}(t,l) \Delta SOC(t,l) \\ &\leq SOC_0 - SOC_{\min} \quad \forall j = 1, \ldots, T \end{aligned} \tag{3.28}$$

It's worth noting that the minimum SOC here indicated $SOC^{min}$, which refers to the lowest SOC value set in the whole process under the premise of protecting the battery life as much as possible. In this way, the original problem is transformed into a Mixed Integer Linear Programming (MILP) problem and can easily be solved by numerous efficient solvers [49]. In this paper, we used the GUROBI OPTIMIZER [126] to solve this MILP problem.

## 3.6/ DATA PREPARATION

The data preparation for establishing the GPR model is described first to implement the proposed stochastic eco-driving system. To achieve realistic traffic patterns, the arrival of vehicles in the simulator is determined at random by using a probability distribution, the car-following models' parameters are also picked at random from a pre-defined distribution. The traffic light is settled with a fixed cycle and splits the last 3 seconds of the green period actually is yellow signal, but for simplicity we will treat the yellow sign within the green signal, and the buffer time is considered for safety. Each vehicle in the simulator follows the signal strictly.

The traffic flow rate is set to be moderate and non-congested, the parameters of IDM are $v^{des} = 27 - 60km/h$, $s_0 = 2m$,$t_{hw} = 1.5sec$, $a = 1.5m/s^2$, and $b = 2.5m/s^2$. The green-yellow and red traffic signal durations are set as $t_g = 45s$, $t_r = 30s$ respectively, but in fact the last 3 seconds is yellow signal. Then, the selected road for simulation has a single lane with total length of 1.5 km and the intersection is located at 1.0 km, but in order to evaluate fuel consumption, the analysis boundary of the road section is set to 600 m before and 200 m after the intersection. In the simulation, all the vehicles are assumed to be the same type, and the simulation is run in a discrete-time framework with time step $\Delta t = 1$.

We collected the crossing data from driving on the test road net, all the vehicles were set with random trips during 20000 seconds, here we only considered the uncertainty of the car on the road and ignored people for simplicity. Once the traffic signal changes, the speed and position of vehicles in the analysis area of the test road will be recorded, and the moment that vehicles cross through the intersection will also be recorded by a detector placed 5 meters through the intersection. Then the crossing time of passing through the intersection for a series of vehicles could be calculated and normalized with respect to green-yellow and red signal durations, if $\delta n\left(t_{en}\right) = 1$, then $\overline{\tau_n} = \left(\tau_n - t_r\right)/t_r$ and if $\delta n - \left(t_{en}\right) = 0$, then $\overline{\tau_n} = \left(\tau_n - t_g\right)/t_g$. According to the collected data samples, which contains 116 groups in total, there are 49 groups with $\delta n = 1$ and 67 groups with $\delta n = 0$, they are used to build a GPR model for estimating the probability of a vehicle crossing the intersection when an event occurs. As the Fig 3.10 shows, the estimated normalized cross time is predicted by this data-driven model, it is seen that when $\delta n = 0$, the estimated normalized average crossing time $\overline{\tau_n} > 0$, which means that the actual crossing time is likely to be less than or equal to 45 seconds, but as can be seen from Fig 3.11a, there is still a possibility of failure due to some Uncertainty. However, for $\delta n = 0$, the vehicle often have to stop at the intersection, the normalized cross time $\overline{\tau_n} \leq 0$, which means the actual crossing time is more than or equal to 30 seconds as shown in Fig 3.11b. After the training by two-dimensional data samples, the normalized output of the Bayesian network is translated back into the original scale. Finally, the GPR model is used to predict the average cross time and estimate the host vehicle's possibility, which become the basis of stochastic eco-driving decision subsystem to give the recommended velocity.

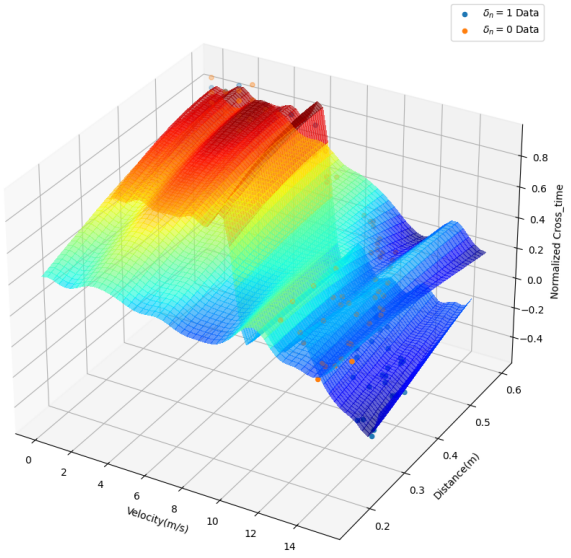


Figure 3.10: 3-D plot of the average normalized cross time predicted by GPR

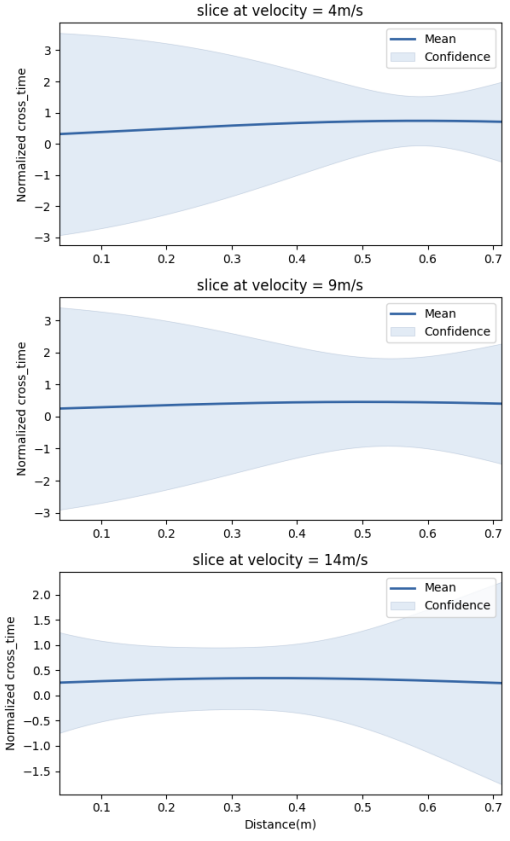


(a) 1-D slice plot with 95% confidence interval when $\delta n = 0$

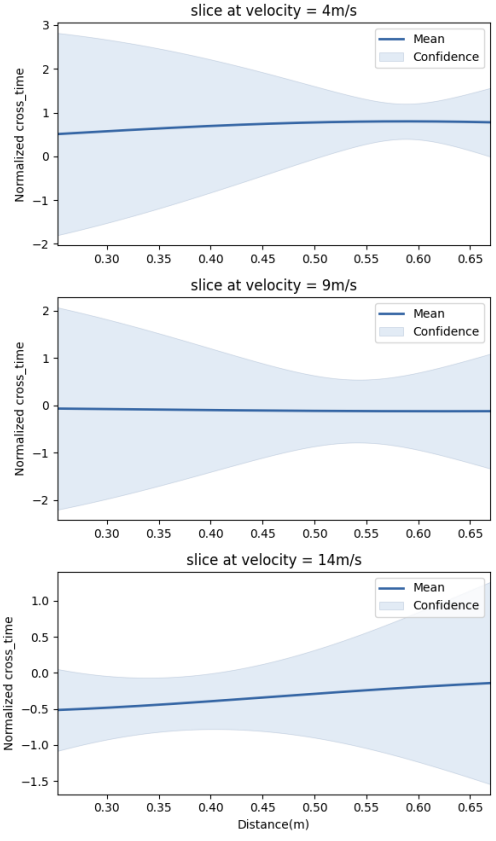


(b) 1-D slice plot with 95% confidence interval when $\delta n = 1$

Figure 3.11: GPR model training by two-dimensional data samples to approximate crossing time

## 3.7/ RESULTS AND ANALYSIS

The performance of S-EDS is analyzed and compared through four simulation experiments with the same traffic characteristics. Firstly, start from several individual tests, when the initial SOC of a host HEV satisfied $SOC_0 > SOC_{MIN}$, taking into account the short driving distance, the proposed stochastic eco-driving system will optimize the energy consumption by adjusting the desired set speed. The performance of the proposed S-EDS is evaluated and compared with the IDM model (without S-EDS) in a free-flow traffic scenario. The distance-velocity, distance-acceleration, distance-time, and distance-cost plots for events $\delta n = 0$ and $\delta n = 1$ are shown in Fig.3.12. In Fig. 3.12a, the IDM model adjusts the $v^{des}$ of the host HEV in the situation where there is a preceding vehicle, when event $\delta n = 0$ (traffic signal from green to red) occurs, so that the speed of the host HEV is always maintained at 12.5$m/s$ until has to stop aggressively near the intersection, but with the proposed S-EDS based on the relatively lower probability, the host HEV is recommended to decelerate early to 10$m/s$ to avoid aggressive braking. Thus the cumulative cost of energy consumption of S-EDS is lower than the IDM vehicle though the travel time of both cars is similar. While as for the event $\delta n = 1$ (traffic signal from red to green), the host HEV is recommended to increase its velocity to have a higher probability of crossing the intersection, but still limited by the speed of the preceding vehicle, and the cumulative energy consumption of S-EDS outperforms the IDM because the brake recovery system of host HEV makes deceleration more advantageous than slow acceleration. At the same time, the host vehicle still has the chance of failing to cross the intersection during this traffic signal cycle with the traditional IDM strategy, as shown in the case of $\delta n = 1$ in Fig. 3.12b, then if there's no speed limit, the S-EDS system will recommend accelerating early to a relatively high speed to obtain the higher probability to cross. In addition, similarly, for the case of $\delta n = 0$ without limit speed, the host vehicle will also be recommended to decelerate in advance to avoid idling at the red light signal.

All of the above analyses and comparisons are individual trajectories, the performance with and without S-EDS are compared in non-congested traffic flow at last. Four traffic simulation experiments with the same traffic flow and distribution are established, S-EDS is applied by two of the four groups, and one group is selected to set $SOC_0 = 0.9$. The other group is $SOC_0 = 0.35$, HEV with a higher initial value of SOC means that the electric energy is sufficient at this time, so the electric mode is applied in this area, but when the initial value of SOC is low, the system will optimize the powertrain operation of HEV according to the predicted vehicle speed to achieve the better energy consumption effect. The other two groups without S-EDS use the same settings. The four groups are divided into two comparison groups; in the first comparison group, the energy costs, which are calculated in pure-electric mode through the optimized set speed, are noted as group 1 (with/without S-EDS1), and in the second comparison group, the energy costs that by applying powertrain optimization are reported as group 2 (with/without S-EDS2). Be-

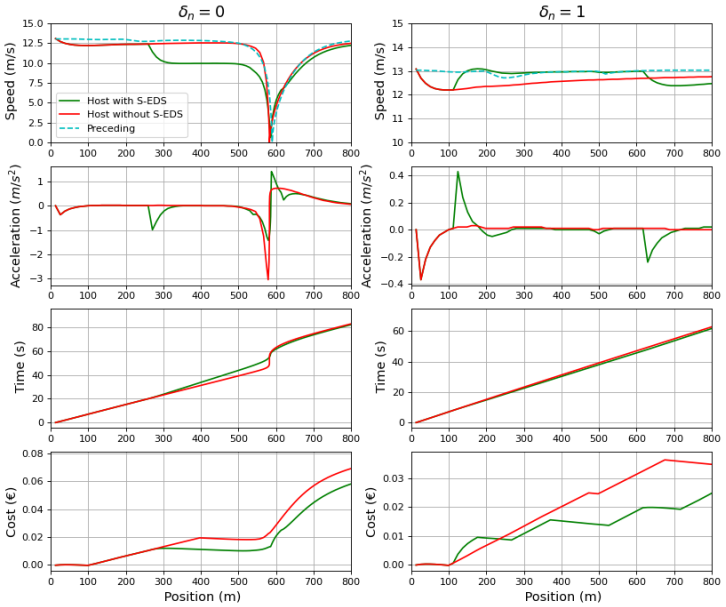


(a) Cases with the speed limit of the preceding vehicle

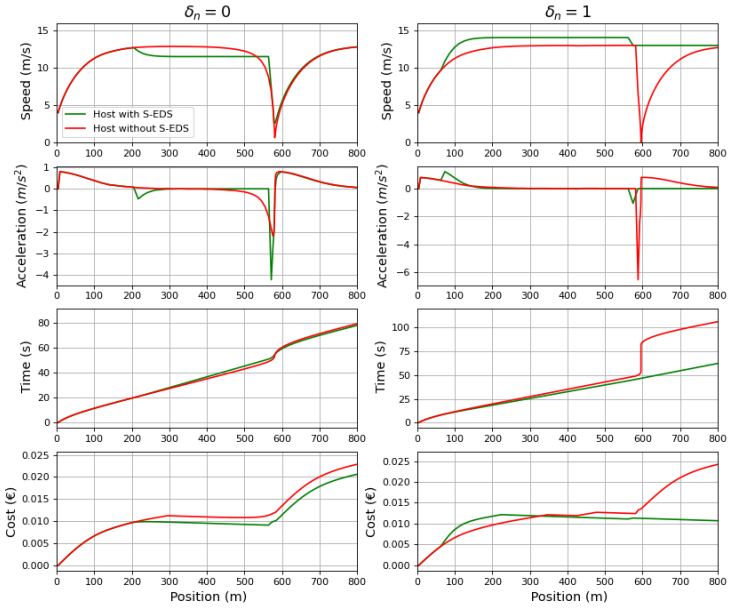


(b) Cases without the speed limit of the preceding vehicle

Figure 3.12: Comparison of the driving performance with and without the stochastic eco-driving system when passing through an 800m intersection, and $\delta n = 0$ represents the traffic signal change from green to yellow to red, $\delta n = 1$ represents the traffic signal change from red to green.

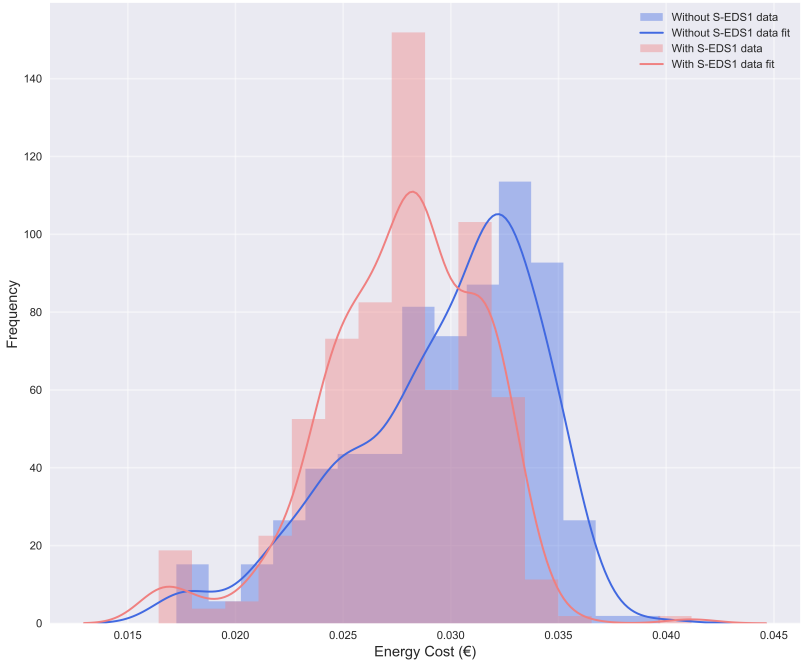


Figure 3.13: Energy costs with/without S-EDS1

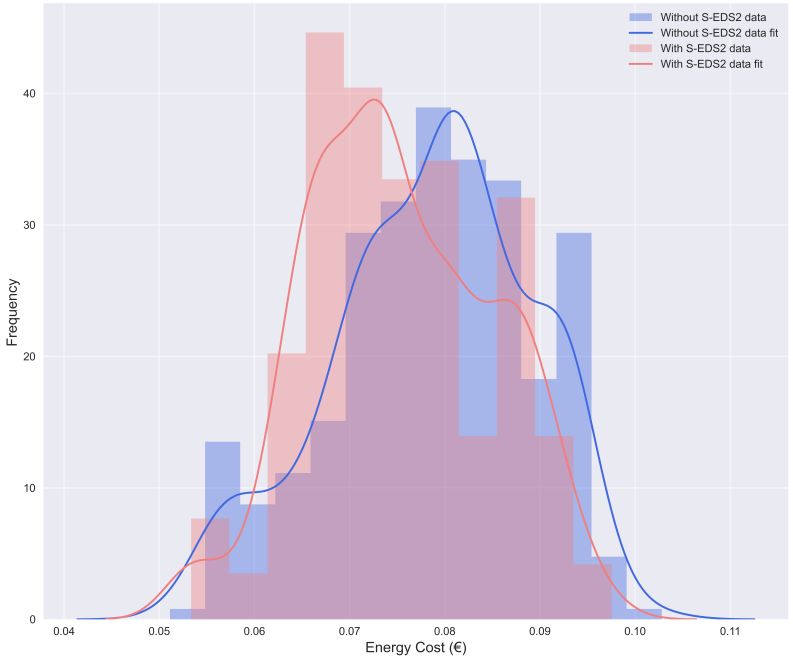


Figure 3.14: Energy costs with/without S-EDS2

cause the time when HEVs appear is uncertain and the total simulation time is set to a fixed value, the numbers of HEVs counted in the four simulation experiments are not the same, the final statistical results indicated the numbers are 345 and 357(with S-EDS),

338 and 341(without S-EDS) respectively. Eventually, the histograms of energy costs are shown in Fig3.13 and Fig3.14, and the percentage improvement in energy cost is given in TABLE 3.2.

Table 3.2: Energy costs improvement with/without S-EDS

| | Energy costs with/without S-EDS1(€) | Energy costs with/without S-EDS2(€) |
|---|---|---|
| Mean value | Without S-EDS1: 0.0297<br>With S-EDS1: 0.0277 | Without S-EDS2: 0.0785<br>With S-EDS2: 0.0752 |
| Energy consumption reduce percentage | 6.49% | 4.17% |

## 3.8/ CONCLUSION

In this chapter, a stochastic eco-driving system with co-optimization of vehicle dynamics and hybrid powertrain operations for power-split HEV is presented and evaluated, which contains a stochastic eco-driving decision subsystem and hybrid powertrain control decision subsystem. For the upper-level stochastic eco-driving decision subsystem, taking into account the randomness of the traffic environment, we used a dual-driven (data and model) approach to suggest the optimal desired set speed or predict the trajectory through stochastic optimization. As for the hybrid powertrain control decision subsystem, the rule-based control strategy is developed to optimize the energy cost of host HEV considering the particularity of the intersection. At last, the performance of the proposed stochastic eco-driving system is evaluated by the simulation cases which were built in SUMO traffic simulation environment; the simulation results show that the energy consumption is reduced by 6.49% and 4.17% respectively compared with the groups without stochastic eco-driving system. Furthermore, this system does not rely on full connectivity with traffic infrastructure, which is its greatest advantage because the realization of connectivity at all intersections is not only costly but also impossible to achieve in the near future. Moreover, the optimization driven by data and model is a promising technology perspective facing future massive traffic data and intelligent transportation systems. Although we have not used real traffic data simulations, our method can be extended relatively easily to consider multiple traffic environments (such as the scenarios where connected and automated hybrid electric vehicles are mixed with human-driven vehicles or pedestrians) and multiple intersections, which is also the direction of future research.

# 4

# A DATA-DRIVEN TRAJECTORY PLANNING STRATEGY

## 4.1/ INTRODUCTION

In Chapter 3, we focus on a power-split HEV as the subject of our research, designing a cooperative optimization framework to enhance fuel economy while ensuring the drive comfort. To simplify the process, we extract stochastic traffic data from the SUMO simulator, as real-world traffic data often presents greater complexity and challenges. In this chapter, we apply real-world traffic datasets in an attempt to develop a data-driven speed planning strategy for connected vehicles (CVs) to achieve fuel efficiency and safety. In this context, we initially choose a general vehicle model for our study rather than using an HEV directly in order to reduce the complexity of data processing. This approach allows for the subsequent extension of our research to scenarios involving the coexistence of HEVs/PHEVs with regular vehicles. Normally we assume in an ITS system, a host vehicle can easily access information about surrounding through V2V and V2I communication, this information may include SPaT data for upcoming intersections, as well as the position information of preceding vehicles. However, when the preceding vehicle is not ”connected” or encounters unforeseen situations, uncertainties in position information may arise. To account for the potential influence of realistic process noise or unexpected changes, we tackle the relative distance between the host and preceding vehicles as a random variable. Therefore, a non-parametric regression (Gaussian Process Regression) is constructed based on historical data to represent the uncertain relative distance between the preceding and host vehicle. Then a optimal control problem is formulated and solved using a Receding Horizon Control (RHC) framework, through transforming the probabilistic constraint into a deterministic constraint within a shorter control interval. Based on these efforts, the numerical simulation applied the NGSIM (Next Generation SIMulation) dataset, demonstrate the effectiveness of the proposed method in improving fuel economy while guarantee the safety simultaneously.

The rest of this chapter is structured as follows: Section 4.2 introduces mathematical for-

mulations of the uncertainty in shared traffic information and treat it as an optimal control problem, while also presenting the normal longitudinal vehicle dynamics. Section 4.3 reviews the Gaussian sampling planner method for handling chance constraints. Section 4.4 provides details on our proposed method, which is based on the GPR-based predictor and the receding control framework. Section4.5 exhibits the process of data preparation. Section 4.6 presents the simulation results for the reviewed Gaussian sampling planner method and the proposed GPR-based method, comparing their outcomes to demonstrate effectiveness. Lastly, Section4.7 offers the conclusion and discusses future work.

## 4.2/ Problem Formulation

### 4.2.1/ Uncertainty in Shared Information

As described in the introduction, the host vehicle can easily access information about its surroundings via V2V or V2I communication in a CAV system, which may include SPaT information of upcoming intersection, as well as the position information of preceding vehicle, denoted as $s_j$. But once the preceding vehicle can not be "connected" or encounter some unforeseen situation, there will be uncertainties in position information provided by the preceding vehicle. To model the potential influence of the realistic process noise or

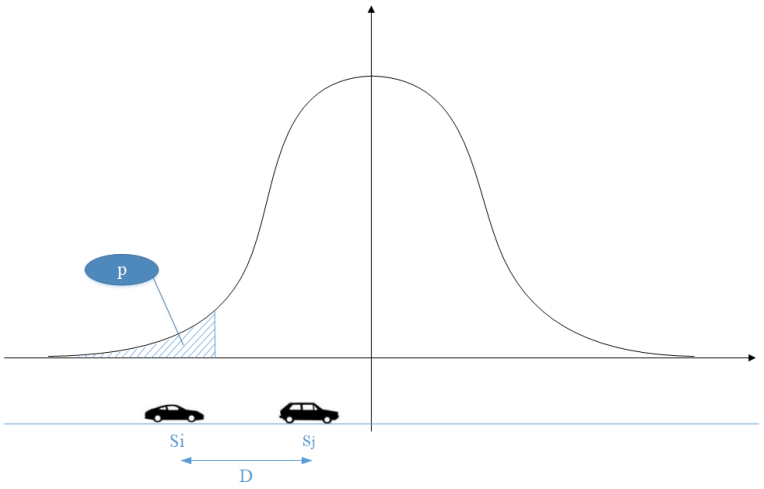


Figure 4.1: Schematic of the probability of collision between the preceding and the host vehicles

unforeseen changes, we consider the relative distance between the host and preceding vehicle as a random variable $D$, it is worth noting that the true distribution of $D$ is unknown. The probability distribution diagram in Fig.4.1 is only a schematic representation, but a probabilistic constraint would capture the collision avoidance requirement.

### 4.2.2/ VEHICLE MODEL

Firstly, we use the regular vehicle model and energy model for the numerical modeling. The longitudinal vehicle dynamics [113] of $i$ th vehicle is given by,

$$f_i\left(x^i, u^i\right) = \begin{bmatrix} v^i(t) \\ u^i(t) - \frac{1}{2M_i} C_D^i \rho A_v^i v^i(t)^2 - \mu g - g\theta \end{bmatrix} \tag{4.1}$$

where the control variable is $u^i$, tractive force per unit of mass, the state variable $x^i = \left[s^i, v^i\right]^T$ includes the position $s^i$ and the velocity $v^i$ of a host vehicle. And for simplicity, we assume that road gradients are small, thus there is $\sin(\theta) \approx \theta$ and $\cos(\theta) \approx 1$. The rest parameters, $M_i$, $C_D^i$, $\rho$, $A_v^i$, $\mu$, $g$ and $\theta$ are the vehicle mass, air drag coefficient, air density, front area, rolling resistance coefficient, gravitational acceleration, and road gradient separately.

And the energy model can be estimated as [26],

$$\begin{aligned} m_f^i(t) = b_0 + b_1 V^i(t) + b_2 V^i(t)^2 + b_3 V^i(t)^3 \\ + \bar{a}^i(t)\left(c_0 + c_1 V^i(t) + c_2 V^i(t)^2\right) \end{aligned} \tag{4.2}$$

where $m_f$ denotes the fuel consumption rate (in ml/sec),$b_0$, $b_1$, $b_2$, $b_3$, $c_0$, $c_1$ and $c_2$ are the consumption parameters. $\bar{a}^i(t)$ is the non-negative acceleration and given by

$$\bar{a}^i(t) = \begin{cases} a^i(t) + g\sin\theta, & \text{if } a^i(t) + g\sin\theta \geq 0 \\ 0, & \text{otherwise} \end{cases} \tag{4.3}$$

### 4.2.3/ OPTIMAL CONTROL PROBLEM

The goal of host vehicle is to improve its fuel economy while avoiding rear-end collisions, thus the objective function is

$$\min \sum_{t=k}^{k+T-1} \frac{m_f^i(t)}{v^i(t)} \tag{4.4}$$

where $t$ is the discrete time, the finite time horizon length $T$ is chosen to be the time remaining until the end of the current or the next green-light window from any time $k$ begins. Here it's worth noted that $v$ and $V$ in the Eq.4.2 both is velocity, but the difference is that the unit of $V$ is $km/h$ and $v$ is $m/s$.

The probability of relative distance between the host vehicle (index $i$) and preceding vehicle (index $j$) is required to drop below a threshold $d_{\min}$ to be less than $\beta$ at each time step for avoiding a potential collision, which is given by

$$P\left(s^j(t) - s^i(t) < d_{\min}\right) \leq \beta \tag{4.5}$$

And the predicted states from any time $k$ are denoted by $x^i(t+1 \mid k)$ and discretized system dynamics are calculated by

$$x^i(t+1 \mid k) = f_{di}\left(x^i(t \mid k), u^i(t \mid k)\right) \tag{4.6}$$

At last, the boundary of each time step velocity is road speed limits, $v_{\min}$ and $v_{\max}$, the control bounds are $u_{\min}$ and $u_{\max}$.

$$\begin{aligned} v_{\min} \leq v^i(t \mid k) \leq v_{\max} \\ u_{\max} \leq u^i(t \mid k) \leq u_{\min} \end{aligned} \tag{4.7}$$

## 4.3/ Review Method

### 4.3.1/ Deterministic Equivalent of Chance Constraint

The review method comes from the reference [114], the authors model the uncertainties by defining the position of preceding vehicle as a random variable and suppose it obey the Gaussian distribution for over-approximation. Then for the constraint Eq 4.5, the probability of collision avoidance constraint constraint violation must be upper bounded by $\beta$, if the position of preceding vehicle is considered as a random vector $S_j(t)$, whose elements follow a Gaussian distribution $S_j(t) \sim \mathcal{N}\left(s_j(t), \sigma_j^2(t)\right)$ with changing mean $s_j(t)$ and variance $\sigma_j^2(t)$. Here, the mean is the shared or predicted position, the time-varying standard deviation captures the amount of possible deviation. Increasing standard deviation models the prediction error. So for a given mean $s_j$ and standard deviation $\sigma_j$ of $S_j(t)$, the probability of collision when the host vehicle position $S_i$,

$$p = \mathbb{P}\left(s_i - L_i/2 \leq S_j - L_j/2 \leq s_i + L_i/2\right) \tag{4.8}$$

where $L_i$ and $L_j$ are the lengths of the vehicles $i$, $j$, $s_i$ is the position of host vehicle at each time step, then we suppose,

$$\lambda = \frac{s - (s_j - \frac{L_j}{2})}{\sigma_j} \tag{4.9}$$

By this changes of variable, we can get the following equations,

$$\begin{aligned} p &= \int_{\lambda_1}^{\lambda_2} \frac{1}{\sqrt{2\pi}} e^{\frac{-\lambda^2}{2}} d\lambda \\ \lambda_1 &= \frac{-D + \frac{L_j - L_i}{2}}{\sigma_j} \\ \lambda_2 &= \frac{-D + \frac{L_j + L_i}{2}}{\sigma_j} \\ D &= s_j - s_i \end{aligned} \tag{4.10}$$

if the relative distance of $D$ is confirmed, the probability of collision would be $p$. Here we can obtain an analytical approximation of the minimum distance that the host vehicle should keep with its preceding vehicle so that the probability of collision is less than $\beta$. Then taking a first-order Taylor expansion around $\lambda_0 = \frac{-D + \frac{L_j}{2}}{\sigma_j}$

$$p \simeq \frac{1}{\sqrt{2\pi}} \int_{\lambda_1}^{\lambda_2} e^{\frac{-\lambda_0^2}{2}} \left(1 - \lambda_0 \left(\lambda - \lambda_0\right)\right) d\lambda \tag{4.11}$$

Hence,

$$p \simeq \underbrace{\left(\lambda_2 - \lambda_1\right)}_{=L_i/\sigma_j} \frac{e^{\frac{-\lambda_0^2}{2}}}{\sqrt{2\pi}} [\left(1 + \lambda_0^2\right) - \frac{\lambda_0}{2} \underbrace{\left(\lambda_2 + \lambda_1\right)}_{=2\lambda_0}] \simeq \frac{L_i e^{\frac{-\lambda_0^2}{2}}}{\sqrt{2\pi\sigma_j^2}} \tag{4.12}$$

After considering $p < \beta$, we can get an analytical approximation of the required relative distance $D\left(\sigma_j, \beta\right)$, which is a function of the standard deviation of the uncertainty and the chosen probability threshold in constraint Eq 4.5, which can be forced as,

$$s_j(t) - s_i(t) \geq D\left(\sigma_j(t), \beta, \tau\right) \tag{4.13}$$

$$D\left(\sigma_j(t), \beta, \tau\right) \simeq \frac{L_j}{2} + \sigma_j(t) \sqrt{\log\left(\frac{L_i^2}{2\pi\sigma_j^2(t)\beta^2}\right)} \tag{4.14}$$

### 4.3.2/ Gaussian Sampling-Based Planner

Based on the above analysis, the chance constraint Eq.4.5 can be transformed to a deterministic interval through the approximation and assumption of Gaussian distribution. However, the finite horizon length $T$ in Eq.4.4 is typically large enough to obtain a feasible solution, which increases the computational complexity to solve the nonlinear optimization. Still in [114], a sampling-based method is employed to sample the control space and retain only those solutions that fulfill the constraints and objective function. Specifically, the control solution is obtained by Gaussian distribution as,

$$u_s(k) \sim \mathcal{N}\left(\mu(k), \sigma_c^2(k)\right) \tag{4.15}$$

where $u_s(k)$ is the control input sampled at each time step following the Gaussian distribution with mean $\mu(k)$ and standard deviation, $\sigma_c(k)$ depend on current target velocity and the relative distance between the host and the preceding vehicle. This distribution is different from the probability distribution followed by the information/prediction uncertainty. Here,

$$\begin{aligned} \mu(k) &= a(k) + \frac{1}{2M_i} C_D^i \rho_a A_v^i v_i(k)^2 + \mu g + g\theta \\ \sigma_c(k) &= \frac{\beta_1}{\left| \frac{\Delta s_a(k)}{\Delta s_c(k) - \beta_2} \right|} \end{aligned} \tag{4.16}$$

where $\mu(k)$ of the Gaussian distribution is chosen as the acceleration that maintains the target velocity $v_{\text{target}}$ for the host vehicle as the following,

$$a(k) = \frac{v_{\text{target}}\,(k) - v(k)}{\Delta t} \tag{4.17}$$

The target velocity is calculated wisely using SPAT information that helps the vehicle avoid stopping at red light,

$$v_{\text{target}}\,(k) = \frac{d_{ia}(k)}{g_a} \tag{4.18}$$

where $d_{ia}$ is the distance between $s_i(k)$ (location of the host vehicle) and the traffic signal $a$, $g_a$ is the time to green signal of the traffic signal $a$, which creates a feasible velocity space for making the vehicle move past traffic signal $a$ through a green light window.

In addition, the following equations will give the definition of $\Delta s_a$ and $\Delta s_c$ in Eq.4.16.

$$\begin{aligned} \Delta s_a &= s_j - s_i \\ \Delta s_c &= d_{\min} + \alpha v_i \end{aligned} \tag{4.19}$$

Since the host vehicle is required to perform rear-end collision avoidance, the standard deviation $\sigma_c(k)$ is computed to smaller if the relative distance $\Delta s_a$ between the host and the preceding vehicle is larger. And the highly probable control solution space expands when the relative distance decreases, facilitating collision avoidance control actions, the vehicle tends to cruise at the target velocity. Vice versa, the standard deviation will be smaller when the relative distance is smaller.

## 4.4/ Proposed Method

### 4.4.1/ GPR-based Relative Distance Prediction

The reviewed method in section 4.3 is based on the assumption that the position of preceding vehicle follows Gaussian distribution. Next, inspired by this review method, the actual distribution of the preceding vehicle's position, as well as the relative distance between the host and the preceding vehicle, is actually unknown. In this case, the variable

can be considered a random vector. As the relative distance is characterized by a random vector, it can be inferred that a nonlinear stochastic relationship exists between the distance difference and the traffic environment. To address this, Gaussian Process Regression (GPR) can generate the predicted output after learning a functional mapping from the training inputs and outputs, which can be implemented by parameterizing a covariance function.

Given a training set including $n$ input-output pairs, where an arbitrary element $X = [x_1, x_2, \ldots, x_n]^{\mathrm{T}}$ is a D-dimension vectors. The training input $x_i$ is related to a scalar value $y_i$, $y = [y_1, y_2, \ldots, y_n]^{\mathrm{T}}$, each output $y_i$ is related to the relevant input vector $x_i$ under a latent function $\gamma_i$ and is disturbed by gaussian noise $\varepsilon_i$, which can be written as,

$$\begin{aligned} y_i &= \gamma_i + \varepsilon_i \\ \varepsilon_i &\sim N\left(0, \sigma^2\right) \end{aligned} \tag{4.20}$$

where the $n$ latent variables are collected into a vector form $\gamma = [\gamma_1, \gamma_2, \ldots, \gamma_n]^T$, the $\gamma$ is considered to follow a joint Gaussian distribution and a random single $\gamma_i$ follows a GP, which is fully specified by a mean function and covariance function [111],

$$\gamma_i \sim \mathcal{GP}\left(\mu_i\left(x_i\right), k\left(x_i, x_j\right)\right) \quad i, j = 1, 2, \ldots, n \tag{4.21}$$

where is also called a Gaussian process prior, $x_i$, $x_j$ are two arbitrary inputs, $\mu_i(\cdot)$ is the mean function, $k(\cdot)$ is the covariance function. From the Gaussian process prior, the collection of training points $(x, y)$ and test points $X_*$ are joint multivariate Gaussian distributed as follows [62],

$$\begin{pmatrix} y \\ \gamma_* \end{pmatrix} \sim \mathcal{N}\left(0, \begin{pmatrix} K + \sigma^2 I & K_* \\ K_*' & K_{**} \end{pmatrix}\right) \tag{4.22}$$

$\gamma_*$ is predict function value set at $m$ test points $X_*$, where, $X_* = \left[x_1^*, x_2^*, \ldots, x_m^*\right]^T$, $\gamma_* = \left[\gamma_1^*, \gamma_2^*, \ldots, \gamma_m^*\right]^T$ and $K$ is the covariance kernel matrix where its entries correspond to the covariance function evaluated at observations, $(K)_{ij} = k\left(x_i, x_j\right)$, $(K_*)_{ij} = k\left(x_i, x_j^*\right)$, $(K_*')_{ij} = k\left(x_i^*, x_j\right)$ and $(K_{**})_{ij} = k\left(x_i^*, x_j^*\right)$. As the joint distribution is Gaussian,it is able to have predictive posterior distribution,

$$\begin{aligned} p\left(\gamma_* \mid y, \theta, \sigma^2\right) &= \mathcal{N}\left(\gamma_* \mid \mu_*, \Sigma_*\right) \\ \mu_* &= K_*'\left(K + \sigma^2 I\right)^{-1} y \\ \Sigma_* &= K_{**} - K_*'\left(K + \sigma^2 I\right)^{-1} K_* \end{aligned} \tag{4.23}$$

where the hyperparameter $\theta$ should be the optimal to build the kernel function. Normally

the optimization is realized by maximizing the marginal likelihood

$$\theta_{\max} = \arg\max\{\log(p(y \mid X, \theta))\} \tag{4.24}$$

In this work, we assume the predicted relative distance $D_*$ at each step $\Delta t$ from the current time $t$ follows the GP as

$$p\left(D_* \mid X_*, X_{tr}, y_{tr}\right) \sim \mathcal{GP}\left(\mu(\cdot), K(\cdot)\right) \tag{4.25}$$

where the inputs $X_{tr}$ represent the effect of the traffic information on the relative distance. Specifically, the following information is recorded as Fig.3.11 indicated,

1) The relative distance between the preceding and host vehicle $y_{tr} = s^j(t+\Delta t) - s^i(t+\Delta t)$

2) The relative velocity between the preceding and host vehicle $x_{tr,i} = v^j(t) - v^i(t)$

3) The distance to from the host vehicle to intersection $x_{tr,j} = s - s^i(t)$

The uncertainties in position information make the true distribution of relative distance at each step is unknown, but after training the GPR model by optimizing the hyperparameter $\theta$ with historical traffic information, the real distribution model of relative distance can be approximated. Once the relative distance $D_*$ is predicted from the GPR model with new

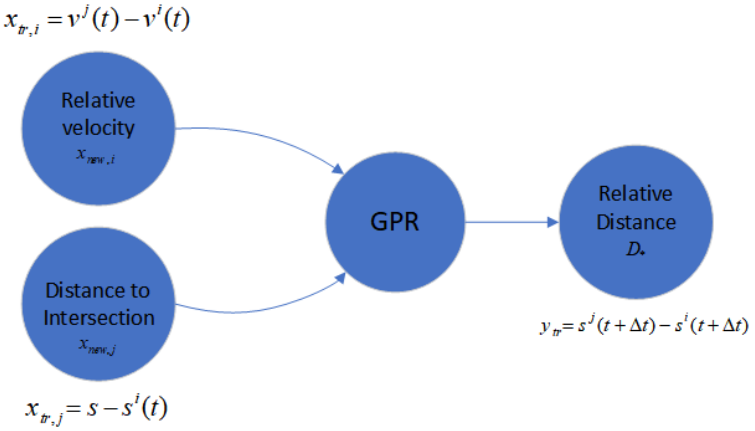


Figure 4.2: Gaussian Process Regression Prediction Model

inputs $x_{new,i}, x_{new,j}$, we obtain the mean $\mu_{D_*}$ and the covariance matrix $\Sigma_{D_*}$, i.e., $D_* \sim N(\mu_{D_*}, \Sigma_{D_*})$. Then, once the exact collision possibility $\beta$ is settled, like less than 5%, 1%, the constraint in Eq.4.5 is calculated using the inverse cumulative distribution function as,

$$\begin{aligned} &P\left(s^j(t+\Delta t) - s^i(t+\Delta t) < d_{\min}\right) \\ &= P\left(D_* < d_{\min}\right) \leq \beta \end{aligned} \tag{4.26}$$

### 4.4.2/ Receding Horizon Control Problem

The optimal control model is built in Section 4.2.3 as a nonlinear optimization methods for solving the problem. However, the finite horizon length $T$ in Eq.4.4 is sometimes too large to obtain a feasible solution. Thus a data-driven Receding Horizon Control (RHC) framework, which has the shorter horizon, is proposed to solve the dynamic control problem, as shown in Fig.4.3.

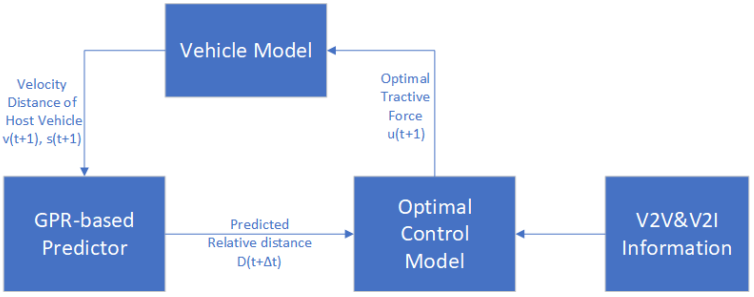


Figure 4.3: The structure of data-driven receding horizon control model

To ensure the constraints Eq.4.5, the following constraints will be added to each control interval,

$$\tau_c \frac{ds_t}{dt} + s_t = sp \tag{4.27}$$

$$v^i\left(t_f\right) = v_t = v^j(t_0) + a^j(t_0)\Delta t \tag{4.28}$$

where $\tau_c$ is the time constant of desired controlled variable response, $sp$ is the target bounds to final set-point dead-band, $s_t, v_t$ is the desired location and velocity target, $d_{min}$ is the minimum safe distance with certain probability, which is calculated from (4.26). Then in order to solve this nonlinear receding horizon control problem, the optimization suite for Python named Gekko [83] is employed in this work, which is a powerful toolbox to perform estimation, optimization, and predictive control via multiple solvers, including active set solver (APOPT) and interior point solver (IPOPT). For more details, please refer [45], and one of the simultaneous approaches for solving nonlinear control problems is to convert dynamic equations to algebraic equations by orthogonal collocation on finite elements. In this strategy, the dynamic optimization is converted to LP, quadratic programming (QP), nonlinear programming (NP), MILP, or mixed-integer nonlinear programming problems (MINLP) that large-scale solvers can solve.

## 4.5/ Data Description

The NGSIM Peachtree dataset was collected from an arterial segment on Peachtree in Atlanta, Georgia; the arterial segment was approximately 640 meters (2100 feet) in length with 4 signalized intersections. It includes the spatial and temporal information of all the

vehicles as well as the traffic light information from 12:45 p.m. to 1:00 p.m.and 4.00 p.m. to 4.15 p.m. on November 8, 2006 [1]. For data preparation, the traffic data between 12th Street NE and 14th Street NE, as shown in Fig. 4.4, will be used for training and testing the relative distance prediction and evaluation. The intersection of 14th St. NE and Peachtree St. NE is 600 meters from the first intersection, and the distance from the intersection of 12th NE to the stop line of 14th St. NE is measured to be about 221 meters (726 feet). In addition, to simplify as much as possible, the final selection of the number of host vehicles in the study area meets the requirements in the presence of the previous vehicle restrictions, and no lane change, overtaking, and other driving behavior is 44. The SPaT information at the 14th St. NE is also obtained based on the phase start/end time provided in the data. Then we record the relative speed and the position of the host vehicle from the signalized intersection at $t$ moment, as well as the relative distance at the future $t + \Delta t$ timestep. The latter record variable includes both spatial and temporal information.

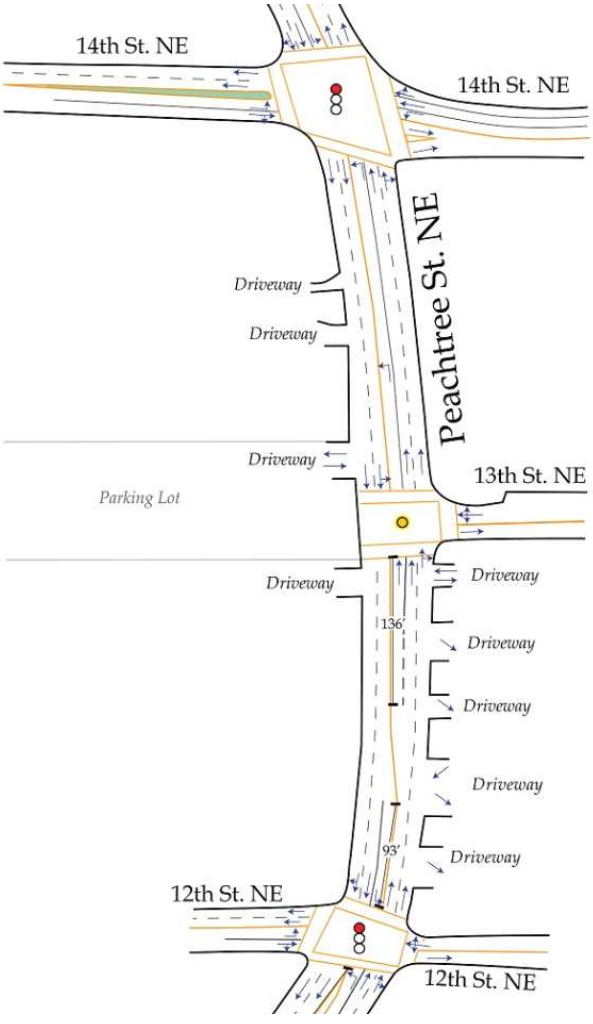


Figure 4.4: Study area schematic

## 4.6/ RESULTS AND ANALYSIS

### 4.6.1/ SIMULATION RESULTS OF REVIEW METHOD

According to the previous method, the simulation scenario is built with traffic light at 200m intervals on a single lane urban road. The case is settled considering standard deviation of uncertainty increasing over time to model the prediction uncertainty as the Eq.4.14 described.

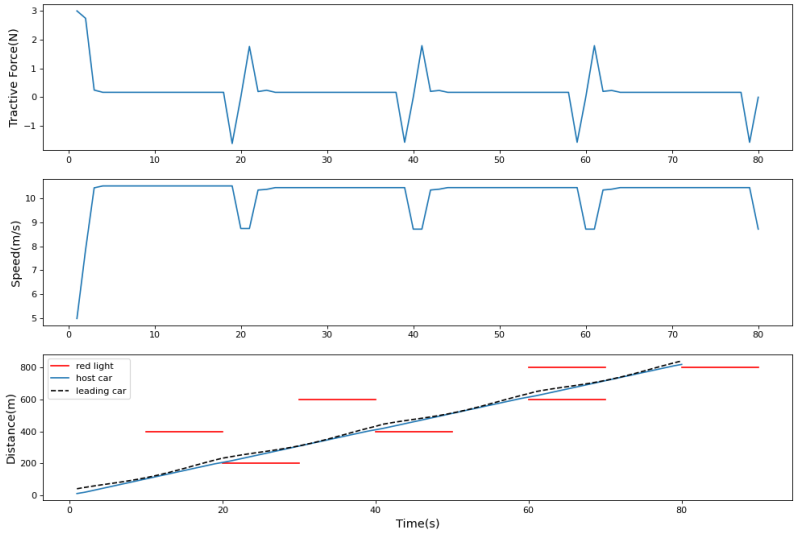


(a) Results without gaussian planner (Baseline)

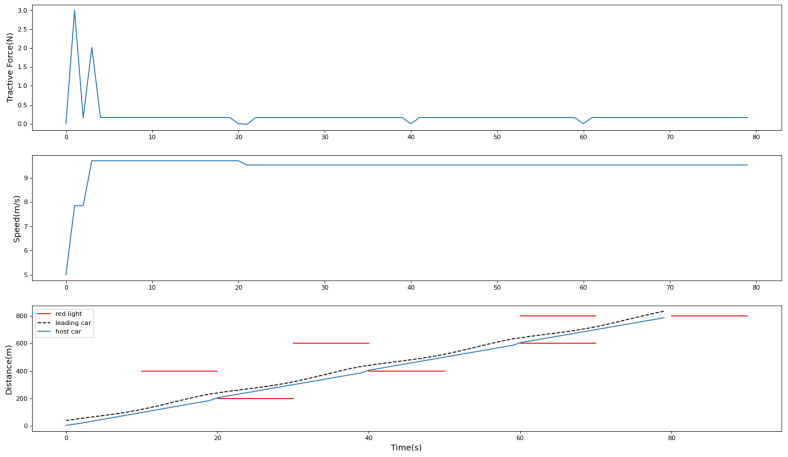


(b) Results with gaussian planner (Gaussian Planner)

Figure 4.5: Simulation Results

Fig.4.5 shows the tractive force, velocity and distance profiles without/with gaussian planner, respectively. We use the MPC based fuel efficient controllers without gaussian planner as baseline methods, compare the fuel consumption and the average computation time per iteration. As expected, with the gaussian sampling planner limit the initial value for the MPC controller, the computation time and fuel consumption are both decreased as the Table.4.1 recorded. Fig.4.6 shows the details of the distance-time diagram for the host car and the leading car, from which we can see that the control of the host car relative distance is more conservative when using the gaussian sampling planner compared with the baseline relative distances, and because the speed range of the initial limit minimize the tractive force adjustment and thus reduce the fuel consumption based on gaussian sampling planner method, which verifies the effectiveness of the reviewed method.

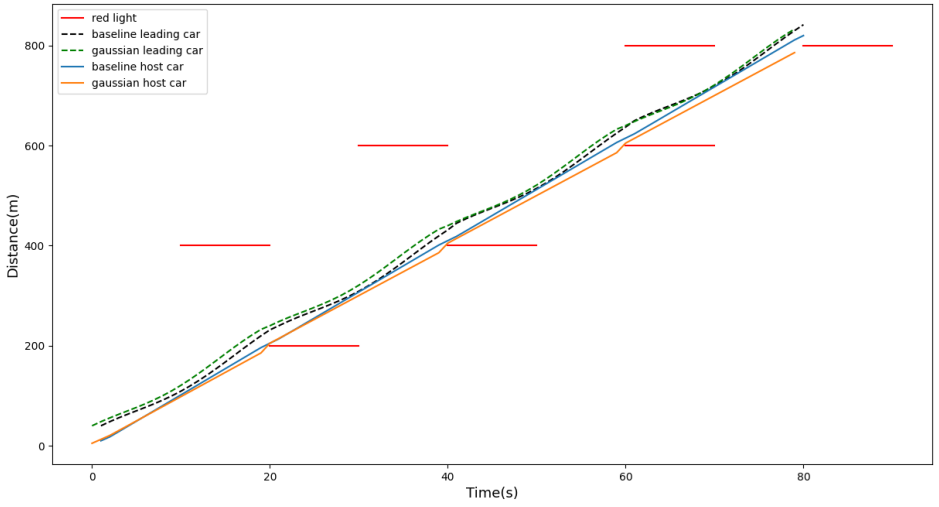


Figure 4.6: Distance-time diagram comparison

Table 4.1: Simulation results with time varying standard deviation

| Method | Fuel Consumption (ml) | Average Time/Iteration (s) |
|---|---|---|
| Baseline | 2603.82 | 8.75 |
| Gaussian Planner | 2032.88 | 3.75 |

### 4.6.2/ Simulation Results for Prediction

According to the proposed method, we train the real-world traffic data after processing for modeling the probability of relative distances. The prediction results for relative distance are presented in this subsection. As shown in Fig.3.11, the speed difference between the host vehicle and the preceding vehicle and the distance to intersection are used as inputs to predict the relative distance between the preceding vehicle and the following vehicle after $\Delta t$ time steps.For simplicity, the relative distance is normalized for the standard

minimum safe distance, which is calculated as the followings,

$$D_{st} = \begin{cases} 30, & V \leq 40 \\ 40, & 40 < V \leq 50 \\ V, & V > 50 \end{cases} \tag{4.29}$$

$$\overline{y_{tr}} = \frac{y_{tr} - D_{st}}{D_{st}} \tag{4.30}$$

where $D_{st}$ is the standard minimum safe distance, $V$ is the velocity $km/h$, $\overline{y_{tr}}$ is the normalized relative distance. Then in order to select the appropriate forecasting time step as well as the size of the training data, the mean absolute error (MAE) is adopted to measure the accuracy of, which is defined as

$$MAE = \frac{\sum_{i=1}^{N} |\hat{y} - y|}{N} \tag{4.31}$$

where *N* is the number of observations, $\hat{y}$ is predicted value and $y$ is the observed value.

A summary of the comparative results of different training sizes and forecasting times can be seen in Table 4.2. In terms of computational cost for training, when the prediction time is set to 3 seconds or 5 seconds, and the scale of the training data only accounts for 10% of the total sample size, the computational time for training is the shortest. Nevertheless, once the prediction accuracy is considered, it is observed that the best results are obtained when the prediction time is set to 5s, and 30% of the total sample data is used for training. Therefore, compared to the 50% and 70% training scale, 30% training time is acceptable, and with the highest accuracy, it will be chosen to do the subsequent calculation. For example, fig 4.8 shows the slices of the GPR model with 30% of the training data at a distance of 80m from the intersection for different horizons (3s and 5s), respectively, from which we can see more intuitively that compared to the 3s prediction horizon, 5s prediction horizon covers more data points within the 95% confidence interval.

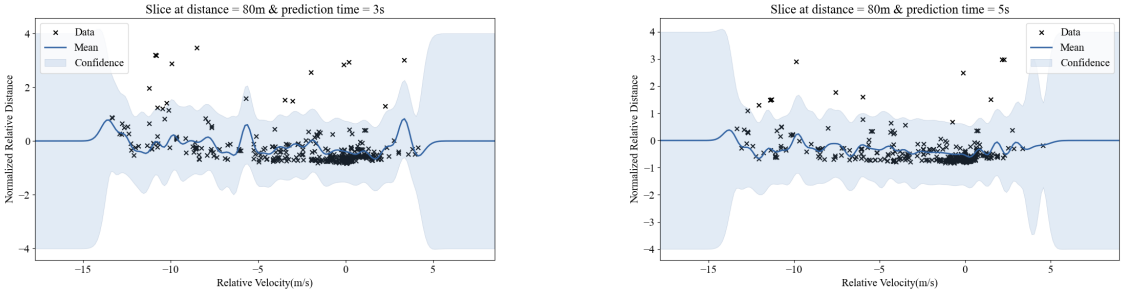


(a) 10% training with prediction time = 3s

(b) 10% training with prediction time = 5s

Figure 4.7: Relative distance prediction for different horizons by 10% training

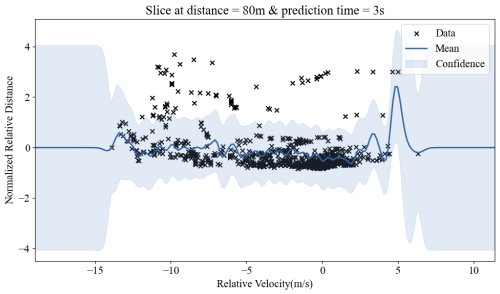


(a) 30% training with prediction time = 3s

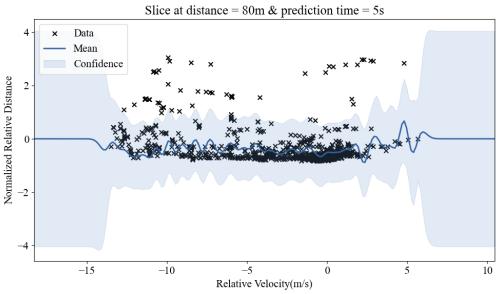


(b) 30% training with prediction time = 5s

Figure 4.8: Relative distance prediction for different horizons by 30% training

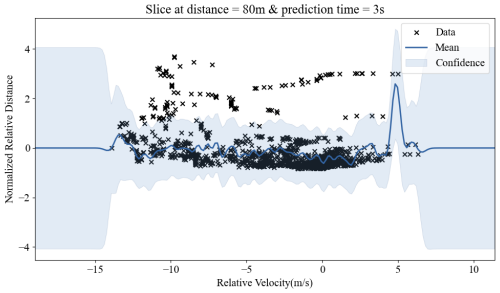


(a) 50% training with prediction time = 3s

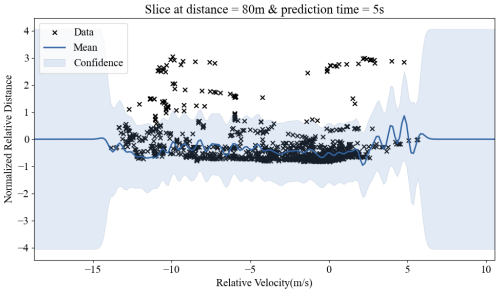


(b) 50% training with prediction time = 5s

Figure 4.9: Relative distance prediction for different horizons by 50% training

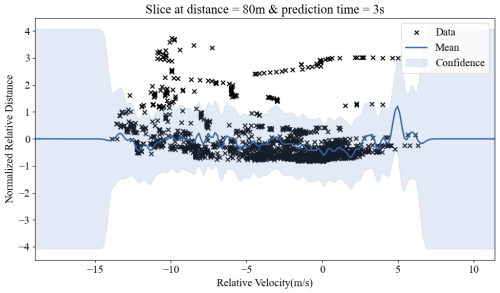


(a) 70% training with prediction time = 3s

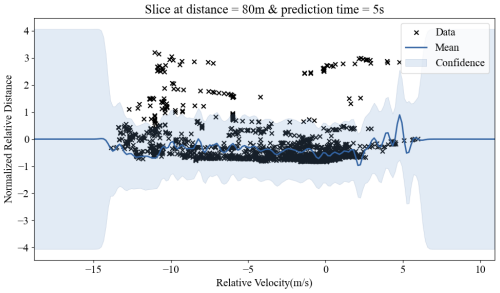


(b) 70% training with prediction time = 5s

Figure 4.10: Relative distance prediction for different horizons by 70% training

### 4.6.3/ Simulation Results for Optimization

To evaluate the performance of optimization results, the parameters for simulation are designed uniformly with host vehicle as shown in Table 4.3. Next, based on the input variables and prediction horizon selected in the previous subsection, we obtain the simulation results of energy consumption corresponding to different $\beta$ values. Required in the constraint (4.26), the probability that the relative distance between the host and the preceding vehicle is then less than the threshold $d_{min}$ in each time step to be less than $\beta$ for avoiding a potential collision.

Table 4.2: Comparative results of relative distance prediction model

| | Prediction Time(s) | MAE(m) | Training Time(s) |
|---|---|---|---|
| 10% Training | 3 | 0.2 | 2.25 |
| | 5 | 0.144 | 2.41 |
| 30% Training | 3 | 0.183 | 21.98 |
| | 5 | 0.123 | 17.21 |
| 50% Training | 3 | 0.155 | 71.92 |
| | 5 | 0.136 | 68.75 |
| 70% Training | 3 | 0.172 | 180.64 |
| | 5 | 0.131 | 152.1 |

Table 4.3: List of vehicle parameters

| Definition | Symbol | Value |
|---|---|---|
| vehicle mass | $M$ | 1200 |
| frontal vehicle area | $A_v$ | 2.5 |
| drag coefficient | $C_d$ | 0.32 |
| air density | $\rho$ | 1.184 |
| rolling resistance | $\mu$ | 0.013 |
| gravity acceleration | $g$ | 9.8 |
| consumption parameters | $b_0$ | 0.1569 |
| | $b_1$ | 0.0245 |
| | $b_2$ | $-7.415\text{e}{-04}$ |
| | $b_3$ | $5.975\text{e}{-05}$ |
| | $c_0$ | 0.0722 |
| | $c_1$ | $9.68\text{e}{-02}$ |
| | $c_2$ | $1.075\text{e}{-03}$ |

The simulation scenario uses accurate trajectories of 44 cars, with the time step of the original dataset resampled from $0.1s$ to $1s$. It is important to note that driving behaviors, such as no overtaking and lane changing, are restricted only for the host vehicle, as mentioned in Section 4.5, however, the corresponding preceding vehicle(s) in the specified study area are not subject to these restrictions.

This leads to a range of situations. At times, there may be only one preceding vehicle, with its trajectory serving as the safety constraint. In other instances, there may be more than one preceding car. For example, the first vehicle might temporarily change lanes, causing the second car to suddenly appear. Alternatively, a car in another lane may

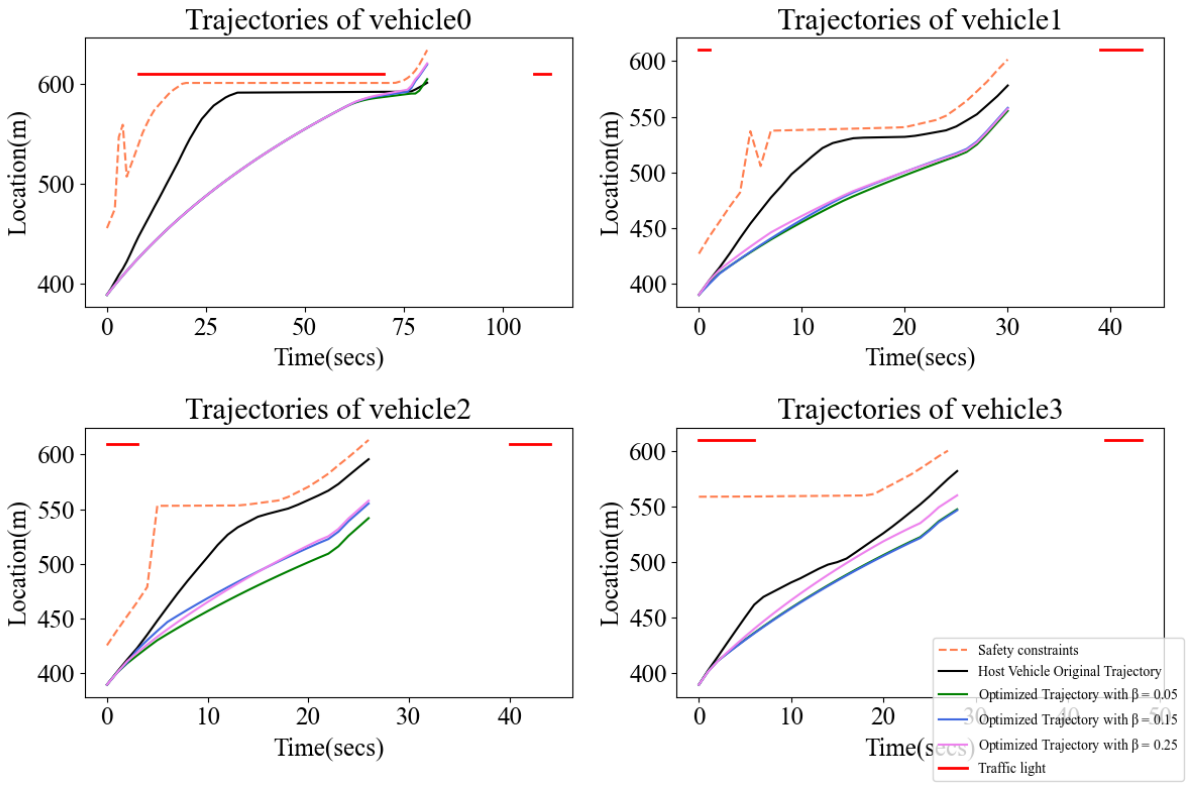


Figure 4.11: A comparison of different time-space trajectories for host vehicles

abruptly switch lanes and become the host vehicle's preceding car, making the safety distance between the preceding vehicle and the host car highly uncertain. To explore the relationship between driving trajectories and fuel consumption of host vehicles, we set different values for the parameter $\beta$.

Table 4.4: Performance of the proposed prediction-based strategy

| | Fuel consumption(ml/m) | | | | | | |
|---|---|---|---|---|---|---|---|
| Vehicles | Original trajectory | Optimized trajectory with $\beta$ = 0.05 | Percentage reduction | Optimized trajectory with $\beta$ = 0.15 | Percentage reduction | Optimized trajectory with $\beta$ = 0.25 | Percentage reduction |
| vehicle0 | 2.32 | 1.53 | 33.97% | 1.70 | 26.62% | 1.73 | 25.45% |
| vehicle1 | 4.44 | 3.69 | 16.95% | 3.55 | 20.02% | 3.74 | 15.66% |
| vehicle2 | 3.76 | 2.82 | 24.86% | 4.43 | -17.82% | 3.40 | 9.56% |
| vehicle3 | 2.83 | 3.50 | -23.70% | 2.78 | 1.89% | 2.77 | 2.21% |

From the above dataset, 10% of the host vehicles are randomly selected for simulation. Fig **??** displays the comparison of trajectories for 4 different host vehicles driven by the driver and calculated using the proposed strategy, while Fig 4.12 shows their corresponding fuel consumption performance, and the specific fuel consumption values are presented in TABLE 4.4.

As mentioned earlier, the safe constraint in Fig.4.11 may be a set of a complete trajectory or may be determined by the position of multiple preceding vehicles. Moreover, we can also observe that as the parameter $\beta$ increases, the relative distance between the optimized trajectory and the safety constraint slightly expands, indicating a higher poten-

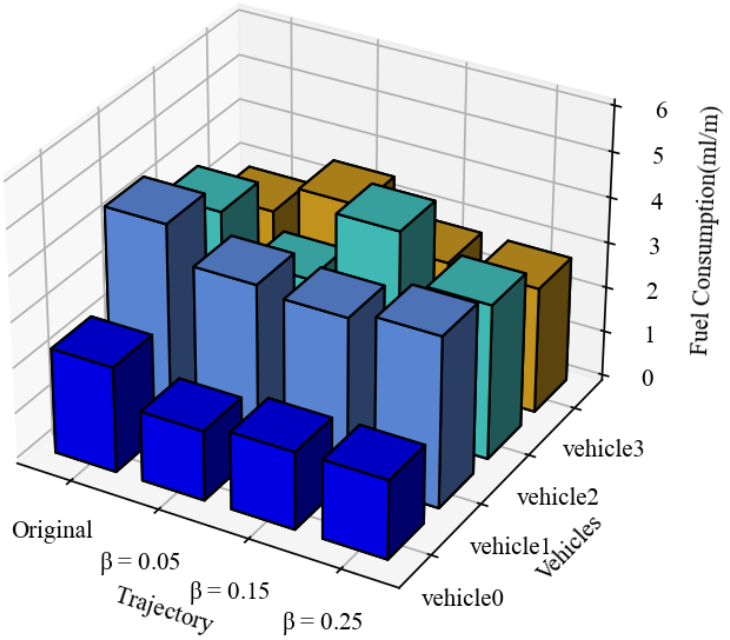


Figure 4.12: Fuel consumption performance of different host vehicles with different $\beta$ values

tial crash risk due to the relaxation of $\beta$, However, there are no safety issues within the studied road segment.

From the viewpoint of fuel consumption, the fuel consumption per unit distance of all optimized trajectories (with $\beta$ = 0.05, $\beta$ = 0.15 and $\beta$ = 0.25) are smaller than the original trajectory from data set for vehicle0 and vehicle1, with a maximum reduction of 33.97% and a minimum reduction of 15.66%, but for vehicle2 and vehicle3, the overall reduction in fuel consumption per unit distance after optimization is not as significant as that of vehicle0 and vehicle1, the maximum reduction is 22.86% and the minimum reduction is only 2.21% and even the fuel consumption per unit distance of the optimized trajectory increases with $\beta$ = 0.05 and $\beta$ = 0.15.

It can be observed from the original host vehicle trajectories that when there is a long waiting time, the relative distance prediction (part of the proposed strategy) tends to be more stable, resulting in more effective fuel consumption optimization. In contrast, for vehicles without waiting or with shorter waiting times (vehicle2 and vehicle3), the accuracy of the predicted values significantly impacts the subsequent optimization calculations.

## 4.7/ CONCLUSION

In this chapter, we proposed a data-driven trajectory planning strategy for connected vehicles, taking into account the uncertainty in shared information. Initially, we reviewed the

Gaussian sampling-based method, which effectively handles chance constraints in trajectory planning problems. Inspired by this, we developed a strategy that solves the optimal control problem by converting the chance constraint into a deterministic equivalent interval at each time step, based on a Gaussian Process Regression prediction model. To evaluate the effectiveness of our proposed strategy, we utilized the Next Generation SIMulation (NGSIM) dataset, simulating various scenarios and examining vehicle trajectory and fuel consumption performance under different probability values. The results showcase improvements in fuel economy, proving the merit of our approach. As for future research directions, expanding this strategy to longer routes featuring a larger number of signalized intersections could be considered. This would further test and refine the proposed method in more complex traffic situations, potentially leading to even greater efficiency improvements.

# 5

# Conclusion and Future Work

## 5.1/ Conclusion

In this thesis, we have explored various strategies for improving energy efficiency and reducing emissions in transportation sector across four chapters. Each focusing on different aspects of optimization and control.

In chapter 1, a comprehensive introduction is provided about HEV/PHEV/PEV, as well as a review of the state-of-the-art EMS for HEV/PHEV, eco-driving strategies for CAVs, and cooperative optimization approaches for CAHEVs. This chapter set the stage for our contributions to the field by identifying the gaps and challenges in existing methods.

In chapter 2, a velocity planning strategy for PHEB is presented, focusing on energy and time savings. By simplifying a 3D-DP to 2D-DP with optimal SOC from empirical data, we developed a deterministic spatial-discrete nonlinear optimization problem. Our simulation results demonstrated a 3.98% reduction in energy consumption and a 4.84% time saving. However, the premise of such a case assumes that the traffic signal information under a fixed route can be obtained completely and accurately in the context of ITS. However, in the absence of full ITS, more often than not, we do not have access to very accurate information of surrounding traffic information, and one of the solutions to this situation is to combine historical data to predict or extrapolate possible scenarios for better control.

In chapter 3, we try to combine data and model-driven strategies and proposed a stochastic eco-driving system for a power-split HEV, featuring co-optimization of vehicle dynamics and hybrid powertrain operations. The system comprises a dual-driven upper-level decision subsystem that suggests optimal set speeds or predicts trajectories and a rule-based hybrid powertrain control subsystem for optimizing energy consumption at intersections. Simulations in the SUMO traffic environment showed energy reductions of 6.49% and 4.17% compared to groups without the system, highlighting the system's independence from full traffic infrastructure connectivity, which could reduce to some extent the investment in traffic infrastructure renewal.

In chapter 4, similar to chapter 3, our goal was to optimize eco-driving strategies using a

data-driven model. However, in this chapter, we went a step further by employing data that is more representative of real-world conditions. By utilizing the NGSIM dataset, we were able to simulate various traffic scenarios and examine the performance of our proposed strategy in terms of vehicle trajectory and fuel consumption under different probability values. Firstly we reviewed the Gaussian sampling-based method for handling chance constraints in trajectory planning and developed a strategy using Gaussian Process Regression prediction models to transform chance constraints into deterministic equivalent intervals. The use of the NGSIM dataset allowed us to account for uncertainties in shared information, making our data-driven trajectory planning strategy more robust and adaptable to real-world situations. As a result, we were able to demonstrate improvements in fuel economy, validating the effectiveness of our approach in a more realistic context.

Moving forward, the successful implementation of our data-driven trajectory planning strategy using the NGSIM dataset paves the way for further research and development in this area. By refining our approach and extending it to other datasets or real-world traffic data, we can continue to enhance the energy efficiency and eco-friendliness of connected vehicles in increasingly complex traffic situations. Overall, this thesis has made significant contributions to the development of novel strategies and methodologies for energy-efficient and eco-friendly vehicle control, showcasing the potential for substantial advancements in fuel economy and traffic management.

## 5.2/ Ongoing Research

### 5.2.1/ Exploring Lateral Vehicular Interactions and Heterogeneous Traffic for Enhanced EMS and Eco-driving Strategies

In the Chapter 1, literature analysis highlights that the integration of various data sources, such as traffic data, routes, and vehicle information presents opportunities for cooperative optimization of vehicle dynamics and powertrain systems, with a considerable potential to reduce emissions and energy consumption. However, despite the wealth of research on this topic, there is a notable gap in the literature regarding the rigorous mathematical treatment of lateral vehicular interactions and their implications for trajectory planning along multi-lane road segments near signalized intersections. In realistic traffic conditions, lane-changing and merging maneuvers occur frequently. To address these challenges, several methods [78, 99, 120] have been proposed for legacy vehicles, which adopt stochastic controls to minimize the risk of collisions. The focus on safety can also be extended to connected HEV/PHEVs. As a result, how to manage the single/double-vehicle or platoon considering the lateral vehicular interaction behaviors in the future ITS environment, while ensuring safety and achieving better fuel economy simultaneously, will be one of the future research trends.

In addition, the heterogeneous traffic environment in the future will become another interesting subject to explore. According to [50], full market penetration of CAV technologies is not expected until the 2060s. Consequently, mixed traffic streams consisting of Human-Driven Vehicles (HDVs) and connected PEV/HEV/PHEVs will face heterogeneous dynamics and stability. Recent studies have made progress for the platoon with the consideration of lateral vehicular interactions. For example, [122] proposed distributed MPC method for a heterogeneous platoon, and [116] addresses control problems for heterogeneous vehicle platoons subject to disturbances and modeling errors. Nevertheless, it is crucial to develop a controller that can respond effectively to real-world traffic conditions while maintaining string stability to ensure safe transitional platoon maneuvers. This has been the main goal of the control algorithms proposed in most research to date and into the future.

### 5.2.2/ Harnessing Machine Learning and Edge Computing for Advanced EMS and Eco-driving Solutions

As the level of sophistication of cooperative optimization of EMS and Eco-driving is gradually advancing, to address many human factors-related issues, machine learning methods have become popular. These data-driven models integrated predictive models that the driver's compliance with speed advice systems or other interactions with V2I and V2V services. By doing so, these models provide a more realistic representation of how these services may affect systems. In addition, leveraging empirical observations that encompass different driver types, vehicle types, and traffic conditions can enable accurate predictions regarding the performance of co-optimization applications. An example like [110], deep learning is used to model state transitions based on an offline-trained graphical model, significantly reducing the time complexity. Further, hybrid two or more learning algorithms will be the direction of approaches for solving the cooperative optimization problem with more and more data sources, one of the applications direction of the learning algorithm is to extract useful traffic information and perceive the behavioral characteristics of human-related factors from huge amounts of data, which makes the ”brain” of connected HEV/PHEVs smarter, and another is application is the onboard implementation of EMS, which makes their ”behavior” more reliable.

Besides, online control requirements need more powerful calculation and processing capacity. To improve working efficiency, cooperative optimization frameworks must be able to allocate computing resources reasonably according to different calculation tasks. With the advent of the Internet of Things and 5G communications, centralized mobile cloud computing has given way to Mobile Edge Computing (MEC) in recent years. The primary feature of MEC is to push mobile computing, network control, and storage to network edges, enabling computation-intensive and latency-critical applications on resource-limited mobile devices [71]. Therefore, the analysis and study of cooperative optimization

under the mobile edge computing architecture represent another important research direction.

### 5.2.3/ Assessing the Real-World Impact of EMS and Eco-driving Strategies

Ultimately, experimental validation of any proposed controllers is essential for evaluating their efficacy in real-life scenarios. While simulation tests are the primary validation tool in most reviewed works, they may not provide a precise approach that can be implemented and improved upon in a real-life environment. Although simulation tests satisfy the essential requirement of initial evaluation, several testing-related elements, including communication devices (sensors, V2V/V2I equipment), trajectory planning algorithms, and EMS for determining the optimal power-split for HEVs/PHEVs, pose a challenge to evaluating the real performance of proposed methods. To address this challenge, some researchers have developed HIL testing for relatively simple traffic conditions [80, 123, 125]. Therefore, there is a need to systematically investigate efficient approaches (such as those that are low-cost and easy to implement) to validate the co-optimization performance.

# BIBLIOGRAPHY


[1] **Next generation simulation, improved simulation of stop bar driver behavior at signalized intersections-los angeles, ca and atlanta, ga data sets, 2014**. http://www.webpages.uidaho.edu/ngsim/ATL/ATL.htm.

[2] SALMAN, M., SCHOUTEN, N. J., AND KHEIR, N. A. **Control strategies for parallel hybrid vehicles**. In *Proceedings of the 2000 American Control Conference. ACC (IEEE Cat. No. 00CH36334)* (2000), vol. 1, IEEE, pp. 524–528.

[3] BENGTSSON, J. **Adaptive cruise control and driver modeling**. Department of Automatic Control, Lund Institute of Technology, 2001.

[4] CHAU, K., AND WONG, Y. **Overview of power management in hybrid electric vehicles**. *Energy conversion and management 43*, 15 (2002), 1953–1968.

[5] PAGANELLI, G., DELPRAT, S., GUERRA, T.-M., RIMAUX, J., AND SANTIN, J.-J. **Equivalent consumption minimization strategy for parallel hybrid powertrains**. In *Vehicular technology conference. IEEE 55th vehicular technology conference. VTC spring 2002 (cat. No. 02CH37367)* (2002), vol. 4, IEEE, pp. 2076–2081.

[6] LIN, C.-C., PENG, H., AND GRIZZLE, J. **A stochastic control strategy for hybrid electric vehicles**. In *Proceedings of the 2004 American control conference* (2004), vol. 5, IEEE, pp. 4710–4715.

[7] RAKHA, H., SNARE, M., AND DION, F. **Vehicle dynamics model for estimating maximum light-duty vehicle acceleration levels**. *Transportation Research Record 1883*, 1 (2004), 40–49.

[8] KARBOWSKI, D., ROUSSEAU, A., PAGERIT, S., AND SHARER, P. **Plug-in vehicle control strategy: from global optimization to real time application**. In *22th International Electric Vehicle Symposium (EVS22), Yokohama* (2006), Citeseer.

[9] GAO, W., AND MI, C. **Hybrid vehicle design using global optimisation algorithms**. *International Journal of Electric and Hybrid Vehicles 1*, 1 (2007), 57–70.

[10] GONG, Q., LI, Y., AND PENG, Z.-R. **Trip based power management of plug-in hybrid electric vehicle with two-scale dynamic programming**. In *2007 IEEE vehicle power and propulsion conference* (2007), IEEE, pp. 12–19.

[11] JOHANNESSON, L., ASBOGARD, M., AND EGARDT, B. **Assessing the potential of predictive control for hybrid vehicle powertrains using stochastic dynamic programming**. *IEEE Transactions on Intelligent Transportation Systems 8*, 1 (2007), 71–83.

[12] GONG, Q., LI, Y., AND PENG, Z.-R. **Computationally efficient optimal power management for plug-in hybrid electric vehicles with spatial domain dynamic**

**programming**. In *Dynamic Systems and Control Conference* (2008), vol. 43352, pp. 1019–1026.

**[13]** ROUSSEAU, A., PAGERIT, S., AND GAO, D. W. **Plug-in hybrid electric vehicle control strategy parameter optimization**. *Journal of Asian Electric Vehicles 6*, 2 (2008), 1125–1133.

**[14]** TATE JR, E. D., GRIZZLE, J. W., AND PENG, H. **Shortest path stochastic control for hybrid electric vehicles**. *International Journal of Robust and Nonlinear Control: IFAC-Affiliated Journal 18*, 14 (2008), 1409–1429.

**[15]** WU, J., ZHANG, C.-H., AND CUI, N.-X. **Pso algorithm-based parameter optimization for hev powertrain and its control strategy**. *International Journal of Automotive Technology 9*, 1 (2008), 53–59.

**[16]** BANVAIT, H., ANWAR, S., AND CHEN, Y. **A rule-based energy management strategy for plug-in hybrid electric vehicle (phev)**. In *2009 American control conference* (2009), IEEE, pp. 3938–3943.

**[17]** MANDAVA, S., BORIBOONSOMSIN, K., AND BARTH, M. **Arterial velocity planning based on traffic signal information under light traffic conditions**. In *2009 12th International IEEE Conference on Intelligent Transportation Systems* (2009), IEEE, pp. 1–6.

**[18]** SERRAO, L., ONORI, S., AND RIZZONI, G. **Ecms as a realization of pontryagin's minimum principle for hev control**. In *2009 American control conference* (2009), IEEE, pp. 3964–3969.

**[19]** VAN KEULEN, T., NAUS, G., DE JAGER, B., VAN DE MOLENGRAFT, R., STEINBUCH, M., AND ANEKE, E. **Predictive cruise control in hybrid electric vehicles**. *World Electric Vehicle Journal 3*, 3 (2009), 494–504.

**[20]** ASADI, B., AND VAHIDI, A. **Predictive cruise control: Utilizing upcoming traffic signal information for improving fuel economy and reducing trip time**. *IEEE transactions on control systems technology 19*, 3 (2010), 707–714.

**[21]** HUANG, X., TAN, Y., AND HE, X. **An intelligent multifeature statistical approach for the discrimination of driving conditions of a hybrid electric vehicle**. *IEEE Transactions on Intelligent Transportation Systems 12*, 2 (2010), 453–465.

**[22]** KIM, N., CHA, S., AND PENG, H. **Optimal control of hybrid electric vehicles based on pontryagin's minimum principle**. *IEEE Transactions on control systems technology 19*, 5 (2010), 1279–1287.

**[23]** TIELERT, T., KILLAT, M., HARTENSTEIN, H., LUZ, R., HAUSBERGER, S., AND BENZ, T. **The impact of traffic-light-to-vehicle communication on fuel consumption and emissions**. In *2010 Internet of Things (IOT)* (2010), IEEE, pp. 1–8.

**[24]** BARTH, M., MANDAVA, S., BORIBOONSOMSIN, K., AND XIA, H. **Dynamic eco-driving for arterial corridors**. In *2011 IEEE Forum on Integrated and Sustainable Transportation Systems* (2011), IEEE, pp. 182–188.

**[25]** BORHAN, H., VAHIDI, A., PHILLIPS, A. M., KUANG, M. L., KOLMANOVSKY, I. V., AND DI CAIRANO, S. **Mpc-based energy management of a power-split hybrid electric vehicle**. *IEEE Transactions on Control Systems Technology 20*, 3 (2011), 593–603.

**[26]** KAMAL, M. A. S., MUKAI, M., MURATA, J., AND KAWABE, T. **Ecological vehicle control on roads with up-down slopes**. *IEEE Transactions on Intelligent Transportation Systems 12*, 3 (2011), 783–794.

**[27]** PEDREGOSA, F., VAROQUAUX, G., GRAMFORT, A., MICHEL, V., THIRION, B., GRISEL, O., BLONDEL, M., PRETTENHOFER, P., WEISS, R., DUBOURG, V., VANDERPLAS, J., PASSOS, A., COURNAPEAU, D., BRUCHER, M., PERROT, M., AND DUCHESNAY, E. **Scikit-learn: Machine learning in Python**. *Journal of Machine Learning Research 12* (2011), 2825–2830.

**[28]** SCHURICHT, P., MICHLER, O., AND BÄKER, B. **Efficiency-increasing driver assistance at signalized intersections using predictive traffic state estimation**. In *2011 14th International IEEE Conference on Intelligent Transportation Systems (ITSC)* (2011), IEEE, pp. 347–352.

**[29]** BERTSEKAS, D. **Dynamic programming and optimal control: Volume I**, vol. 1. Athena scientific, 2012.

**[30]** HE, Y., RIOS, J., CHOWDHURY, M., PISU, P., AND BHAVSAR, P. **Forward powertrain energy management modeling for assessing benefits of integrating predictive traffic data into plug-in-hybrid electric vehicles**. *Transportation Research Part D: Transport and Environment 17*, 3 (2012), 201–207.

**[31]** MAHLER, G., AND VAHIDI, A. **Reducing idling at red lights based on probabilistic prediction of traffic signal timings**. In *2012 American Control Conference (ACC)* (2012), IEEE, pp. 6557–6562.

**[32]** MURPHEY, Y. L., PARK, J., CHEN, Z., KUANG, M. L., MASRUR, M. A., AND PHILLIPS, A. M. **Intelligent hybrid vehicle power control—part i: Machine learning of optimal vehicle power**. *IEEE Transactions on Vehicular Technology 61*, 8 (2012), 3519–3530.

**[33]** MURPHEY, Y. L., PARK, J., KILIARIS, L., KUANG, M. L., MASRUR, M. A., PHILLIPS, A. M., AND WANG, Q. **Intelligent hybrid vehicle power control—part ii: Online intelligent energy management**. *IEEE Transactions on Vehicular Technology 62*, 1 (2012), 69–79.

**[34]** RAKHA, H. A., KAMALANATHSHARMA, R. K., AHN, K., AND OTHERS. **Aeris: Eco-vehicle speed control at signalized intersections using i2v communication**. Tech. rep., United States. Joint Program Office for Intelligent Transportation Systems, 2012.

**[35]** SIVAK, M., AND SCHOETTLE, B. **Eco-driving: Strategic, tactical, and operational decisions of the driver that influence vehicle fuel economy**. *Transport Policy 22* (2012), 96–99.

**[36]** TAGHAVIPOUR, A., VAJEDI, M., AZAD, N. L., AND MCPHEE, J. **Predictive power management strategy for a phev based on different levels of trip information**. *IFAC Proceedings Volumes 45*, 30 (2012), 326–333.

**[37]** ZHANG, Y., AND LIU, H.-P. **Fuzzy multi-objective control strategy for parallel hybrid electric vehicle**. *IET Electrical Systems in Transportation 2*, 2 (2012), 39–50.

**[38]** DI CAIRANO, S., BERNARDINI, D., BEMPORAD, A., AND KOLMANOVSKY, I. V. **Stochastic mpc with learning for driver-predictive vehicle control and its application to hev energy management**. *IEEE Transactions on Control Systems Technology 22*, 3 (2013), 1018–1031.

**[39]** FRANCO, V., KOUSOULIDOU, M., MUNTEAN, M., NTZIACHRISTOS, L., HAUSBERGER, S., AND DILARA, P. **Road vehicle emission factors development: A review**. *Atmospheric Environment 70* (2013), 84–97.

**[40]** MOHAN, G., ASSADIAN, F., AND LONGO, S. **Comparative analysis of forward-facing models vs backwardfacing models in powertrain component sizing**. In *IET hybrid and electric vehicles conference 2013 (HEVC 2013)* (2013), IET, pp. 1–6.

**[41]** SAERENS, B., RAKHA, H. A., DIEHL, M., AND VAN DEN BULCK, E. **A methodology for assessing eco-cruise control for passenger vehicles**. *Transportation research part D: transport and environment 19* (2013), 20–27.

**[42]** XIA, H., BORIBOONSOMSIN, K., AND BARTH, M. **Dynamic eco-driving for signalized arterial corridors and its indirect network-wide energy/emissions benefits**. *Journal of Intelligent Transportation Systems 17*, 1 (2013), 31–41.

**[43]** BODENHEIMER, R., BRAUER, A., ECKHOFF, D., AND GERMAN, R. **Enabling glosa for adaptive traffic lights**. In *2014 ieee vehicular networking conference (vnc)* (2014), IEEE, pp. 167–174.

**[44]** CHEN, Z., ZHANG, Y., LV, J., AND ZOU, Y. **Model for optimization of ecodriving at signalized intersections**. *Transportation Research Record 2427*, 1 (2014), 54–62.

**[45]** HEDENGREN, J. D., SHISHAVAN, R. A., POWELL, K. M., AND EDGAR, T. F. **Nonlinear modeling, estimation and predictive control in apmonitor**. *Computers & Chemical Engineering 70* (2014), 133–148.

**[46]** LANG, D., SCHMIED, R., AND DEL RE, L. **Prediction of preceding driver behavior for fuel efficient cooperative adaptive cruise control**. *SAE International Journal of Engines 7*, 1 (2014), 14–20.

**[47]** PANDAY, A., AND BANSAL, H. O. **A review of optimal energy management strategies for hybrid electric vehicle**. *International Journal of Vehicular Technology 2014* (2014).

**[48]** SCIARRETTA, A., SERRAO, L., DEWANGAN, P., TONA, P., BERGSHOEFF, E., BORDONS, C., CHARMPA, L., ELBERT, P., ERIKSSON, L., HOFMAN, T., AND OTHERS. **A control benchmark on the energy management of a plug-in hybrid electric vehicle**. *Control engineering practice 29* (2014), 287–298.

**[49]** WU, G., BORIBOONSOMSIN, K., AND BARTH, M. J. **Development and evaluation of an intelligent energy-management strategy for plug-in hybrid electric vehicles**. *IEEE Transactions on Intelligent Transportation Systems 15*, 3 (2014), 1091–1100.

**[50]** ALESSANDRINI, A., CAMPAGNA, A., DELLE SITE, P., FILIPPI, F., AND PERSIA, L. **Automated vehicles and the rethinking of mobility and cities**. *Transportation Research Procedia 5* (2015), 145–160.

**[51]** CHEN, W., LIU, Y., YANG, X., BAI, Y., GAO, Y., AND LI, P. **Platoon-based speed control algorithm for ecodriving at signalized intersection**. *Transportation Research Record 2489*, 1 (2015), 29–38.

**[52]** FANG, Y., SONG, C., XIA, B., AND SONG, Q. **An energy management strategy for hybrid electric bus based on reinforcement learning**. In *The 27th Chinese control and decision conference (2015 CCDC)* (2015), IEEE, pp. 4973–4977.

**[53]** HAO, P., WU, G., BORIBOONSOMSIN, K., AND BARTH, M. J. **Developing a framework of eco-approach and departure application for actuated signal control**. In *2015 IEEE Intelligent Vehicles Symposium (IV)* (2015), IEEE, pp. 796–801.

**[54]** HE, X., LIU, H. X., AND LIU, X. **Optimal vehicle speed trajectory on a signalized arterial with consideration of queue**. *Transportation Research Part C: Emerging Technologies 61* (2015), 106–120.

**[55]** LUO, Y., CHEN, T., ZHANG, S., AND LI, K. **Intelligent hybrid electric vehicle acc with coordinated control of tracking ability, fuel economy, and ride comfort**. *IEEE Transactions on Intelligent Transportation Systems 16*, 4 (2015), 2303–2308.

**[56]** MEULENERS, L., AND FRASER, M. **A validation study of driving errors using a driving simulator**. *Transportation research part F: traffic psychology and behaviour 29* (2015), 14–21.

**[57]** CONTI, J., HOLTBERG, P., DIEFENDERFER, J., LAROSE, A., TURNURE, J. T., AND WESTFALL, L. **International energy outlook 2016 with projections to 2040**. Tech. rep., USDOE Energy Information Administration (EIA), Washington, DC (United States). Office of Energy Analysis, 2016.

**[58]** GUO, L., GAO, B., GAO, Y., AND CHEN, H. **Optimal energy management for hevs in eco-driving applications using bi-level mpc**. *IEEE Transactions on Intelligent Transportation Systems 18*, 8 (2016), 2153–2162.

**[59]** HOMCHAUDHURI, B., LIN, R., AND PISU, P. **Hierarchical control strategies for energy management of connected hybrid electric vehicles in urban roads**. *Transportation Research Part C: Emerging Technologies 62* (2016), 70–86.

**[60]** LI, S. E., GUO, Q., XIN, L., CHENG, B., AND LI, K. **Fuel-saving servo-loop control for an adaptive cruise control system of road vehicles with step-gear transmission**. *IEEE Transactions on Vehicular Technology 66*, 3 (2016), 2033–2043.

**[61]** MARTINEZ, C. M., HU, X., CAO, D., VELENIS, E., GAO, B., AND WELLERS, M. **Energy management in plug-in hybrid electric vehicles: Recent progress and a connected vehicles perspective**. *IEEE Transactions on Vehicular Technology 66*, 6 (2016), 4534–4549.

**[62]** RASMUSSEN, C. E., AND WILLIAMS, C. K. I. **Gaussian Processes for Machine Learning**. MIT press Cambridge, MA, 2016.

**[63]** SABRI, M., DANAPALASINGAM, K. A., AND RAHMAT, M. F. **A review on hybrid electric vehicles architecture and energy management strategies**. *Renewable and Sustainable Energy Reviews 53* (2016), 1433–1442.

**[64]** ZHOU, M., JIN, H., AND WANG, W. **A review of vehicle fuel consumption models to evaluate eco-driving and eco-routing**. *Transportation Research Part D: Transport and Environment 49* (2016), 203–218.

**[65]** ALTAN, O. D., WU, G., BARTH, M. J., BORIBOONSOMSIN, K., AND STARK, J. A. **Glidepath: Eco-friendly automated approach and departure at signalized intersections**. *IEEE Transactions on Intelligent Vehicles 2*, 4 (2017), 266–277.

**[66]** HUANG, Y., WANG, H., KHAJEPOUR, A., HE, H., AND JI, J. **Model predictive control power management strategies for hevs: A review**. *Journal of Power Sources 341* (2017), 91–106.

**[67]** JAZAR, R. N. **Vehicle dynamics: theory and application**. Springer, 2017.

**[68]** JIANG, H., HU, J., AN, S., WANG, M., AND PARK, B. B. **Eco approaching at an isolated signalized intersection under partially connected and automated vehicles environment**. *Transportation Research Part C: Emerging Technologies 79* (2017), 290–307.

**[69]** LUO, Y., LI, S., ZHANG, S., QIN, Z., AND LI, K. **Green light optimal speed advisory for hybrid electric vehicles**. *Mechanical Systems and Signal Processing 87* (2017), 30–44.

**[70]** MA, G., GHASEMI, M., AND SONG, X. **Integrated powertrain energy management and vehicle coordination for multiple connected hybrid electric vehicles**. *IEEE Transactions on Vehicular Technology 67*, 4 (2017), 2893–2899.

**[71]** MAO, Y., YOU, C., ZHANG, J., HUANG, K., AND LETAIEF, K. B. **A survey on mobile edge computing: The communication perspective**. *IEEE communications surveys & tutorials 19*, 4 (2017), 2322–2358.

**[72]** QI, X., WU, G., HAO, P., BORIBOONSOMSIN, K., AND BARTH, M. J. **Integrated-connected eco-driving system for phevs with co-optimization of vehicle dynamics and powertrain operations**. *IEEE Transactions on Intelligent Vehicles 2*, 1 (2017), 2–13.

**[73]** QIU, L., QIAN, L., ZOMORODI, H., AND PISU, P. **Global optimal energy management control strategies for connected four-wheel-drive hybrid electric vehicles**. *IET Intelligent Transport Systems 11*, 5 (2017), 264–272.

**[74]** REZAEI, A., BURL, J. B., AND ZHOU, B. **Estimation of the ecms equivalent factor bounds for hybrid electric vehicles**. *IEEE Transactions on Control Systems Technology 26*, 6 (2017), 2198–2205.

**[75]** SANGUINETTI, A., KURANI, K., AND DAVIES, J. **The many reasons your mileage may vary: Toward a unifying typology of eco-driving behaviors**. *Transportation Research Part D: Transport and Environment 52* (2017), 73–84.

**[76]** STEBBINS, S., HICKMAN, M., KIM, J., AND VU, H. L. **Characterising green light optimal speed advisory trajectories for platoon-based optimisation**. *Transportation Research Part C: Emerging Technologies 82* (2017), 43–62.

**[77]** TAJEDDIN, S., AND AZAD, N. L. **Ecological cruise control of a plug-in hybrid electric vehicle: A comparison of different gmres-based nonlinear model predictive controls**. In *2017 American Control Conference (ACC)* (2017), IEEE, pp. 3607–3612.

**[78]** VAN DE HOEF, S., JOHANSSON, K. H., AND DIMAROGONAS, D. V. **Efficient dynamic programming solution to a platoon coordination merge problem with stochastic travel times**. *IFAC-PapersOnLine 50*, 1 (2017), 4228–4233.

**[79]** ZHANG, S., LUO, Y., WANG, J., WANG, X., AND LI, K. **Predictive energy management strategy for fully electric vehicles based on preceding vehicle movement**. *IEEE Transactions on Intelligent Transportation Systems 18*, 11 (2017), 3049–3060.

**[80]** ZULKEFLI, M. A. M., MUKHERJEE, P., SUN, Z., ZHENG, J., LIU, H. X., AND HUANG, P. **Hardware-in-the-loop testbed for evaluating connected vehicle applications**. *Transportation Research Part C: Emerging Technologies 78* (2017), 50–62.

**[81]** ABDEL-BASSET, M., ABDEL-FATAH, L., AND SANGAIAH, A. K. **Metaheuristic algorithms: A comprehensive review**. *Computational intelligence for multimedia big data on the cloud with engineering applications* (2018), 185–231.

**[82]** BARIK, B., KRISHNA BHAT, P., ONCKEN, J., CHEN, B., ORLANDO, J., AND ROBINETTE, D. **Optimal velocity prediction for fuel economy improvement of connected vehicles**. *IET Intelligent Transport Systems 12*, 10 (2018).

**[83]** BEAL, L. D., HILL, D. C., MARTIN, R. A., AND HEDENGREN, J. D. **Gekko optimization suite**. *Processes 6*, 8 (2018), 106.

**[84]** HAO, P., WU, G., BORIBOONSOMSIN, K., AND BARTH, M. J. **Eco-approach and departure (ead) application for actuated signals in real-world traffic**. *IEEE Transactions on Intelligent Transportation Systems 20*, 1 (2018), 30–40.

**[85]** HE, X., AND WU, X. **Eco-driving advisory strategies for a platoon of mixed gasoline and electric vehicles in a connected vehicle system**. *Transportation Research Part D: Transport and Environment 63* (2018), 907–922.

**[86]** HUANG, Y., NG, E. C., ZHOU, J. L., SURAWSKI, N. C., CHAN, E. F., AND HONG, G. **Eco-driving technology for sustainable road transport: A review**. *Renewable and Sustainable Energy Reviews 93* (2018), 596–609.

**[87]** LI, G., AND GÖRGES, D. **Ecological adaptive cruise control and energy management strategy for hybrid electric vehicles based on heuristic dynamic programming**. *IEEE Transactions on Intelligent Transportation Systems 20*, 9 (2018), 3526–3535.

**[88]** MORLOCK, F., AND SAWODNY, O. **An economic model predictive cruise controller for electric vehicles using gaussian process prediction**. *IFAC-PapersOnLine 51*, 31 (2018), 876–881.

**[89]** QI, X., WANG, P., WU, G., BORIBOONSOMSIN, K., AND BARTH, M. J. **Connected cooperative ecodriving system considering human driver error**. *IEEE Transactions on Intelligent Transportation Systems 19*, 8 (2018), 2721–2733.

**[90]** SAKHDARI, B., AND AZAD, N. L. **Adaptive tube-based nonlinear mpc for economic autonomous cruise control of plug-in hybrid electric vehicles**. *IEEE Transactions on Vehicular Technology 67*, 12 (2018), 11390–11401.

**[91]** SHARMA, A., ALI, Y., SAIFUZZAMAN, M., ZHENG, Z., HAQUE, M., AND OTHERS. **Human factors in modelling mixed traffic of traditional, connected, and automated vehicles**. In *International Conference on Applied Human Factors and Ergonomics* (2018), Springer, pp. 262–273.

**[92]** SUN, C., SHEN, X., AND MOURA, S. **Robust optimal eco-driving control with uncertain traffic signal timing**. In *2018 annual American control conference (ACC)* (2018), IEEE, pp. 5548–5553.

**[93]** WANG, Y., WANG, W., XIANG, C., AND WANG, X. **Pmp-based equivalent fuel consumption optimization for power distribution of power-split hevs**. In *2018 Chinese Control And Decision Conference (CCDC)* (2018), IEEE, pp. 3445–3450.

**[94]** YE, F., HAO, P., QI, X., WU, G., BORIBOONSOMSIN, K., AND BARTH, M. J. **Prediction-based eco-approach and departure at signalized intersections with speed forecasting on preceding vehicles**. *IEEE Transactions on Intelligent Transportation Systems 20*, 4 (2018), 1378–1389.

**[95]** ZHAO, P., WANG, Y., CHANG, N., ZHU, Q., AND LIN, X. **A deep reinforcement learning framework for optimizing fuel economy of hybrid electric vehicles**. In *2018 23rd Asia and South Pacific design automation conference (ASP-DAC)* (2018), IEEE, pp. 196–202.

**[96]** BAE, S., CHOI, Y., KIM, Y., GUANETTI, J., BORRELLI, F., AND MOURA, S. **Real-time ecological velocity planning for plug-in hybrid vehicles with partial communication to traffic lights**. In *2019 IEEE 58th Conference on Decision and Control (CDC)* (2019), IEEE, pp. 1279–1285.

**[97]** BAE, S., KIM, Y., GUANETTI, J., BORRELLI, F., AND MOURA, S. **Design and implementation of ecological adaptive cruise control for autonomous driving with communication to traffic lights**. In *2019 American Control Conference (ACC)* (2019), IEEE, pp. 4628–4634.

**[98]** BAKIBILLAH, A., KAMAL, M. A. S., TAN, C. P., HAYAKAWA, T., AND IMURA, J.-I. **Event-driven stochastic eco-driving strategy at signalized intersections from self-driving data**. *IEEE Transactions on Vehicular Technology 68*, 9 (2019), 8557–8569.

**[99]** GAO, Y., JIANG, F. J., JOHANSSON, K. H., AND XIE, L. **Stochastic modeling and optimal control for automated overtaking**. In *2019 IEEE 58th Conference on Decision and Control (CDC)* (2019), IEEE, pp. 1273–1278.

**[100]** HU, X., LIU, T., QI, X., AND BARTH, M. **Reinforcement learning for hybrid and plug-in hybrid electric vehicle energy management: Recent advances and prospects**. *IEEE Industrial Electronics Magazine 13*, 3 (2019), 16–25.

**[101]** QIU, S., QIU, L., QIAN, L., AND PISU, P. **Hierarchical energy management control strategies for connected hybrid electric vehicles considering efficiencies feedback**. *Simulation Modelling Practice and Theory 90* (2019), 1–15.

**[102]** ZHANG, F., HU, X., LANGARI, R., AND CAO, D. **Energy management strategies of connected hevs and phevs: Recent progress and outlook**. *Progress in Energy and Combustion Science 73* (2019), 235–256.

**[103]** GONÇALVES, T. R., VARMA, V. S., AND ELAYOUBI, S. E. **Vehicle platooning schemes considering v2v communications: A joint communication/control approach**. In *2020 IEEE Wireless Communications and Networking Conference (WCNC)* (2020), IEEE, pp. 1–6.

**[104]** MINTSIS, E., VLAHOGIANNI, E. I., AND MITSAKIS, E. **Dynamic eco-driving near signalized intersections: Systematic review and future research directions**. *Journal of Transportation Engineering, Part A: Systems 146*, 4 (2020), 04020018.

**[105]** PETTERSSON, P., JACOBSON, B., BRUZELIUS, F., JOHANNESSON, P., AND FAST, L. **Intrinsic differences between backward and forward vehicle simulation models**. *IFAC-PapersOnLine 53*, 2 (2020), 14292–14299.

**[106]** SUN, C., GUANETTI, J., BORRELLI, F., AND MOURA, S. J. **Optimal eco-driving control of connected and autonomous vehicles through signalized intersections**. *IEEE Internet of Things Journal 7*, 5 (2020), 3759–3773.

**[107]** WANG, J. **An intuitive tutorial to gaussian processes regression**. *arXiv preprint arXiv:2009.10862* (2020).

**[108]** WANG, S., AND LIN, X. **Eco-driving control of connected and automated hybrid vehicles in mixed driving scenarios**. *Applied Energy 271* (2020), 115233.

**[109]** XU, F., AND SHEN, T. **Look-ahead prediction-based real-time optimal energy management for connected hevs**. *IEEE transactions on Vehicular Technology 69*, 3 (2020), 2537–2551.

**[110]** YE, F., HAO, P., WU, G., ESAID, D., BORIBOONSOMSIN, K., GAO, Z., LACLAIR, T., AND BARTH, M. **Deep learning-based queue-aware eco-approach and departure system for plug-in hybrid electric buses at signalized intersections: A simulation study**. Tech. rep., Oak Ridge National Lab.(ORNL), Oak Ridge, TN (United States), 2020.

**[111]** ZHANG, B., ZHANG, J., XU, F., AND SHEN, T. **Optimal control of power-split hybrid electric powertrains with minimization of energy consumption**. *Applied Energy 266* (2020), 114873.

**[112]** ZHANG, J., AND XU, F. **Real-time optimization of energy consumption under adaptive cruise control for connected hevs**. *Control Theory and Technology 18*, 2 (2020), 182–192.

**[113]** BHATTACHARYYA, V., CANOSA, A. F., AND HOMCHAUDHURI, B. **Fast Data-Driven Model Predictive Control Strategy for Connected and Automated Vehicles**. *ASME Letters in Dynamic Systems and Control 1*, 4 (2021).

**[114]** BHATTACHARYYA, V., CANOSA, A. F., AND HOMCHAUDHURI, B. **Fast data-driven model predictive control strategy for connected and automated vehicles**. *ASME Letters in Dynamic Systems and Control 1*, 4 (2021).

**[115]** Le Rhun, A., Bonnans, F., De Nunzio, G., Leroy, T., and Martinon, P. **A bilevel energy management strategy for hevs under probabilistic traffic conditions**. *IEEE Transactions on Control Systems Technology 30*, 2 (2021), 728–739.

**[116]** Luo, Q., Nguyen, A.-T., Fleming, J., and Zhang, H. **Unknown input observer based approach for distributed tube-based model predictive control of heterogeneous vehicle platoons**. *IEEE Transactions on Vehicular Technology 70*, 4 (2021), 2930–2944.

**[117]** Baby, T. V., Bhattacharyya, V., Shahri, P. K., Ghasemi, A. H., and Hom-Chaudhuri, B. **A suggestion-based fuel efficient control framework for connected and automated vehciles in heterogeneous urban traffic**. *Transportation Research Part C: Emerging Technologies 134* (2022), 103476.

**[118]** Davis, S., and Boundy, R. G. **Transportation energy data book: Edition 40**. Tech. rep., Oak Ridge National Lab.(ORNL), Oak Ridge, TN (United States), 2022.

**[119]** Du, A., Han, Y., and Zhu, Z. **Review on multi-objective optimization of energy management strategy for hybrid electric vehicle integrated with traffic information**. *Energy Sources, Part A: Recovery, Utilization, and Environmental Effects 44*, 3 (2022), 7914–7933.

**[120]** Medina-Lee, J. F., Jiménez, V., Godoy, J., and Villagra, J. **Maneuver planner for automated vehicles on urban scenarios**. In *2022 IEEE International Conference on Vehicular Electronics and Safety (ICVES)* (2022), IEEE, pp. 1–7.

**[121]** Peng, J., Fan, Y., Yin, G., and Jiang, R. **Collaborative optimization of energy management strategy and adaptive cruise control based on deep reinforcement learning**. *IEEE Transactions on Transportation Electrification* (2022).

**[122]** Qiang, Z., Dai, L., Chen, B., and Xia, Y. **Distributed model predictive control for heterogeneous vehicle platoon with inter-vehicular spacing constraints**. *IEEE Transactions on Intelligent Transportation Systems* (2022).

**[123]** Shao, Y., Deter, D., Cook, A., Wang, C. R., Thompson, B., and Perry, N. **Real-sim interface: Enabling multi-resolution simulation and x-in-the-loop development for connected and automated vehicles**. *SAE International Journal of Connected and Automated Vehicles 5*, 12-05-04-0026 (2022).

**[124]** Sun, C., Zhang, C., Sun, F., and Zhou, X. **Stochastic co-optimization of speed planning and powertrain control with dynamic probabilistic constraints for safe and ecological driving**. *Applied Energy 325* (2022), 119874.

**[125]** Xu, Z., Jiang, T., and Zheng, N. **Developing and analyzing eco-driving strategies for on-road emission reduction in urban transport systems-a vr-enabled digital-twin approach**. *Chemosphere 305* (2022), 135372.

**[126]** Gurobi, L. **Optimization, gurobi optimizer reference manual. 2020**.

**[127]** USEPA. **Vehicle and fuel emission testing - engine testing regulations**. https://www.epa.gov/vehicle-and-fuel-emissions-testing/engine-testing-regulations#engine-test-procedures.

# List of Figures

# List of Tables

Document generated with LaTeX and:
the LaTeX style for PhD Thesis created by S. Galland — http://www.multiagent.fr/ThesisStyle
the tex-upmethodology package suite — http://www.arakhne.org/tex-upmethodology/